Investigations on the Optimal Planning of Electric Vehicle Charging Stations in coupled network using Meta Heuristic Techniques

Submitted in partial fulfilment of the requirements
for the award of the degree of

Doctor of Philosophy

in

Electrical Engineering

By

Vutla Vijay

Roll No: 718016

Supervisor:

Dr. Chintham Venkaiah

Professor

Department of Electrical Engineering

NATIONAL INSTITUTE OF TECHNOLOGY

WARANGAL

(An Institute of National Importance)

HANUMAKONDA - 506004, TELANGANA, INDIA

July 2024

Approval

This Thesis entitled **"Investigations on the Optimal Planning of Electric Vehicle Charging Stations in coupled network using Meta Heuristic Techniques"** by **Mr. Vutla Vijay**, bearing **Roll No. 718016** is approved for the degree of **Doctor of Philosophy** in **Electrical Engineering** from **National Institute of Technology, Warangal.**

Examiners

_____

_____

_____

Supervisor

_____

Dr. Chintham Venkaiah
Professor
Department of Electrical Engineering
NIT Warangal

Chairman

_____

Dr. S. Srinivasa Rao
Professor
Department of Electrical Engineering
NIT Warangal

Date: /07/24
Place: NIT Warangal

DEPARTMENT OF ELECTRICAL ENGINEERING
NATIONAL INSTITUTE OF TECHNOLOGY WARANGAL
HANUMAKONDA-506004, TELANGANA, INDIA

CERTIFICATE

This is to certify that the thesis entitled "**Investigations on the Optimal Planning of Electric Vehicle Charging Stations in coupled network using Meta Heuristic Techniques**" which is being submitted by **Vutla Vijay**, bearing Roll No. **718016**, is a bonafide work submitted to National Institute of Technology, Warangal in partial fullfillment of the requirements for the award of the degree of Doctor of Philosophy in Department of Electrical Engineering. To the best of my knowledge, the work incorporated in this thesis has not been submitted elsewhere for the award of any degree.

Date: /07/2024
Place: NIT Warangal

Dr. Chintham Venkaiah
(Supervisor)
Professor
Department of Electrical Engineering
NIT Warangal

DECLARATION

This is to certify that the work presented in the thesis entitled "**Investigations on the Optimal Planning of Electric Vehicle Charging Stations in coupled network using Meta Heuristic Techniques**" is a bonafide work done by me under the supervision of **Dr. Chintham Venkaiah**, Professor, Department of Electrical Engineering, National Institute of Technology Warangal, India and is not submitted elsewhere for the award of any degree.

I declare that this written submission represents my ideas in my own words and where others ideas or words have been included, I have adequately cited and referenced the original sources. I also declare that I have adhered to all principles of academic honesty and integrity and have not misrepresented or fabricated or falsified any idea / data / fact / source in my submission. I understand that any violation of the above will be a cause for disciplinary action by the Institute and can also evoke penal action from the sources which have thus not been properly cited or from whom proper permission has not been taken when needed.

_____

Vutla Vijay

(**718016**)

Date: /07/2024
Place: NIT warangal

ACKNOWLEDGEMENTS

The research work and the current thesis are outcomes of constant inspiration and support of the kind people around me. I would like to convey my most sincere recognition to each and every one for their respective assists.

Foremost, I would like to express my deepest gratitude to my respected research supervisor, **Dr. Chintham Venkaiah**, Professor, Department of Electrical Engineering, National Institute of Technology Warangal, for his guidance, scholarly input and consistent encouragement. This work is possible only because of the unconditional moral support provided by him. I had great freedom to plan and execute my ideas in research without any pressure. This made me identify my strengths and drawbacks and boosted my self-confidence.

I am very much thankful to **Dr. S. Srinivasa Rao**, Chairman of DSC, Professor, Department of Electrical Engineering for his constant technical suggestions, encouragement, support, and cooperation.

I would like to express my sincere gratitude to **Dr. D. M. Vinod Kumar (HAG)**, Professor (Rtd)), Department of Electrical Engineering, for his constant encouragement, support, and cooperation.

I thank all my DSC Committee members, **Dr. A. V. Giridhar**, Associate Professor, Department of Electrical Engineering, **Dr. A. Kirubakaran**, Associate Professor, Department of Electrical Engineering and **Dr. Debashis Dutta**, Professor, Department of Mathematics, for their detailed technical review, constructive suggestions and excellent advice during the progress of this research work.

I am very much thankful to **Dr. Srikanth N V**, Professor, Head, Department of Electrical Engineering for his constant encouragement, support and cooperation.

I am very much thankful to Dr. **M. Raja Vishwanathan**, Associate Professor in Department of Humanities & Social Science for his continuous support and encouragement.

I wish to express my sincere thanks to **Prof. Bidyadhar Subudhi**, Director, NIT Warangal for his official support and encouragement.

I also appreciate the encouragement from teaching, non-teaching members, and the Department of Electrical Engineering fraternity of NIT Warangal. They have always been

encouraging and supportive.

Finally, I would like to express profound gratitude to my family members for all they have undergone to bring me up to this stage. I wish to express gratitude to my parents, **Sh. Jyothi Prakash** and **Smt. Venkata Laxmi**, for their kind support, the confidence and the love they have shown to me. You are my greatest strength, and I am blessed to be your son. I want to thank my wife, **Swathi** for her continuous support and belief in me. Thanking you is a small thing for the precious thing you have given me, our child **Chi. Shivansh**. You have supported and motivated me and believed in me for who I am. I also would like to thank my elder sister and brother in law, **Smt. Veena Adulapuram** and **Sh. Ravikanth Adulapuram**, younger sister and brother in law **Smt. Vani Thipparthi** and **Sh. Ranjith kumar Thiparthi** for being such good friends and reaching out to me when i needed someone to empathise and keep me going.

Vutla Vijay

ABSTRACT

Growing oil prices, rapid depletion of fossil fuels, and emission of Green House Gases have compelled a shift from conventional combustion engine to Electric Vehicle (EV). It is anticipated that the share of EV is going to rise within a short time. However, driving range and charging time are issues that limit the share of EV. Providing proper charging infrastructure along the road side of urban roads and utilization of advanced technology in charging could tackle the above mentioned issues.

There are many charging methods available for EVs, and one of them is DC Rapid Charging, which can quickly charge an EV battery. The performance of the distribution system is impacted by increased power loss and voltage deviation caused by additional load brought on by EVs. Furthermore, positioning charging stations haphazardly throughout a power distribution network does great harm. In addition, planning of charging station considering only distribution networks is not a reliable approach. Moreover, the location of the charging station should offer convenience to the EV user in a given EV driving range and benefits the charging station owner. All of the aforementioned issues were the rationale for the thesis, which aims to plan charging stations in a coupled network involving power distribution network and road transportation network.

Initially, a multi-objective approach for optimal planning of Rapid Charging Stations (RCSs) and distributed generators (DGs) was proposed. The method suggested aims to achieve reduced active power loss, EV user costs, and voltage deviation for effective RCSs and DGs planning. IEEE 33 bus power distribution network superimposed with a 25-node road transportation network was considered as the test system. Rao 3 algorithm was applied for optimization, and the results were compared with PSO and JAYA algorithms.

The number of charging connectors at charging station not only impacts the station installation cost but also waiting time. Hence, determination of optimal number of connectors is necessary in optimal planning. Therefore, a two-stage optimal planning is proposed in this thesis to address the issues stated above. In the first stage, simultaneous optimal planning of RCSs and distributed generators is done to minimize active power loss, voltage deviation, EV user cost and to maximize voltage stability index. In the second stage, an optimal number of connectors was decided to minimize the installation cost and waiting time in queue at RCS. Here, $M1/M2/C$ queuing model was considered to determine the waiting time.

In addition, integration of D-STATCOMs was done along with charging station and DGs to improve the performance of distribution system through a two stage approach. In Stage 1, RCSs, DGs, and D-STATCOMs were planned optimally by improving voltage stability index, active power loss, voltage deviation, and EV user cost. RCS connectors count was identified in Stage 2 by reducing building cost and waiting time.

Further, network reconfiguration was employed along with optimal planning of RCSs, DGs, and D-STATCOMs to improve the performance of the distribution system. Minimization of active power loss, voltage deviation, EV user cost, waiting time, installation cost, and improvement of voltage stability index were considered in optimal planning.

The proposed approach was tested using an IEEE 33 bus RDN coupled with transportation network. Daily load variation at buses and hourly charging probability of EVs were used in the analysis. The optimization problem was solved using the novel Multi-Objective Rao 3 Algorithm (MORA), and the solutions validated using NSGA-II. The results demonstrate the effectiveness of the suggested strategy by MORA in determining optimal sizes and locations to benefit EV users, charging station owners, and distribution network operators.

Contents

List of Symbols

λ	Arrival rate of EVs at charging station
μ	Service rate of connector at charging station
ρ	Utilization rate of connector at charging station
C_{con}	Connector cost of charging station ($)
$CS^i_{connector}$	Connectors at i^{th} CS
$CS^i_{capacity}$	Capacity of i^{th} CS
C_{init}	Initial investment cost of charging station ($)
C_{land}	Land cost of charging station ($)
CS^i_{load}	EV load at i^{th} CS
C^{max}	Upper limit of connectors at charging station
C^{min}	Lower limit of connectors at charging station
D_n	Distribution network node number
$d_{z_n - c_m}$	Distance between n^{th} zone to m^{th} charging station
$EV^{max}_{usercost}$	Maximum EV user cost
i_b	Current through the b^{th} branch of distribution network (A)
l_{DG}	Location of DG
l_{DST}	Location of D-STATCOM
l_{RCS}	Location of RCS
N^{iCS}_{ev}	Number of EVs charging at i^{th} CS
P_b	EV battery capacity (kWh)
P_c	Connector rating (kW)
P_D	Active power Demand
P_{dg}	Real power output of DG
P_e	Electricity cost ($/kWh)
$P_{effectiveload}$	Effective real power load
P_{load}	Base real power load
P_{loss}	Active power loss
P^{min}_{dg}	Lower bound of real power output of DG
P^{max}_{dg}	Upper bound of real power output of DG
$P^{T,max}_{DG}$	Real power contribution of all DGs
$P^{fcs/dg}_{loss}$	Active power loss after including fast charging station/DGs
P_{sub}	Substation real power output
Pevc	Probability of EVs getting charged at charging station
pf_{DG}	DG operating power factor

pf_{EV}	EV charging station operating power factor
$P_r(k)$	Real power demand at receiving end of k^{th} line of distribution network (kW)
Q_D	Reactive power Demand
Q_{DST}	Reactive power of D-STATCOMs
Q_{dg}	Reactive power output of DG
$Q_{effectiveload}$	Effective reactive power load
Q_{load}	Base reactive power load
Q_{loss}	Reactive power loss
$Q_r(k)$	Reactive power demand at receiving end of k^{th} line of distribution network (kVAr)
Q_{sub}	Substation reactive power output
R_b	Resistance of b^{th} branch of distribution network (Ω)
R_n	n^{th} node of road network
S_{DG}	Size of DG (kW)
S_{DST}	Size of D-STATCOM (kVAr)
T_n	Road network node number
V_{min}	Lower bound of bus voltage
V_{max}	Upper bound of bus voltage
VD_{max}	Maximum value of Voltage Deviation
$V_r(k)$	Voltage at receiving end of k^{th} line of distribution network (V)
$V_s(k)$	Voltage at sending end of k^{th} line of distribution network (V)
VSI^{min}	Minimum value of Voltage stability index
W_T	Total waiting time in min
x_{z_n}	X coordinate of n^{th} zone
x_{c_m}	X coordinate of m^{th} charging station
y_{z_n}	Y coordinate of n^{th} zone
y_{c_m}	Y coordinate of m^{th} charging station
ABC	Artificial Bee colony
APLRI	Active power loss reduction index
BEV	Battery Electric Vehicle
CO_2	Corbon dioxide
CS	Charging Station
DG	Distributed Generator
DR	Demand Response

DS	Distribution System
D-STATCOM	Distribution Static Compensator
EC	Specific energy consumption of EV (kWh/km)
EV	Electric Vehicle
EVCS	Electric Vehicle Charging Station
EVRCS	Electric Vehicle Rapid Charging Station
EVUC	EV user cost ($)
EVUCI	EV user cost index
FCEV	Fuel Cell Electric Vehicle
FCS	Fast Charging Station
G-V	Grid to Vehicle
GWO	Grey Wolf Optimizer
HA	Heuristic Algorithm
HEV	Hybrid Electric Vehicle
ICE	Internal Combustion Engine
ICRCS	Installation cost of RCS
MHA	Meta Heuristic Algorithm
MOF	Multi objective function
MORA	Multi Objective Rao Algorithm
MVD	Maximum voltage deviation
MVDRI	Maximum voltage deviation reduction index
NRT	Network Reconfiguration Technique
NSGA II	Non dominated Sorting Genetic Algorithm II
pf	Power factor
PHEV	Plug in Hybrid Electric Vehicle
Ploss	Active power loss (kW)
PSO	Particle Swarm Optimization
PV	Photo Voltaic
RCS	Rapid Charging Stations
RDN	Radial Distribution Network
RDS	Radial distribution system
SC	Shunt Capacitor
SS	Substation
TLBO	Teaching-Learning-Based Optimization

TPL Total power loss of the distribution network including EV load

V-G Vehicle to Grid

VSI Voltage stability index

List of Figures

List of Tables

Chapter 1
Introduction

The effects of global warming and other issues brought on by carelessness have recently been recognized as harmful to the planet by the global community. The primary cause of global warming is the emission of carbon dioxide (CO_2) and other pollutants by internal combustion engines (ICE), which are regarded as one of the most significant elements in the transportation sector for causing such issues [6]. The depletion of fossil fuels is another issue posing a challenge to transportation system [7]. Rising oil prices, greenhouse gas emissions, and increased public awareness of environmental damage are encouraging individuals to consider other options to favor green transportation. The transport industry in India is the primary source of the country's greenhouse gas emissions [8]. In this context, electrification of the road transportation system by Electric Vehicles is a potential solution to reduce the damage caused by environmental pollution. The deployment of 20 million Electric Vehicles (EVs) globally is a promising beginning to reduce greenhouse gas emissions by 2020. Such a global deployment of EVs will replace 62 % of fleet vehicles by 2050.

1.1 Electric Vehicles

EVs have gained attention in the transportation industry as they offer low noise and emissions. Advancements in battery technology, the evolution of electric vehicle industry, and other factors are escalating the population of EVs on the roads. Also, globalization has witnessed a reduction in 1 kWh battery price from 1000 $ in 2007 to 200 $ in 2020, which favors EV sales. There are four types of EVs: Battery Electric Vehicle (BEV), Hybrid Electric Vehicles (HEV), Plug in Hybrid Electric Vehicles (PHEV), and Fuel Cell Electric Vehicles (FCEV) [9].

1. BEVs are electric vehicles driven by the energy stored in the battery, where the energy required to charge the EV is taken from the grid. In BEVs the inverter converts the available DC power to AC power, and the control module sends a signal according to the acceleration and deceleration [10]. TATA tigor, TATA Nexon, and Mahindra E20 plus are a few examples.

2. HEVs consist of both an engine and a motor. The engine uses conventional fuel, and the motor is powered by a battery. The energy captured during the braking is

utilized to charge the battery [11]. In HEV, the transmission is supported by both an electric motor and an engine at the same time. Volvo XC90 and Toyota Prius are a few examples.

3. PHEV consists of both an engine and an electric motor. Here, the battery is charged by both regenerative braking and an external source [12]. It starts and runs with battery energy, and once the battery drains, transmission is supported by an engine. Porsche Cayenne S E-Hybrid, and BMW 330e are a few examples.

4. FCEV utilizes fuel cell technology to drive the EV. Here, chemical reactions in the fuel cell generate the required energy to run the FCEV [13]. These are also called zero-emission EVs. Riversimple Rasa, Honda Clarity Fuel Cell, and Hyundai Nexo are a few examples.

1.2 Charging methodology for EVs

The installation of proper charging infrastructure is necessary to charge the batteries of EVs. There are three main types of charging: 1. Conductive charging, 2. Inductive charging, 3. Battery swapping

1. Conductive charging includes direct contact between the charging inlet and EV connector. This methodology has the benefits of economic viability, quick charging, and efficient operation. It is categorized into onboard charging systems and off-board charging systems. In an onboard charging system, a power electronic converter is in the EV, which converts the external AC to DC to charge the EV battery. It charges the battery at a slower rate. In off-board charging, the converter is at the charging station that enables fast charging [14].

2. Inductive charging uses two-coil technology, where the charging coil is installed in the EV and another coil is installed at the charging lots and roads. Contactless charging, lower accident risk, and more convenience are a few advantages, whereas eddy current loss would be an issue in inductive charging [15].

3. Battery swapping is a method of battery exchange in which an EV owner can swap his battery with one that has been completely charged. Every swap only takes a few minutes, so it is a rapid operation. The distribution system can profit from the V-G strategy by using battery swapping stations (BSS). However, the investment

cost is very high, as stations have to have various sizes and types of batteries. The EV user also has to pay the utilization fee to station owner [16].

1.2.1 Types of Electric Vehicle Charging modes

By putting up Electric Vehicle Charging Stations (EVCS) in strategic areas throughout the distribution network, green transportation can be promoted. The distribution system must be examined by including EVCS before installing it at a particular location. However, adding EVCS to the distribution system will use more power, which will influence the bus voltage and thermal stability of the branches [17]. Generally, three modes of charging are available at charging stations. Each has a different rate of charging, various voltage levels, and various applications. They are listed below.

1. Level 1 mode uses a 120V AC supply to charge an EV. It has the capability to supply a maximum current capacity of 16 A. These are mostly installed in residential places and other places where 120 V outlets are available. In this mode, AC is converted to DC using the vehicle's onboard charger [18]. The maximum power output of this station is 1.9 kW, and it takes 8–16 hours to charge a battery. The presence of this station has the least impact on the distribution system. The estimated installation cost is around 500 $ to 800 $. It is the least expensive charging method, but it takes more time to charge [19].

2. Level 2 stations can be placed in both residential and commercial places. These are the most commonly installed charging stations [20]. These charging stations operate on a 240 V AC source and have a maximum current capacity of 40 A for domestic use. These charging stations operate on a three-phase 400 V AC supply and support 80 A of current for commercial purposes. These charging stations take 4–10 hours to charge an EV. The maximum charging power is around 12 kW. The estimated installation cost is around 2150 $ to 2300 $ per unit [21].

3. Level 3 charging stations take 20 to 30 minutes to charge an EV battery up to 80 %, so these are called rapid charging stations. These are installed in public places, mostly along the roadside. These are supplied from 400 V to 600 V AC and have a current capacity of 200 A [22]. It has a maximum power outlet of 36–240 kW. These are bulk loads; hence, locating them at random locations in the distribution system hinders performance. The estimated installation cost is around 50000 $ to 150000 $ [23].

1.3 Literature Review

The transportation industry uses a lot of fossil fuels, which results in 37 % of total greenhouse gas (GHG) emissions across all sectors. The introduction of EVs into road transportation can reduce GHG emissions [24]. EVs have two modes of operation: one is the G-V mode, which deals with charging EVs from the grid and acts as a load on the distribution system. The second is V-G mode, where EVs can inject power into the grid, i.e., act as spinning reserves, and can be utilized to improve resilience, reliability, and performance of distribution systems [25] [26].

Although EVs have several advantages, they also have the drawbacks of low driving range and high charging time, and these are the major reasons for the slow expansion of EVs [27]. Adoption of advanced charging technologies and the installation of proper charging infrastructure are potential solutions to above-mentioned issues. There are three charging methodologies: level 1 and level 2 take a few hours for charging, while level 3 (DC rapid charging) takes 15-20 minutes [28]. Therefore, level 3 charging methodology is used at Rapid charging stations (RCSs). The deployment of RCS can encourage customers to switch to EV-based transportation over combustion engines. However, the load caused by the charging station (CS) acts as a bulk load on the distribution system, whether it is deployed at home or in public areas. The distribution system's ability to operate normally is altered by extra CS load. Further, peak-hour EV charging can put greater strain on the grid. Because they are mobile in nature and their power usage is dependent on how far they go each day, electric cars are regarded as highly dynamic loads. The unpredictable fluctuation of CS load causes violations of voltage limitations. This has an impact on the power network's stability [29] [30].

Voltage deviation at the lowest possible value and the voltage stability index at the highest possible value are always anticipated for a healthy power system. The load due to CS cause extra power flows across the power network, resulting in increased power loss, voltage deviations, and component overloading. Converters are typically used to convert AC power into DC power while charging an EV battery. This conversion may introduce harmonics into the power network. This affects the life of transformers and other components in power networks [31]. Further, the placement of CS at improper locations can increase the harmful impact on the distribution system that alters the healthy operating conditions of the power system [32].

It is observed from an extensive literature survey that the following two major categories

of optimal planning of charging stations exist:

1. Electric Vehicle charging stations in the Power network
2. Electric vehicle charging stations in a coupled power distribution network and road transportation network.

1.3.1 Optimal planning of EVCS in power distribution network

The EVCS hurts the distribution system. In the literature, most of the authors concentrated on the minimization of power loss and voltage deviation as objectives to support distribution systems in the presence of charging stations. EVCS integration into the distribution system changes operational parameters. Further, placing EVCS at inappropriate locations escalates the damage [33]. Installing charging stations in a distribution network could change the operation of the power network, driving behaviour of EV users, traffic flow, increase power loss, and voltage variations [34]. It is not advisable to install charging stations at random locations because it may lead to performance degradation of the radial distribution network and burden the EV user. Hence, there is a need to find optimal locations for charging stations [35].

The design and feasibility analysis of a charging station was done in [36] by considering different configurations and techno-economic performance. Integration of EVCS has a significant influence on system losses, supply-demand imbalance, and harmonic injection in the Distribution System (DS) [37]. The authors in [38] considered minimizing power loss, reducing average voltage deviation, and improving voltage stability index for optimal planning of charging stations in a radial distribution network using Teaching learning-based optimization algorithm for solving optimization problems. In [39], the researchers considered the unstable nature of the distribution network with the uncertainty of loads while planning charging stations using a fuzzy-based differential evolution algorithm for solving the optimization problem. In [40], the installation of level 1, level 2, and level 3 connectors was done at the charging station by considering power loss, installation cost, and transformer loading, where the uncertainty of the EV load was modelled using stochastic process. The authors in [41] presented a CS planning approach that considers reliability while minimizing investment, maintenance, and operational costs. Similarly, in [42], the concept of an incentive-based demand response program was used in optimal planning, where minimization of investment cost, connection cost, total cost of losses, and demand response (DR) cost were considered as

objectives for placing CS optimally. In [43], the authors proposed a two-stage strategy to plan fast charging stations. Stage 1 involves the evaluation of the system with existing resources to supply the EV demand, while Stage 2 matches the extra EV load with the installed fast charging station capacity.

Though the charging station is located in proper places, high loading on DS causes an increase in power loss and voltage deviation. Integrating the DGs into the DS could improve DS performance [44, 45]. In [46], the authors analysed the DS with the inclusion of EV charging during peak power and off-peak power EV loading by employing butterfly optimization algorithm to install DGs at optimal locations for improving the performance of the DS. In [47], optimal placement of charging stations and solar power DGs was done by considering the charging station investor decision index, land cost index, and electric vehicle population index. In [48], the authors used a hybrid meta-heuristic algorithm to identify CS locations with randomly distributed PVs in DS by considering the minimization of power loss, voltage deviation, and voltage stability index (VSI). In [49], the authors used demand side management approach for coordination of DGs, Battery Energy Storage, and Photo Voltaic source in the presence of EVs. In [50], the authors used the Arithmetic Optimization Algorithm for optimal planning of charging stations and DGs. In [51], the authors proposed a framework for optimal allocation of renewable based DGs, battery energy storage systems, and EV charging stations to improve the performance of the distribution system. In [52], the authors proposed improved bald eagle search algorithm to optimally allocate fast charging stations and PV-DGs in the distribution system. In this paper, reliability analysis was carried out after the placement of FCS and PV-DGs to analyse the impact of FCS and PV-DGs on the distribution system. Integration of RCS puts stress on RDN and to reduce it, renewable type DGs were installed and energy management scheme was utilised in [53].

Integrating both DGs and reactive power compensating devices in the distribution system could improve the performance reduction caused by the inclusion of RCSs [54]. In [55], the authors proposed a new hybrid technique of grey wolf optimizer and particle swarm optimization for optimal placement of charging station and shunt capacitors. In [56], the authors proposed a novel hybrid optimization approach to plan charging station, DGs, and D-STATCOM optimally by considering the reconfiguration of distribution network. In [57], the authors recommended a strategy for optimal placement of distribution generators and shunt compensator's in distribution system by Adaptive African Vulture Optimization Algorithm by considering minimization of power loss, voltage deviation, and maximization of loading margin. In [58], the authors proposed

a two-stage approach for optimal planning of distributed generators (DGs), shunt capacitors (SCs), and charging stations with grass-hopper optimization based fuzzy multi-objective technique. The optimal planning of DGs and SCs was done in the first stage and the planning of CS was done in the second stage. As RCS load increases on RDN, it could also impact the substation power factor, and to improve power factor, DGs and Shunt capacitors were installed along with charging station in [59].

Further, EV customers always try to take advantage of getting to charging stations early and spending less time in queue to charge their EVs [60]. In [61], the authors used M1/M2/N queue model for modelling EV charging demand, and used optimal planning of CS, BESS, and Photo Voltaic DGs. In [62], the authors used hybrid algorithm in bi-level optimization of CS. Optimal location and capacity of CS were determined by considering minimization of total cost and service tardiness in upper level. Lower level dealt with the allocation of users to each station.

Load growth on power sector is in exponential form these days. As the load is increasing, there is a need to expand the power network, but it results in higher cost and more power loss. In this context, Network Reconfiguration Technique (NRT) is an attractive choice, as it uses existing resources in an optimal way by offering better performance to RDN. In [63], simultaneous optimal planning of charging station and DGs along with NRT was done by considering power loss, voltage deviation, and energy not supplied as objectives using hybrid algorithm comprising ant colony optimization and artificial bee colony optimization. Reactive power regulation was employed in the presence of EVs along with changing topology in [64], where power loss and voltage deviation were considered as objectives. In [65], the authors considered the minimization of initial investment cost and energy loss while planning fast charging stations and network reconfiguration, where a cooperative co-evolutionary genetic algorithm was used for solving the optimization problem.

1.3.2 Optimal planning of EV charging stations in coupled Power distribution and Road transportation network

Generally, both power network and road transportation network are interconnected. The increasing number of EVs on the roads could bring issues of over loading of distribution network. Planning the setting up of charging stations keeping in mind road network ensures a superior site. In planning for CS, very few authors have considered the transportation network.

In [66], the authors considered coupled network in optimal planning of fast charging stations by considering land cost, installation cost, and trip cost. In [67], the authors considered EV energy loss, station development cost, electric gird loss along with location of electric substations on urban roads for optimal sizing and locating fast-charging stations. To plan a CS near an existing CS, the authors in [68] suggested a two-level method by minimizing power loss, voltage deviation and CS installation cost as objectives. In [69], the authors applied Enhanced Heuristic Descent Gradient (EHDG) and Voronoi diagram to optimally plan charging stations by considering route distributions, consumption profile, and operating cost. The author of [70], proposed a method for positioning and sizing the fast charging station (FCS). In addition to reducing power loss and waiting times, FCS positioning was done as efficiently as possible to compensate for reactive power.

In [71], a hybrid algorithm based on genetic algorithm and conventional particle swarm optimization was used to determine optimal planning of fast charging station, where the authors factored power quality parameters of electrical network and investment cost as objectives. In [72], the authors proposed a two stage approach for optimal placement of charging stations. In Stage 1 minimization of land cost and maximization of EV flow were considered, while power loss has been minimized in Stage 2. In [73], the authors developed charging infrastructure for EVs by formulating profit maximizing mixed integer linear programming problem. The planning comprised the identification of EV fleet size, charging station location and size. EVs fuelled from coal fired energy could create more challenges; to address this, fast charging station planning on coupled network was done keeping in mind human health in [74].

In [75–78], the authors formulated a multi objective problem for optimal planning of charging stations. In [75], optimal planning was done with the goals of reducing voltage variation and power loss, maximization of EV flow supplied by fast charging station while confirming the impact of service radius and waiting time on planning. In [76], the authors applied meta-heuristic algorithms to solve problems pertaining to energy loss, voltage deviation, and minimize the land cost to support maximum EVs with low establishment cost. Minimization of VRP (Voltage deviation, Reliability, and Power loss) index, installation and operation cost, and improving accessibility index was considered for optimal planning of charging stations in [77]. In [78], the authors used NSGA II algorithm for simultaneous placing and sizing of FCS, where investment cost, energy losses, waiting time, and traffic flow were considered in planning.

The authors of [79, 80] considered the DG integration in the distribution system to reduce the harmful impact of RCS. In [79], a method for CS and wind based DG planning was proposed while minimizing power loss, voltage deviation, and EV user cost. In addition to operational parameters of distribution system and EV user behaviour, installation cost was considered in optimal planning of fast charging stations and DGs in [80]. In [81], the authors proposed coupled planning for EV parking lots placement and Distribution Network (DN) reinforcement. Initially, the number of EVs at parking lots were calculated by considering EV parking lot profit, DN cost, and EV charging cost.

Queuing theory is rarely used by authors in the domain of electric vehicles. Some authors employed queue theory to set up RCS in the best possible way while taking waiting time into account. By using a queuing analysis, the authors of [82] modelled the load of plug-in electric vehicles. In [83], the authors suggested a method to determine locations and capacity of charging stations optimally along with the multi stage expansion of distribution network considering waiting time. In [84], the best site for charging stations (CS) was determined by minimizing power loss and EV energy loss incurred during the trip to CS, where queue theory was employed to capture the dynamic behavior of CS serviceability. The authors in [85], suggested a queue theory-based CS planning by minimizing power loss, EV User Cost, installation costs, and maximizing VSI for the coupled network. In [86], the waiting time at CS was minimized together with power loss, voltage deviation, and accessibility index.

In the above literature, many authors installed only charging station. However, the load due to CS deteriorates the healthy operation of distribution system. In this context, the inclusion of DGs and providing reactive power support could improve the performance of the distribution system. Moreover, the planning that considers only distribution system may not provide comfort to EV user and CS owner. This thesis factors in the above issues to favour everyone: CS owner, EV user, and Distribution Network Operator.

1.4 Solving methods for charging station placement problem

Modern problems frequently involve the examination of massive data sets and are extremely complex. Assuming that the best solution is typically unknown, this issue can be quite difficult and require solid mathematical analysis. Many real-world problems can be formulated as optimisation problems. Optimisation problem often have goal to

minimise or maximise an objective function to assess the quality of the generated solution [87].

Optimization algorithms can be classified into two major groups, exact and approximate algorithms. Exact algorithms provide an exact answer to the problem, while approximate algorithms may or may not provide exact solutions i.e they provide approximate solutions. Approximate algorithms can further be classified into two groups; heuristic and meta-heuristic algorithms.

1.4.1 Exact algorithms

The optimization technique that can ensure the all optimal solutions is known as exact optimization, where, the optimality of the yielded solution can be verified mathematically, and so it is also called mathematical optimization. However, this technique is not feasible for larger size problems, because the effort and time for solving grows as the dimension of the problem grows. Linear programming, mixed integer programming, and constraint programming are often employed exact algorithms.

1.4.2 Approximate algorithms

Approximate algorithms uses NP (nondeterministic problem) approach to find a solution for the optimization problem. The optimal solution is not always ensured by this method. In an acceptable period of time, which is at most polynomial time, an approximation method aims to get as close to the optimal value as possible.

1.4.2.1 Heuristic algorithms

Heuristic Algorithms (HA) are used for solving mathematical optimization problems when exact algorithms fail to find an optimal solution or take a lot of time. The solutions yielded from HA may not be optimal but are generated in less time. These algorithms are problem-dependent. Hill climbing, best first search, etc. are a few examples of HA.

1.4.2.2 Meta heuristic algorithms

Meta-heuristic Algorithms (MHA) have been developed to find the near optimal solution of complex and high dimensional problems [88]. These are not problem specific i.e any MHA can be applied to all problems. These involves the initialization of solution by

random approach. Random initialization helps in avoiding the trapping of solution in local optima [89].

Exploration and Exploitation are the main components of MHA [90]. Exploration finds a new solution in a search space, while exploitation focuses on searching for the best solution in a local region. A good combination of both exploration and exploitation of MHA makes the search process reach global optima. Primarily, MHAs can be classified as population-based and trajectory-based. Population-based MHAs use a set of solutions and information exchange among them to reach a global optimal solution. Genetic algorithm, particle swarm optimization algorithm, and Ant colony optimization algorithm are some examples. Trajectory based algorithms follows modification of single solution to reach global solution. Simulated annealing, Tabu search algorithm, etc are the few examples [91].

Few MHA algorithms that are nature inspired use evolution and intelligent behaviour of swarms of birds, fish, ants, and other living beings in the optimization process. Genetic algorithm was proposed by Jhon Holland in 1992 [92], it works on the principle of "survival of the fittest". It involves stages of selection, crossover, and mutation in achieving the optimal solution. Particle Swarm Optimization algorithm was proposed by Eberhart and Kannedy et.al [1] in 1995 based on the flocking behaviour of birds. The convergence rate of PSO depends on its control parameters like acceleration coefficients and inertia weight. Another algorithm that works on the behaviour of fireflies movement towards the light is firefly algorithm; it was proposed by Yang et al. in 2010 [93]. The intelligent behaviour of honey bees in searching for food was used to develop Artificial Bee Colony optimization algorithm, which was proposed by Karaboga in 2005 [94]. Generally, ants communicate using pheromone in travelling and find shortest paths while searching for food; this behaviour inspired the Ant colony optimization (ACO) algorithm [95]. However, the above mentioned algorithms are parameter dependent and the accuracy of solution depends on fine tuning of parameters. Rao et al. proposed Teaching and Learning Based Optimization algorithm (TLBO) in 2012 [96]. The influence of teacher on students and communication among students to achieve the goals is the principle involved in TLBO algorithm, where no algorithm specific parameters are required. Rao et al. also proposed Jaya and Rao algorithms, where the ability of candidate solution to move towards best solution and away from the worst solution along with the random interactions among candidate solutions is implemented [2] [97].

Placement problem is complex and nonlinear in nature, while planning on large systems

needs an efficient solution method. In the literature, researchers used various solving methods i.e classical methods and intelligence methods. The ability of exploration, exploitation, and high dimensionality in meta-heuristic algorithms ensures the success in handling complex problems. In the literature, researchers applied various algorithms to solve the complex placement problem. According to "No free lunch theorem" [98] for optimization, there is no guarantee that every optimization technique can solve every optimization issue. In [99], the authors described various nature inspired algorithms used in charging station planning.

In some cases there is a need to consider more than one objective in optimal planning. These can be handled by multi objective approaches [100], [101]. In [4], researchers proposed NSGA-II algorithm for handling multi objective optimization problems that involve the selection, crossover, and mutation to generate off-springs where ideal solutions are chosen through crowding distance and non dominating sorting approach. In [5], the authors proposed multi objective Rao algorithm for constrained and unconstrained problems. The ranking of solutions in optimal front can be done through non dominated sorting and crowding distance.

In conclusion, meta-heuristic algorithms are well suited for optimisation of EVCS planning since the problem formulation necessitates extensive numerical computation, a precise solution that takes into account a wide range of dimensions, and numerous constraints that limit the viability of the solutions.

1.4.3 Research gaps identified

The location and size of EVCS impacts the operation of distribution system and EV user driving behaviour. Based on the limitations that exist in the literature, the following research gaps were identified.

1. Optimal planning of charging station, DGs, and D-STATCOM have not been done by considering coupled network.
2. Optimal number of charging connectors have not been considered.
3. Parameter independent algorithms have not been used for optimization of charging station placement problems.
4. Waiting time at charging stations has not been considered in the optimal planning of charging stations.

1.5 Motivation

Green House Gas (GHG) emission and environment pollution are major issues now a days. Road transportation by conventional combustion engine is the main cause for the emission of GHG. According to US economic sector, around 28% of share GHG was discharged by road transportation from burning fossil fuels for cars, two Wheelers, trucks, and planes. Growing oil prices and environmental degradation due to fossil fuels have led to the search for alternatives for fossil fuels and renewable energy sources.

Transforming the existing road transportation to green transportation by adopting the Electric Vehicle (EV) is a potential solution for reducing GHG emission. The number of EVs is increasing in many countries like China, Europe, and the US. Government initiatives and policies of EVs are supporting EV sales. EV sales tripled in India in 2022 compared to 2021. However, low driving range and high waiting times are limiting the adoption of EVs.

Installation of proper charging infrastructure and adopting new charging technologies can counter the above mentioned issues. Integration of charging stations along the roadside supports EV user. However, the integration of charging station reduces the performance of distribution system through power losses and deteriorating voltage profile. Locating charging stations at random locations can further increase damage to the distribution system. So charging stations have to be placed at optimal locations which do not alter the healthy operation of DS. Further, the optimal planning of charging station should consider EV user behaviour. The EV user always expects charging station to be near, so the energy losses when travelling towards charging station would reduce.

In the literature, most of the authors have used parameter dependent meta-heuristic algorithms in optimal planning. Fine tuning of parameters is necessary for getting accurate and efficient solutions. As the placement problem is complex and computationally burdensome, there is a need to employ novel algorithms which have no algorithm specific parameters in optimal planning. Formulation of single objective function does not always yields feasible solution; hence, the formation of multi-objective problems has to be considered in optimal planning.

Location of EVCS has a significant impact on promoting EVs, since it influences customers' purchasing decisions. Also, the location and size of EVCS effects the operation of distribution system and EV user driving behaviour. As per the limitations that exist in the literature, the motivation of this research is..

1. To plan EVCS using a combination of both Power distribution network and Road transportation network.
2. To explore the reduction of installation cost of EVCS and enhance the comfort of EV user.
3. To ensure the performance of distribution system (power loss, voltage deviation, and voltage stability index).
4. To consider the EV user perspective on installation of EVCS.

1.6 Contributions

The thesis aims to examine various perspectives on issues with respect to planning for charging stations, formulation of complex placement problem, and finding solutions using meta-heuristic algorithms. The planning of Rapid Charging Stations (RCSs) considered in this thesis is shown in Figure 1.1.

The outcomes of the research described in this thesis are highlighted as follows:

1. Optimal planning of Rapid Charging Stations (RCSs) and Distributed Generators (DGs) in a coupled power distribution network and road transportation network.
2. Two-stage optimal planning of RCSs and DGs along with the identification of optimal number of connectors at the RCSs in a coupled network.
3. Improving the performance of distribution system through simultaneous integration of RCSs, DGs, and D-STATCOM in a coupled network.
4. Improving the performance of distribution system through the simultaneous integration of RCSs, DGs, and D-STATCOM in a coupled network, considering network reconfiguration technique.

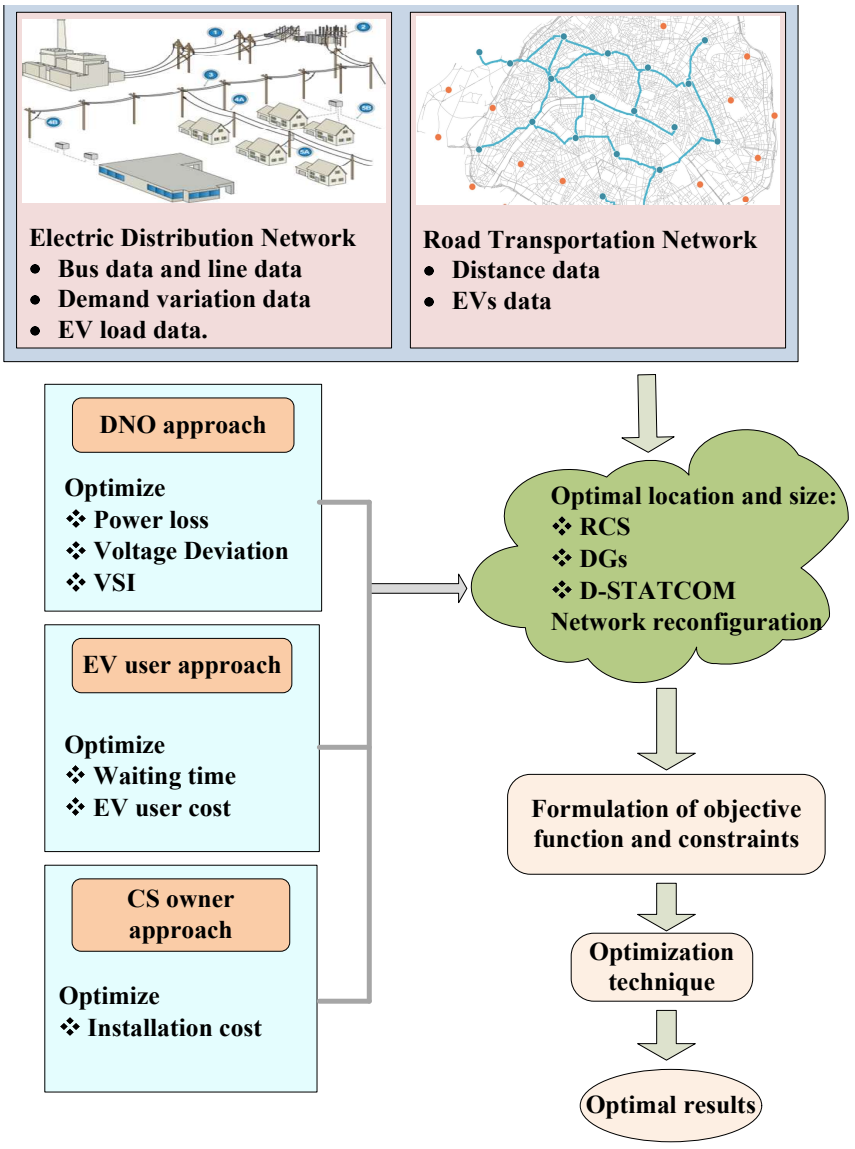

Figure 1.1: Optimal planning of Rapid charging stations in coupled network

The following subsections elaborates the aforementioned research objectives.

1.6.1 Optimal planning of Rapid Charging Stations (RCSs) and Distributed Generators (DGs) in a coupled network

The integration of RCS deteriorates the operational parameters of distribution system. The positioning of RCS should consider EV user convenience and cause less harm to the distribution system. To meet this, the first objective is the simultaneous optimal planning of RCS and DGs in coupled Power distribution network and Road transportation

network. Optimal planning includes the reduction of active power loss, voltage deviation, and EV user cost. Complex placement problem is formulated as a weighted sum multi-objective problem. Novel metaphor-less Rao 3 algorithm was used to solve the optimization problem. The suggested planning was validated on the coupled network of IEEE 33 bus radial distribution network and 25 node transportation network.

1.6.2 Queue theory based optimal planning of RCSs and DGs and identification of optimal connectors in a coupled network

In this thesis, unlike traditional approaches, the number of connectors at RCSs is determined by considering waiting time as an objective. A two stage optimal planning of RCSs and DGs is proposed in a coupled network of Power distribution network and Road transportation network. In Stage 1, reduction of active power loss, voltage deviation, EV user cost and improvement of voltage stability index was taken into consideration. Optimal count of connectors was determined by considering the conflicting objectives of waiting time and installation cost of RCSs in Stage 2. Novel pareto dominance based multi-objective Rao 3 algorithm was used for solving the complex placement problem.

1.6.3 Optimal planning of RCSs, DGs, and D-STATCOMs in a coupled network

The integration of charging station in distribution system increases power loss and voltage deviation. The performance of distribution system is enhanced by the installation of D-STATCOMs along with RCSs and DGs at appropriate locations in a coupled network. A two-stage multi-objective optimization approach is proposed for identifying optimal locations, capacities, and connector count. Reduction of active power loss, voltage deviation, EV user cost and improvement of VSI were considered in Stage 1. Optimal connector count was determined by the minimization of waiting time and RCS's installation cost was considered in Stage 2. Novel metaphor less multi objective Rao 3 algorithm was used for solving the optimization problem and the results were validated using NSGA II.

1.6.4 Network reconfiguration and optimal planning of RCSs, DGs, and D-STATCOMs in a coupled network

Network reconfiguration can enhance the performance of the distribution system. In this context, the system is analysed by employing network reconfiguration technique with prior deployment of RCSs, DGs, and D-STATCOMs. Further, simultaneous network reconfiguration and optimal planning of RCSs, DGs, and D-STATCOM was done in two stages. In Stage 1, optimal locations of RCSs, optimal locations and capacities of DGs and D-STATCOMs were identified by considering minimization of active power loss, voltage deviation, EV user cost, and maximization of voltage stability index. In Stage 2, waiting time and RCSs installation cost were considered to determine the optimal number of connectors at each RCS. The effect of future EV load growth was analysed for the new optimal network. Multi objective Rao 3 algorithm was adopted for solving the optimization problem, and the results were verified by NSGA II.

1.7 Organization of thesis

The thesis has been organized into six chapters.

Chapter 1 provides information regarding the Electric Vehicle, various charging methods, and various levels of charging stations. It also details research done in the field of charging station placement problem and the rationale for research work.

Chapter 2 deals with simultaneous planning of RCSs and DGs in a coupled network of IEEE 33 bus electrical distribution system and 25 node road transportation network.

Chapter 3 discusses two stage multi-objective approach for planning RCSs and DGs along with the identification of optimal number of connectors at RCSs using multi-objective Rao 3 algorithm in a coupled network.

Chapter 4 presents optimal planning of RCSs, DGs, and D-STATCOM using multi-objective Rao 3 algorithm in a coupled network.

Chapter 5 looks at simultaneous network reconfiguration and optimal planning of RCSs, DGs, and D-STATCOM using multi-objective Rao 3 algorithm in a coupled network.

Chapter 6 presents the key findings of the research and describes future research that could be done in the area of optimal planning of charging stations.

1.8 Summary

This chapter provides an introduction to EVs and an extensive review of the literature about optimal location, size, and several issues related to the installation of CS. Finally, the rationale for and contributions of the research study are presented.

Chapter 2
Optimal planning of Rapid Charging Stations and Distributed Generators in coupled network

2.1 Introduction

Greenhouse gas emission, depletion of fossil fuels, and growing oil prices are favouring the choice of Electric Vehicles (EVs) for transportation. The deployment of 20 million EVs globally was a promising beginning to reduce greenhouse gas emissions by 2020. Such a global deployment of EVs will replace 62% of fleet vehicles by 2050. Although EVs have several advantages, they also have the drawbacks of low driving range and high charging time, and these are major reasons for the slow expansion of EVs. Installing proper charging infrastructure (Rapid Charging Stations (RCSs)) can mitigate the problem of low driving range. However, installing these at random locations would reduce the performance of the distribution network. Because EV users always choose the closest RCS to charge their vehicles, considering the road network is crucial for effective planning. Even when RCS is positioned at optimal locations, their presence would increase power loss and voltage deviation. In this regard, DG integration is a feasible solution to address the aforementioned issues.

This chapter presents the optimal planning of RCSs and DGs in a coupled power distribution network and the road transportation network. In addition to the other two goals of minimizing active power loss and voltage deviation, the placement also considered customer convenience through the minimization of EV user costs. A novel metaphor-less Rao 3 algorithm was used for obtaining the optimal location and capacities of RCSs and DGs. A coupled network of an IEEE 33 bus radial distribution network and a 25-node road network is used as a test network for validating the proposed approach.

2.2 Problem formulation

2.2.1 DG modelling

PV or PQ modelling can be used to model distributed generators. In this chapter, PQ (negative load model) mode has been taken for modelling DGs. Here the quantities

emphasized are real power output (P_{dg}) and power factor ($p.f$). Reactive power output (Q_{dg}) can be calculated from the relation governing real power, reactive power, and power factor as shown in Eq. (2.1). Eq. (2.2) and (2.3) shows the calculation of real effective load ($P_{effectiveload}$) and reactive effective load ($Q_{effectiveload}$) at distribution buses, respectively.

$$Q_{dg} = P_{dg} tan(cos^{-1}(pf)) \tag{2.1}$$

$$P_{effectiveload} = P_{load} - P_{dg} \tag{2.2}$$

$$Q_{effectiveload} = Q_{load} - Q_{dg} \tag{2.3}$$

2.2.2 Multi objective function (MOF)

In this chapter, the minimization of active power loss, EV user cost, and voltage deviation were considered for optimal planning of charging stations and DGs. Here, the weighted sum multi-objective formulation was done with equal weights.

$$MOF = min(w_1 \times APLRI + w_2 \times MVDRI + w_3 \times EVUCI) \tag{2.4}$$

In Eq. (2.4), w_1, w_2, and w_3 are weights between [0,1], and the sum of these weights needs to be 1. In this chapter, equal weights were considered for all individual objectives.

2.2.2.1 Active power loss reduction index (APLRI)

Power flow in a power distribution system causes active power loss (Ploss). The addition of rapid charging stations (RCSs) to the power distribution system puts more strain on the network, resulting in higher power losses and voltage magnitude degradation for buses. Further, the placement of RCSs in improper places increases losses abnormally and alters the healthy voltage profile. Usually, RCS is considered as the load at the power distribution substation. Mathematically, the load due to EVs at i^{th} RCS (CS^i_{load}) is calculated as per Eq. (2.5). The connectors at i^{th} RCS ($CS^i_{connectors}$) and the capacity of i^{th} RCS ($CS^i_{capacity}$) are calculated using Eq. (2.6) and (2.7), respectively. Power loss can be reduced by minimizing the active power loss reduction index (APLRI). Here, APLRI (Eq. 2.8) is the ratio of daily Ploss after the placement of CS or DG or both, to

the daily Ploss before the placement of both.

$$CS^{i}_{load} = N^{iCS}_{ev} Pb \tag{2.5}$$

$$CS^{i}_{connectors} = max(P_{evc}) N^{iCS}_{ev} \tag{2.6}$$

$$CS^{i}_{capacity} = CS^{i}_{connectors} R_c \tag{2.7}$$

$$APLRI = \frac{\sum_{t=1}^{24} P^{fcs/dg}_{loss}}{\sum_{t=1}^{24} P_{loss}} \tag{2.8}$$

2.2.2.2 EV user cost index (EVUCI)

Electric vehicle user has a choice to select the nearest RCS to charge their EV. This decision not only helps the user but also reduces the energy loss from travelling to the RCS. Consider m possible charging station locations and q charging demand nodes, which belong to road network nodes. The selection of RCS in optimal planning is done by the calculation of the distance between q^{th} demand node to all available RCSs, which is stored in a D matrix with the order of $[q,z]$ $z \in m$. After comparing the distances of the q^{th} demand node to all RCSs, EVs present at the demand node are assigned to the nearest RCS and the corresponding distance is stored in the DD matrix. Here, the DD matrix has the order of $[q,1]$.

$$D = \begin{bmatrix} d_1c_1 & d_1c_2 & .. & d_1c_z \\ d_2c_1 & d_2c_2 & .. & d_2c_z \\ . & . & . & . \\ . & . & . & . \\ d_qc_1 & d_qc_2 & .. & d_qc_z \end{bmatrix} DD = \begin{bmatrix} min() \\ min() \\ . \\ . \\ min() \end{bmatrix} \tag{2.9}$$

d=$[d_1, d_2, ..., d_q]$ is the set of demand points, and c=$[c_1, c_2, ..., c_m]$ is the set of charging nodes belonging to road network nodes. EV user cost can be calculated from Eq. (2.10). Here, $Nev(i)$ is total number of EVs at i^{th} RCS, EC is the energy consumption of EVs and P_e is the electricity price.

$$EVusercost = \sum_{n=1}^{q} DD(i) Nev(i) ECP_e \tag{2.10}$$

Calculating the distance from q^{th} demand node to all m charging nodes and choosing the longest distance among them offers the maximum distance that an EV customer must

travel from q^{th} demand node. DD_{max} is the result of forming a DD matrix for maximum distances. The values of maximum EV user loss cost and EV user cost index are given by Eqs. (2.11) and (2.12).

$$EV_{usercost}^{max} = \sum_{n=1}^{q} DD_{max}(i)Nev(i)ECP_e \tag{2.11}$$

$$EVUCI = \frac{EVusercost}{EV_{usercost}^{max}} \tag{2.12}$$

2.2.2.3 Maximum voltage deviation reduction index (MVDRI)

Loading the power distribution system with RCS can cause a deviation in voltage beyond its limits. The ac load flow gives the value of the voltage at each bus. The maximum voltage deviation (VD_{max}) can be calculated using Eq. (2.13).

$$VD_{max} = max(1 - v(i)) \qquad i = 1,2,3...N_{distnodes} \tag{2.13}$$

MVDRI refers to the ratio of maximum voltage deviation over the day with the integration of RCS/DG or both to the maximum voltage deviation over the day without the integration of both RCS and DG. It is calculated as follows.

$$MVDRI = \frac{\sum_{t=1}^{24} VD_{max}^{RCS/DG}, t}{\sum_{t=1}^{24} VD_{max}, t} \tag{2.14}$$

2.2.3 System constraints

Each RCS must have at least one charging connector to supply the EVs, and Eq. (2.15) supports this constraint. Eq. (2.16 and 2.17) are the real and reactive power balance constraints, respectively, in the system. Integration of RCS alters the voltage profile, so there is a need to check voltage limits in optimal planning. Eq. (2.18) adds the voltage limits as a constraint. Each DG has maximum and minimum capacity limits (Eq. (2.19)), and the maximum total capacity supplied by all DGs ($P_{DG}^{T,max}$) is a user-defined quantity and should be less than the minimum total real power consumption throughout a day (Eq. (2.20)).

$$CS^{i}_{connector} \geq 1 \qquad i = 1,2,..z(numberofRCS) \tag{2.15}$$

$$P_{sub} + \sum P_{dg} = P_D + \sum P_{RCS} + P_{loss} \tag{2.16}$$

$$Q_{sub} + \sum Q_{DG} = Q_D + Q_{loss} \tag{2.17}$$

$$|V_{min}| \leq |V_n| \leq |V_{max}| \qquad n = 1,2,...N_{bus} \tag{2.18}$$

$$P^{min}_{dg} \leq P_{a,dg} \leq P^{max}_{dg} \qquad a = 1,2,..N_{DG} \tag{2.19}$$

$$\sum_{a=1}^{N_{DG}} P_{a,DG} \leq P^{T,max}_{DG} < min(P_{n,D}) \tag{2.20}$$

Here, P_{sub} and Q_{sub} are the substation real power and reactive power, respectively. P_D, Q_D, P_{loss} and Q_{loss} are real power demand, reactive power demand, real power loss, and reactive power loss in a given test system respectively. Here, RCSs are considered as only real power loads i.e P_{RCS} equal to CS^{i}_{load}. V_{min}, V_{max}, P^{min}_{dg} and P^{max}_{dg} are the voltage minimum limit, voltage maximum limit, DGs minimum real power limit, and DGs maximum real power limit, respectively. $P^{T,max}_{DG}$ is the maximum limit of total active power supplied by all DGs. $P_{n,D}$ real power demand at n^{th} node of the power distribution system.

2.3 Algorithms

2.3.1 PSO algorithm

Particle Swarm Optimization (PSO) is a powerful meta-heuristic optimization algorithm and inspired by swarm behavior observed in nature such as fish and bird schooling. PSO algorithm was proposed by Kennedy in 1995 [1]. Eq. (2.21) gives the position value in $(t+1)^{th}$ iteration, which depends on the position value in t^{th} iteration and velocity in $(t+1)^{th}$ iteration. Eq. (2.22) gives the velocity in $(t+1)^{th}$ iteration. It depends on inertia weight (w), acceleration coefficients (C1 and C2), local best value (P_{best}), global best (G_{best}), and random values (r_1 and r_2). Flow chart of PSO algorithm is shown in Figure 2.1.

$$P^{t+1}_i = P^t_i + V^{t+1}_i \tag{2.21}$$

$$V^{t+1}_i = wV^t_i + C_1 r_1 (P^t_{best} - P^t_i) + C_2 r_2 (g_{best} - P^t_i) \tag{2.22}$$

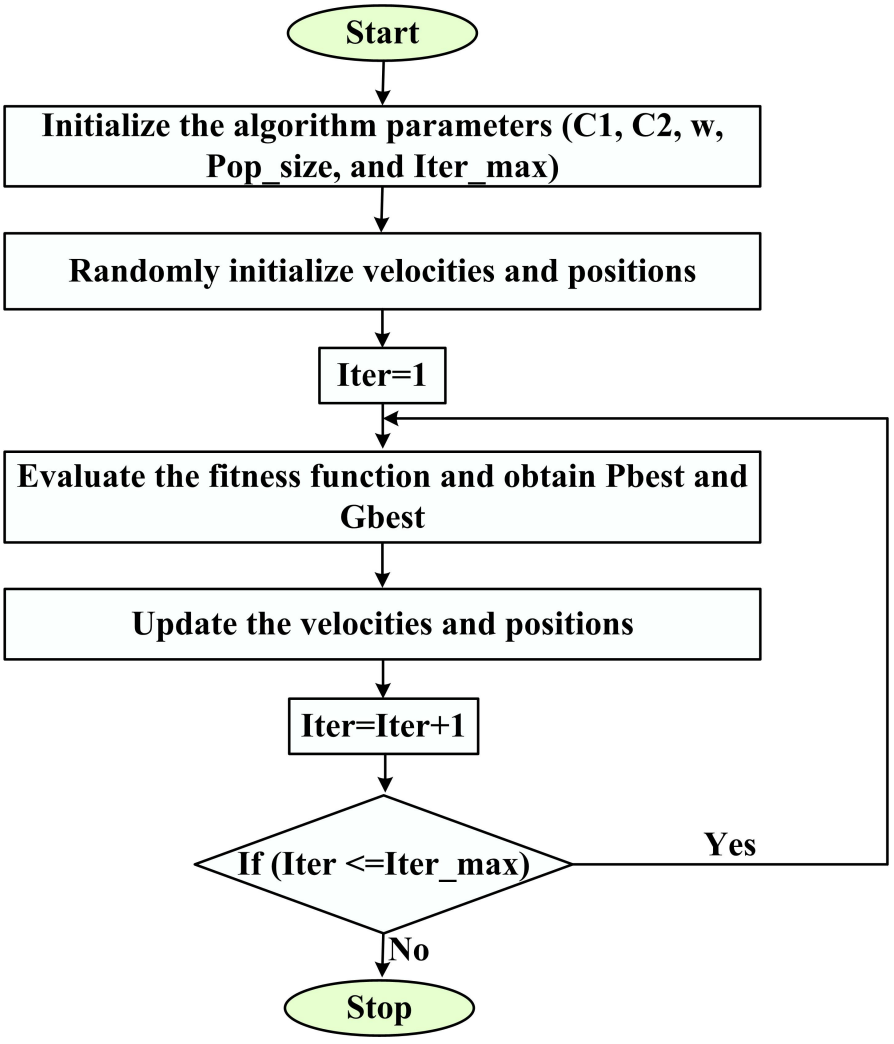

Figure 2.1: Flow chart of PSO algorithm [1]

2.3.2 Jaya algorithm

Rao proposed the Jaya algorithm [2], which is a population based meta-heuristic algorithm. The premise of this algorithm is that the solution to an optimization problem goes towards the global best solution while avoiding the worst solution. It has the advantage that it requires only the common control parameters which are: population size and maximum iterations, and it does not require any algorithm-specific parameter setting. The modified value of k^{th} candidate i^{th} variable in j^{th} iteration is obtained using Eq. (2.23) given below. Figure 2.2 shows the flow chart of jaya algorithm.

$$x'_{k,i,j} = x_{k,i,j} + r1_{i,j}(x_{best,i,j} - x_{k,i,j}) - r2_{i,j}(x_{worst,i,j} - x_{k,i,j}) \tag{2.23}$$

Here $x'_{k,i,j}$ is the modified k^{th} candidate, i^{th} variable in j^{th} iteration, $x_{k,i,j}$ is the present k^{th} candidate, i^{th} variable in j^{th} iteration. $r1$, $r2$ are the random values between 0 and 1 i.e [0 1]. $x_{best,i,j}$ is the best solution of i^{th} variable among all candidates in j^{th} iteration. $x_{worst,i,j}$ is the worst solution of i^{th} variable among all candidates in j^{th} iteration. If the objective value yield by modified $x'_{k,i}$ is better than $x_{k,i}$, then the modified candidate solution is accepted in each iteration. Acceptable solutions are kept in each iteration, and subsequent searches are based on the solutions in the following iteration. When the termination criteria are met, the final optimal solutions are achieved.

2.3.3 Rao 3 algorithm

Rao 3 algorithm was proposed by Rao in 2020 [3]. The algorithm is easy to understand and has the advantage of being metaphor-less with few algorithm-specific parameters. The principle behind this algorithm is random interaction between the candidate solutions, and the candidate solutions move towards the best solutions and away from the worst solutions in the optimization process. This algorithm is a population-based technique and updates equations in each iteration, as shown below.

$$\begin{aligned} X'_{i,j,k} = X_{i,j,k} &+ r1_{j,k}(X_{j,best,k} - |(X_{j,worst,k})|) \\ &+ r2_{j,k}((|X_{i,j,k} or X_{r,j,k}|) - (X_{r,j,k} or X_{i,j,k})) \end{aligned} \tag{2.24}$$

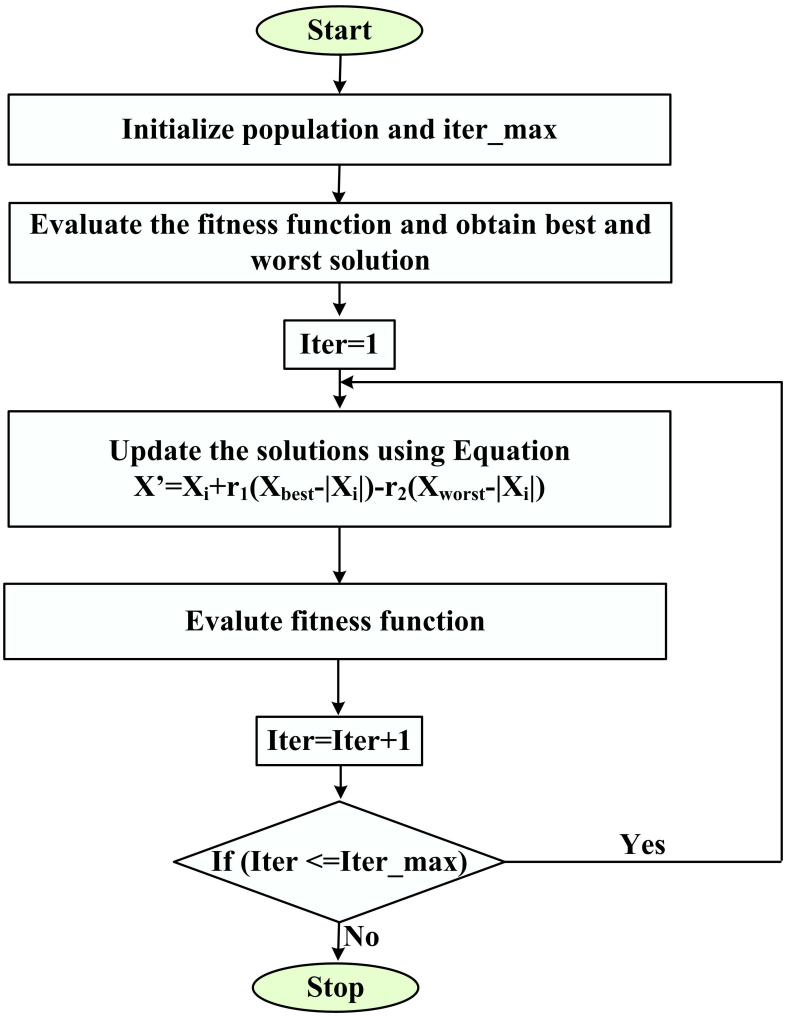

Figure 2.2: Flowchart of JAYA algorithm [2]

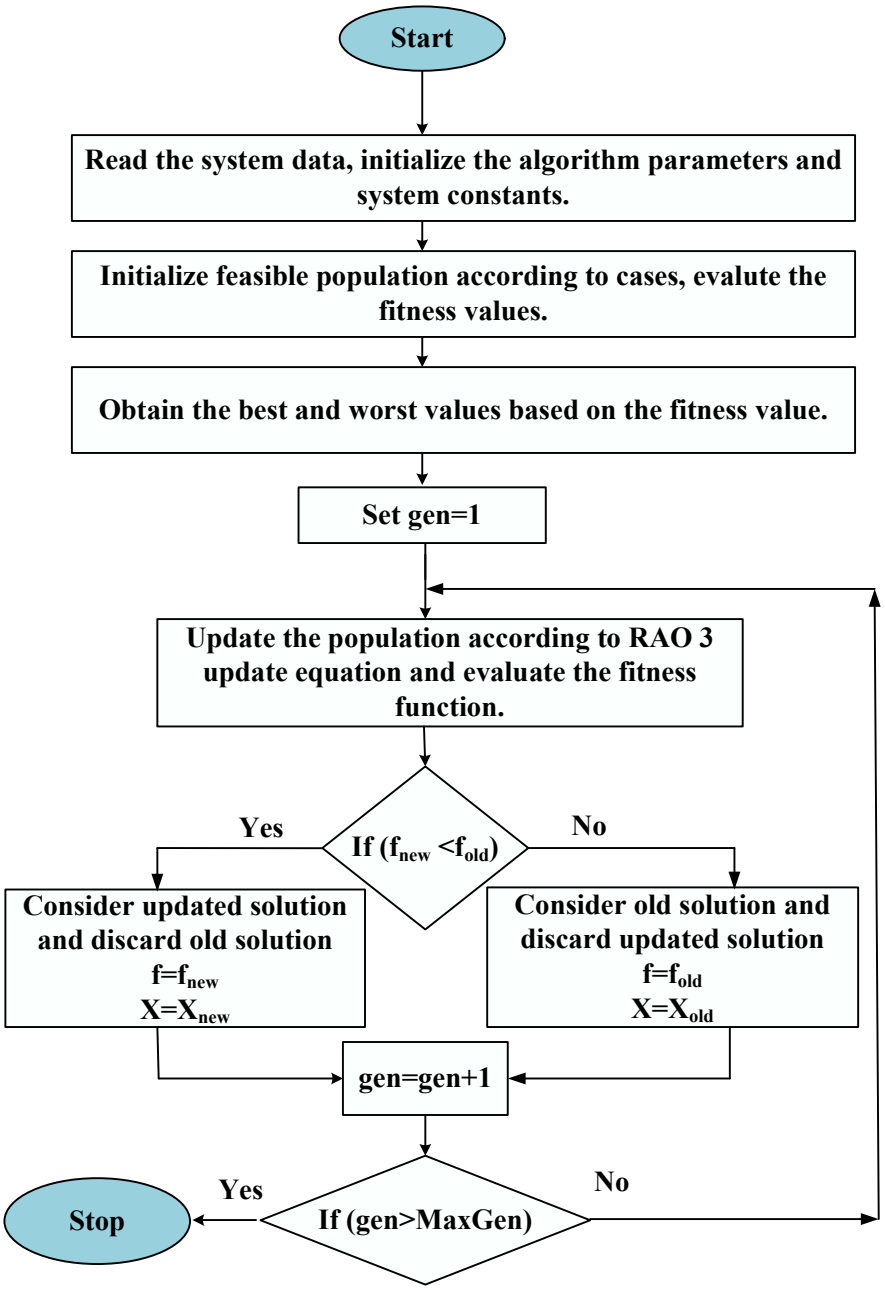

Figure 2.3: Flowchart for implementation of Rao 3 algorithm [3]

Here $X'_{i,j,k}$ is the updated solution of i^{th} candidate, j^{th} variable in k^{th} iteration. $X_{i,j,k}$ is the solution of i^{th} candidate, j^{th} variable in k^{th} iteration, $r1, r2$ are random values between [0,1]. $X_{j,best,k}$ is the best value of j^{th} variable of X in the k^{th} iteration. $X_{j,worst,k}$ is the worst value of j^{th} variable of X in the k^{th} iteration. $X_{r,j,k}$ randomly selected r^{th} candidate, j^{th} variable in k^{th} iteration. The flowchart of Rao 3 algorithm for optimal

planning is shown in Figure. 2.3.

$$L_{cspop} = \begin{bmatrix} X_{1,1} & X_{1,2} & .. & X_{1,z} \\ X_{2,1} & X_{2,2} & .. & X_{2,z} \\ . & . & . & . \\ . & . & . & . \\ X_{pop,1} & X_{pop,2} & .. & X_{pop,z} \end{bmatrix} \tag{2.25}$$

$$L_{dgpop} = \begin{bmatrix} Y_{1,1} & Y_{1,2} & .. & Y_{1,n} \\ Y_{2,1} & Y_{2,2} & .. & Y_{2,n} \\ . & . & . & . \\ . & . & . & . \\ Y_{pop,1} & Y_{pop,2} & .. & Y_{pop,n} \end{bmatrix} \tag{2.26}$$

$$S_{dgpop} = \begin{bmatrix} S_{1,1} & S_{1,2} & .. & S_{1,n} \\ S_{2,1} & S_{2,2} & .. & S_{2,n} \\ . & . & . & . \\ . & . & . & . \\ S_{pop,1} & S_{pop,2} & .. & S_{pop,n} \end{bmatrix} \tag{2.27}$$

$Init_{cspop} = [L_{cspop}]$ is the matrix used for optimal planning of only RCSs (Case 1). This matrix consist of feasible locations of RCSs in a power distribution system. $Init_{dgpop} = [L_{dgpop}, S_{dgpop}]$ is the matrix consisting of randomly initialized feasible locations and the corresponding size of DGs is used in order to plan DGs in the power distribution network optimally (Case 2). $Init_{csdgpop} = [L_{cspop}, L_{dgpop}, S_{dgpop}]$ is the matrix that consists of RCS location, DG location and the corresponding DG size. It is utilised to plan RCSs and DGs at the same time to get the best results (Case 3). Here X indicates the location of RCS, Y indicates the location of DG and S indicates the size of the DG.

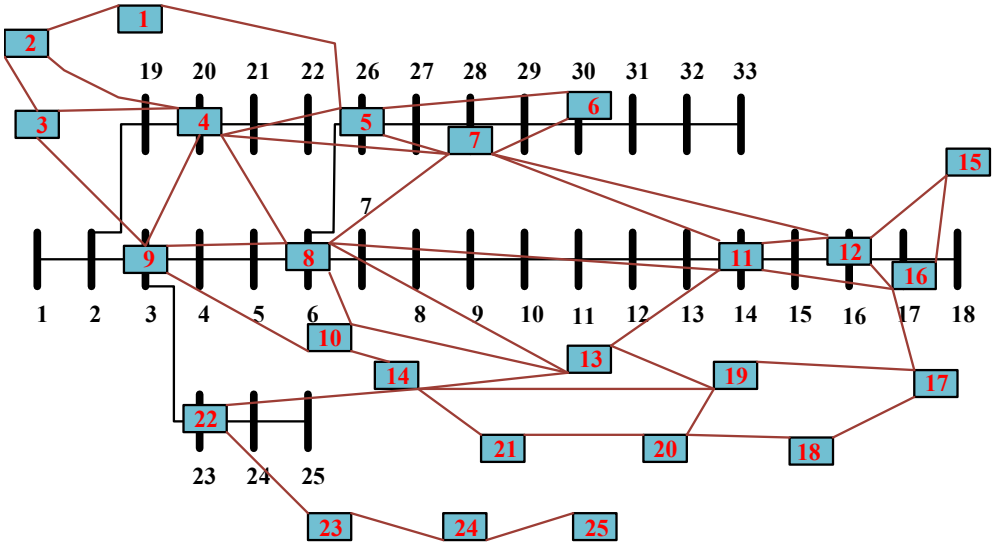

Figure 2.4: Super imposed IEEE 33 bus power distribution system with 25 node road transportation network

2.3.3.1 Implementation of Rao 3 algorithm for optimal planning of RCSs and DGs

Step 1: Read the test system data and initialize the algorithm parameters (population size and maximum iterations).

Step 2: Randomly initialize the population according to cases and determine the respective fitness values.

Step 3: Obtain best and worst solutions based on fitness values.

Step 4: Set gen = 1.

Step 5: Update the candidate solutions based on update equation (2.24) and find the updated fitness value.

Step 6: Accept the modified solution if it is superior to previous solution, otherwise keep the previous solution.

Step 7: Set gen=gen+1.

Step 8: Check terminating criteria, if (gen $>$ MaxGen) prints the results, otherwise continue from step 5 to step 8.

2.4 Simulation Results and Analysis

Superimposed IEEE 33 bus Power distribution network and 25 node road network is considered as test system [77], as shown in Figure 2.4. All the buses in IEEE 33 bus test system were segregated as 17 residential load buses, 9 industrial load buses and 5 commercial load buses shown in Table 2.1. Bus data and line data were taken from [102]. The hourly load at various buses vary according to the load patterns (in p.u) as shown in Figure 2.6. The data regarding road network was taken from [103], and 1 km per unit was considered. Superimposed nodes of the distribution network and road network were taken from [77], which are represented in Table 2.3.

Table 2.1: Identification of types of load buses

Residential loads	Commercial loads	Industrial loads
2,3,5,6	4,11,12,18	22,26,27,28
7,8,9,10	19	29,30,31,32
13,14,15,16	–	33
17,20,21,23,24	–	–

Table 2.2: Electric vehicle technical parameters

Parameter	Value
Total number of EVs (N_{TEV})	238
Connector rating (R_c) (kW)	96
EV battery capacity (P_b) (kWh)	50
Energy Consumption (EC) (kWh/km)	0.219
Electricity Price (P_e) ($/MWh)	87.7

The total number of EV population at road network nodes was assumed to be 238, and were allowed to charge at select charging stations according to the probability of EV charging shown in Figure 2.5. Table 2.4 gives the assumed number of EVs present at the nodes of the road network. In this work, all 25 road network nodes were considered demand nodes. For all optimization algorithms, 100 maximum generations and 30 population size are considered. For the PSO algorithm, inertia constants C1=C2=2 were considered. Simulations were carried out on PC with windows 10 operating system, 4Gb RAM, and MATLAB 2014b software.

In this chapter, analysis was done by considering the Base case, Case 1, Case 2, and Case 3.

- Base case: In this case, the load flow study was done on power distribution system without the integration of RCSs and DG to find daily active power loss and maximum voltage deviation.
- Case 1: In this case, optimal placement and sizing of RCSs were done on the superimposed network to minimize the EV user cost, active power loss, and voltage deviation.
- Case 2: The load due to charging stations from Case 1 is added to the current load at the corresponding distribution bus in Case 2. In this system, optimal placement and sizing of DGs were done to minimize the EV user cost, active power loss, and voltage deviation.
- Case 3: In this case, concurrent placement and sizing of RCSs and DGs were done to minimize active power loss, EV user cost, and voltage deviation.

Table 2.3: Coupling of the road network nodes (R_n) with the distribution network nodes (D_n)

D_n	R_n	D_n	R_n
03	09	20	04
06	08	23	22
14	11	26	05
16	12	28	07
17	16	30	06

Table 2.4: Assumed EVs present at road network nodes

R_n	EVs	R_n	EVs	R_n	EVs	R_n	EVs	R_n	EVs
1	5	6	8	11	3	16	15	21	9
2	9	7	15	12	3	17	8	22	12
3	13	8	6	13	10	18	6	23	15
4	8	9	4	14	12	19	7	24	5
5	5	10	15	15	15	20	15	25	15

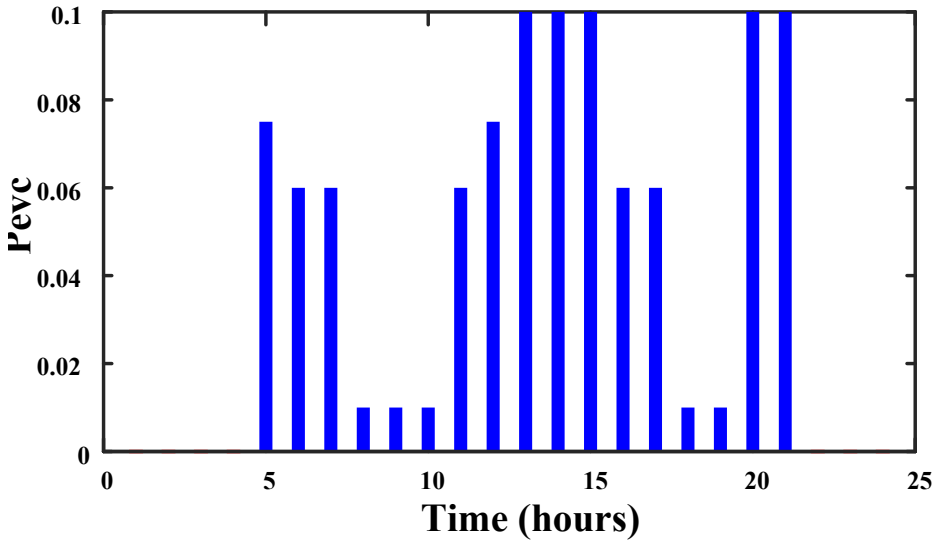

Figure 2.5: Variation of Electric Vehicle charging probability

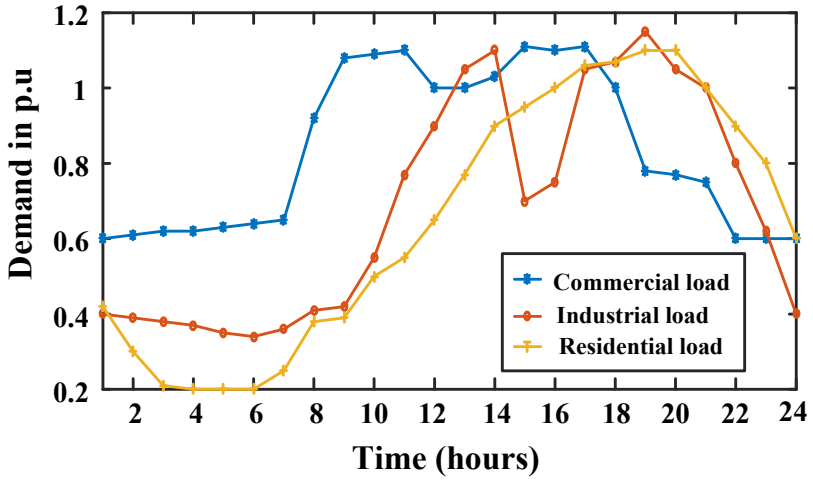

Figure 2.6: Plot of different types of load patterns

2.4.1 Base case

The test system consists of IEEE 33 bus power distribution system. As it is radial and has a high R/X ratio, backward forward sweep load flow algorithm was used for load flow study. In the Base case, the distributed load flow study was simulated without the integration of RCSs and DGs into the test system by considering hourly load patterns of different load types over 24 hours.

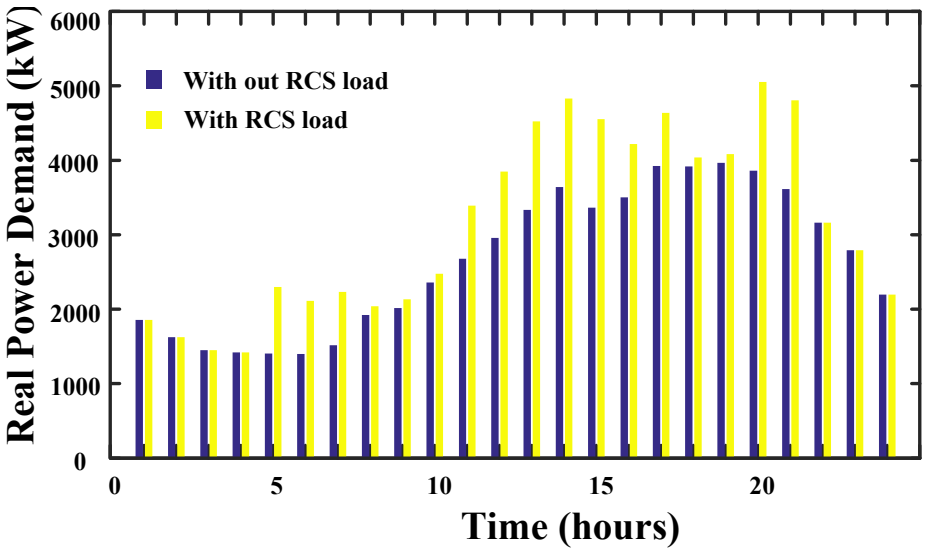

Figure 2.7: Plot of hourly varying load demand with and with out RCSs load

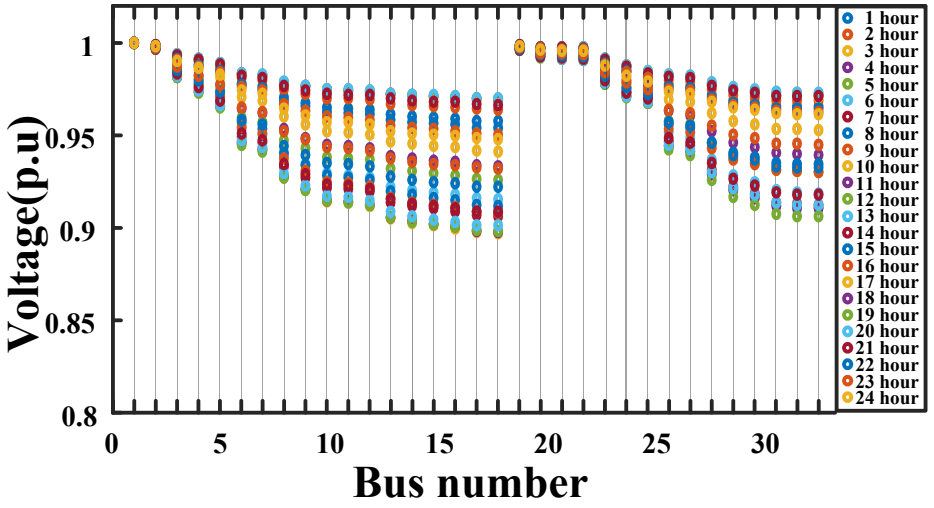

Figure 2.8: Distribution system voltage profile in base case

It was observed that the load flow led to daily active power loss of 2811 kW and daily maximum voltage deviation of 1.5816 (p.u). The lowest voltage of 0.8968 (p.u) was observed at 18^{th} node in 17^{th} hour. Voltage profile over 24 hours is shown in Figure 2.8

2.4.2 Case 1: Optimal planning of RCSs

Case 1 deals with optimal placement and sizing of RCSs. The placement was done based on the following assumptions:

- The superimposed nodes were considered for RCS's placement.
- RCSs can be placed at 3 buses and it is observed that placement at more than 3 buses makes the system unstable.

In Case 1, RCSs were optimally planned. In optimal planning, primarily all the EVs were distributed among initialized RCS locations to minimize EV user costs by selecting the nearest RCS. After adding the RCS load, the distribution load flow algorithm is applied to the test system to find Ploss and MVD. To minimize the multi-objective function, various algorithms were applied. It is observed from Table 2.5 that, power distribution system performance is affected by RCS's installation. Daily active power loss increased by 19.5 %, 12.1 %, and 9.73 % compared with Base case Ploss, that were obtained using PSO, JAYA, and Rao 3 algorithms, respectively. The presence of RCSs was also witnessed by the increased value of MVD (1.6120 (p.u)) in comparison with Base case MVD (1.5816 (p.u)). Here, Rao 3 algorithm gave least MVD compared to other two algorithms. The system's minimum voltage was 0.8949 (p.u), which appeared at the 18^{th} bus in the 17^{th} hour using Rao 3 algorithm, as shown in Figure 2.9.

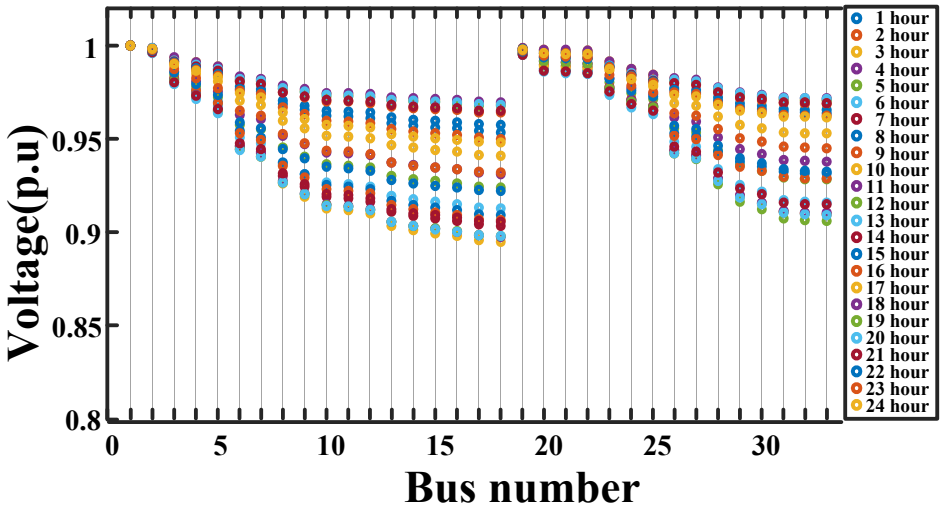

Figure 2.9: Distribution system voltage profile in Case 1

Table 2.5: Comparison of various algorithms for optimal allocation of RCSs in Case 1

Parameter	PSO	JAYA	Rao 3
CS locations	23,20,30	23,20,26	20,23,3
EVs	129,50,59	144,76,18	105,114,19
Connectors	13,5,6	14,8,2	11,11,2
Size (kW)	1248,480,576	1344,768,192	1056,1056,192
Ploss (kW)	3359.8	3151.8	3084.6
EVUC ($)	34.0335	36.1270	36.3383
MVD (p.u)	1.6608	1.6271	1.612
APLRI	1.1952	1.1212	1.0973
EVUCI	0.3643	0.3867	0.3890
MVDRI	1.0501	1.0288	1.0193
MOF	0.8690	0.8447	0.8343
Time (sec)	250.4	169.3	155.6

RCSs placement caused the downfall of system minimum voltage from 0.8968 (p.u, Base case) to 0.8949 (p.u). EVUC is 36.3383 $ with Rao 3 algorithm which is highest among EVUC of PSO and JAYA algorithms. However, the overall objective function value of 0.8343 by Rao 3 algorithm was lowest in comparison with JAYA algorithm (0.8447) and PSO algorithm (0.8690). Rao 3 algorithm took less time for evalution compared to PSO and JAYA algorithms. To counter the effects caused by RCSs installation in the power distribution system, DGs are installed.

2.4.3 Case 2: Optimal planning of DGs

Installing DGs in the power distribution system reduces power loss and improves voltage profile. Renewable type DGs of size 5 kW-1MW were considered for integration. It has been observed that integration of three DGs in a power distribution system outperforms integration of single DG or two DGs. It's also been observed that adding more than three DGs to a power distribution system doesn't significantly increase performance. As a result, three DGs were considered in this study. The hourly total real load demand on the system, which includes RCSs load and the hourly charging probability of EVs, is depicted in Figure 2.7. According to this plot, the minimum real power load demand of 1420.8 kW appeared at the 4^{th} hour. As a result, the total real power injection by all DGs was limited to less than or equal to 1400 kW ($<$1420.8), according to the constraint

(Eq. 2.20).

Table 2.6 shows the optimal placements, DG sizes, and numerous technical observations. When compared to the Base case, active power loss was reduced to 38.42 % in Case 2. This reduction was aided by the insertion of DGs in the power distribution system. The PSO and JAYA algorithms reduced active power loss by 40.06 % and 39.45 %, respectively, but the optimal placements and sizes of DGs obtained by Rao 3 algorithm reduced active power loss to maximum in comparison with other two algorithms. The maximum voltage deviation with Rao 3 algorithm was 0.5215 (p.u), which was higher than 0.5151 (p.u), 0.5162 (p.u) of PSO, and JAYA algorithms, respectively.

Furthermore, compared to 0.3718 of PSO and 0.3699 of JAYA, the multi-objective function (MOF) with Rao 3 algorithm was 0.3675, which was the lowest value. The voltage profile at all buses throughout the day is depicted in Figure 2.10, with DGs placed at optimal locations and sizes using Rao 3 algorithm. A minimum voltage of 0.9626 (p.u) appeared at the 30^{th} bus in the 19^{th} hour, according to Figure 2.10. The lowest voltage at the 18^{th} bus improved from 0.8968 (p.u Base case) to 0.9627 in the 17^{th} hour (p,u). The placement of DGs in appropriate locations is responsible for this improvement. When compared to PSO and JAYA algorithms, Rao 3 produced more efficient outcomes in the shortest time.

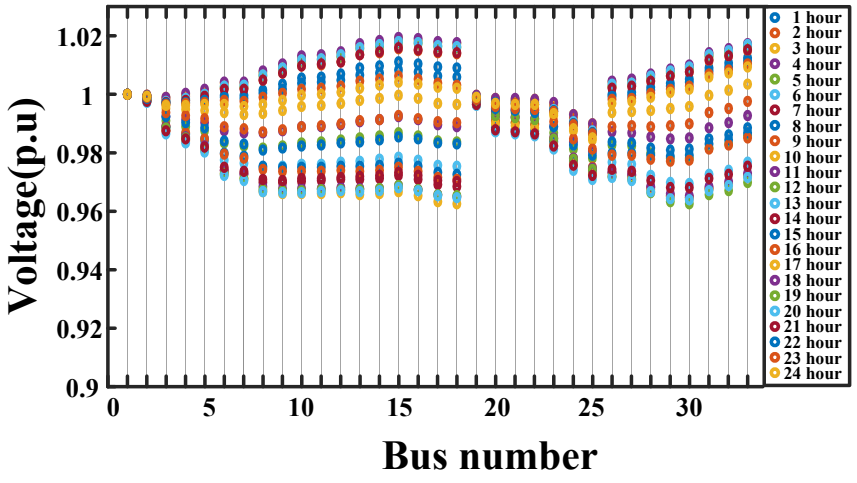

Figure 2.10: Distribution system voltage profile in Case 2

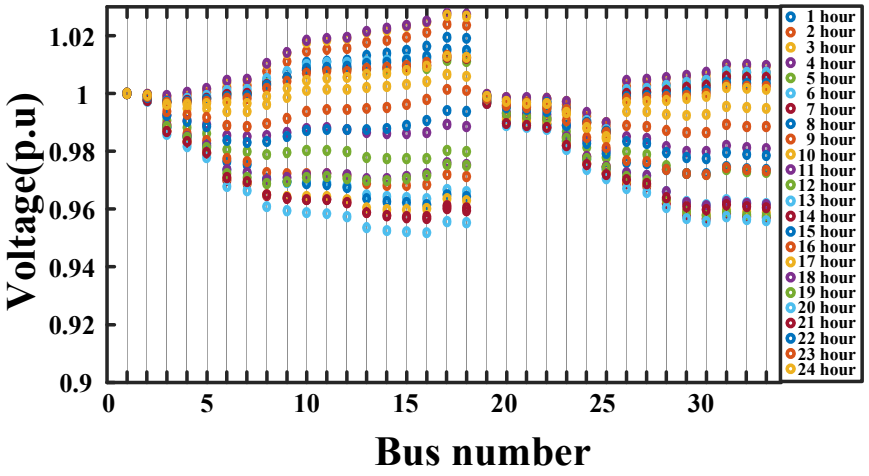

Figure 2.11: Distribution system voltage profile in Case 3

Table 2.6: Comparison of various algorithms for optimal allocation of DGs in Case 2

Parameter	PSO	JAYA	Rao 3
DGs locations	15,33,5	33,15,8	33,15,12
Size (kW)	609,784,5	793,554,52	773,429,196
Ploss (kW)	1126.3	1108.9	1080
EVUC ($)	36.3383	36.3383	36.3383
MVD (p.u)	0.5151	0.5162	0.5215
APLRI	0.4007	0.3945	0.3841
EVUCI	0.3890	0.3890	0.3890
MVDRI	0.3257	0.3264	0.3297
MOF	0.3718	0.3699	0.3675
Time (sec)	274.2	136.1	130.5

Table 2.7: Comparison of various algorithms for concurrent optimal allocation RCSs and DGs in Case 3

Parameter	PSO	JAYA	Rao 3
CS locations	20,28,16	23,20,6	16,20,23
EVs	44,112,82	104,40,94	67,73,98
Connectors	4,11,8	10,4,9	7,7,10
Size (kW)	384,1056,768	960,384,864	672,672,960
DGs locations	13,11,30	14,31,30	31,11,17
Size(kW)	514,69,791	569,461,151	615,389,395
Ploss (kW)	1271.9	1219.2	1079.2
EVUC ($)	42.3306	31.1142	25.3715
MVD (p.u)	0.8192	0.6714	0.5960
APLRI	0.4525	0.4337	0.3839
EVUCI	0.4531	0.3331	0.2716
MVDRI	0.5179	0.4245	0.3768
MOF	0.4745	0.3971	0.3441
Time (sec)	298.8	160.1	148.06

2.4.4 Case 3: Concurrent optimal planning of RCSs and DGs

In this case, Rao 3 algorithm was used to plan RCSs and DGs at the same time. RCS location, DG location, and DG size make up the initialization matrix. The system was examined for improved overall objective function once these two were added. Table 2.7 shows the optimal results by various algorithms. Rao 3 algorithm was shown to generate a better multi-objective function (MOF) of 0.3441. The daily active power loss was 1079.2 kW, or 38.39% of the base active power loss. In comparison to PSO and JAYA algorithms, the maximum voltage deviation (MVD) was 0.5960 (p.u), which was the lowest of the values. With Rao 3 algorithm, EV user cost of electric vehicles was 25.3715 $, which is cost - effective when compared to 42.3306 $ and 31.1142 $ for PSO and JAYA, respectively.

Table 2.8: Comparison of Ploss, MVD, and EVUC in various cases by Rao 3 algorithm

Parameter	Base case	Case 1	Case 2	Case 3
Ploss (kw)	2811	3084.2	1080	1079.3
MVD (p.u)	1.5816	1.6120	0.5215	0.5960
EVUC ($)	–	36.3383	36.3383	25.3715
MOF	–	0.8343	0.3675	0.3441

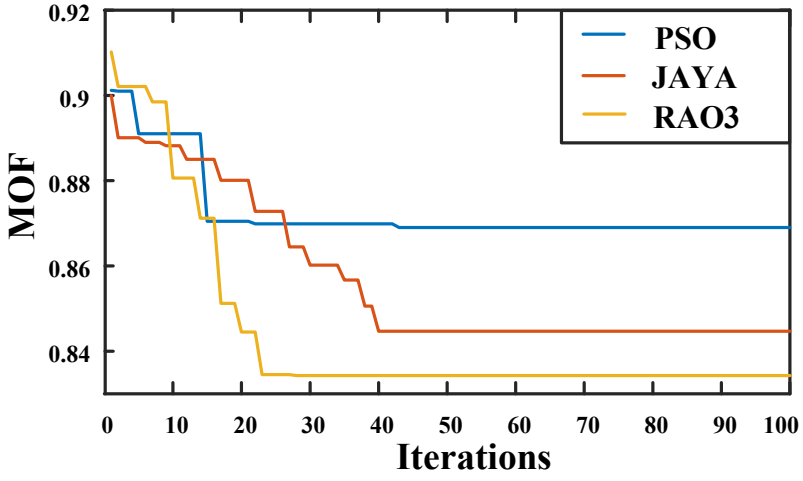

Figure 2.12: Convergence characteristics by various algorithms in Case 1

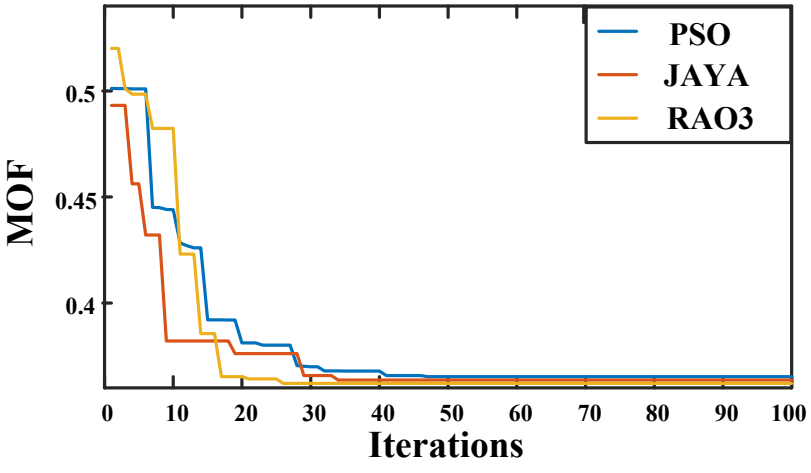

Figure 2.13: Convergence characteristics by various algorithms in Case 2

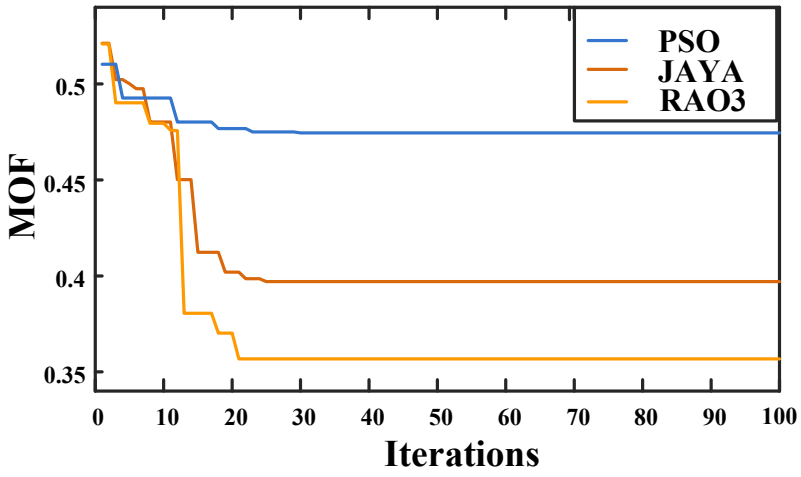

Figure 2.14: Convergence characteristics by various algorithms in Case 3

The system's voltage profile is shown in Figure. 2.11, with RCSs and DGs placed simultaneously using Rao 3 algorithm. At 16^{th} bus in 20^{th} hour, the system's minimum voltage was 0.9518 (p.u). The voltage improved from 0.8968 (p.u, Base case) to 0.9629 (p.u) at the 18^{th} bus in the 17^{th} hour. When compared to other two algorithms, Rao 3 algorithm takes less time to simulate and produce optimal results.

We know from Table 2.8 that, daily active power loss is gradually reduced from Case 1 to Case 3. Though the maximum voltage deviation is slightly higher in Case 3 compared to Case 2, EVUC and overall objective function are the smallest of all cases (Case 1 and Case 2) in Case 3. Based on these findings, it can be inferred that using Rao 3 algorithm to plan RCSs and DGs concurrently (Case 3) generated the best outcomes.

2.5 Summary

The optimal locations and capacities of RCSs and DGs were obtained by considering the following scenarios: i) RCSs alone, ii) Optimal DG planning with prior RCSs outcomes, iii) Concurrent planning of RCSs and DGs. In the proposed planning, variation of load demand and Electric Vehicle charging probability over 24 hours was considered. The use of the metaphor less Rao 3 algorithm yielded faster convergence with better performance for the optimal planning of RCSs and DGs simultaneously. Random interactions between candidate solutions and the ability to move candidate solutions towards the best optimal solution and away from the worst solution of Rao 3 algorithm outperform PSO and Jaya algorithms. Future research will identify the appropriate number of

connectors at each RCS that provide the best trade-off between waiting time and RCS installation cost.

Chapter 3

Queue theory based optimal planning of RCSs, DGs, and identification of optimal connectors in coupled network

3.1 Introduction

In the previous chapter, voltage stability index, charging station installation cost, and waiting time at charging stations were not considered. This chapter, presents a two stage approach for optimal planning of RCSs and DGs in a coupled transportation and distribution network. Optimal location of RCSs and optimal planning of DGs was done in the first stage by minimizing power loss, voltage deviation, EV user cost and maximizing voltage stability index. Optimal number of connectors was determined in second stage by minimizing the waiting time in queue at RCSs and installation cost of RCSs. A novel Multi-Objective Rao 3 algorithm was employed to determine the optimal solutions.

3.2 Problem formulation

This section presents two a stage approach for optimal planning of RCSs and DGs in a coupled network, objective functions, operational constraints considered in each stage, DG modelling, and RCS modelling.

3.2.1 Two stage approach

In this chapter, optimal planning of RCSs and DGs was done in two stages (Figure 3.1). Integration of only RCS into the power distribution system causes performance degradation. In this context, DG integration was adopted and the test system analysed in Stage I. Based on the results achieved from Stage I, optimal number of connectors was determined in Stage II to benefit EV user and RCS owner.

3.2.1.1 Stage I: Optimal location of RCSs and optimal location and sizing of DGs in a coupled network

In stage I, optimal locations of RCSs and optimal planning of DGs were done through two scenarios. In scenario 1, the impact of RCS on the performance of power distribution system was analysed through various cases (explained in Section 3.4.2.1). In scenario 2, concurrent optimal planning of RCSs and DGs was done and the performance of power distribution system was analysed through various cases (explained in Section 3.4.2.2). Optimal location of RCSs, optimal location and sizing of DGs were done by minimizing power loss (P_{loss}), maximum voltage deviation (MVD), EV user cost ($EVUC$), and maximizing voltage stability index (VSI). Eq. (3.1) shows the objective function in Stage I, where feasible locations of RCSs (l_{RCS}), locations of DGs (l_{DG}), and size of DGs (S_{DG}) were decision variables.

$$f(l_{RCS}, l_{DG}, S_{DG}) = min(Ploss, MVD, EVUC, (1/VSI)) \tag{3.1}$$

Here certain constraints exist while planning the RCSs and DGs optimally in the coupled network. Backward forward sweep load flow algorithm was used for load flow study to achieve power loss, node voltages, and voltage stability index. While planning RCSs and DGs in a coupled network optimally in Stage I, some equality and inequality constraints are considered. The real and reactive power balance in the power distribution system was considered using Eqs. (3.2) and (3.3). Addition of RCSs results in deterioration of voltage profile. Hence, to maintain voltage limits, Eq. (3.4) was used as constraint. DG's minimum active power limits and total active power supplied by all DGs were used as constraints using Eq. (3.5) and Eq. (3.6) respectively. In Eq. (3.6), the contribution from all DGs was limited by minimum active power consumption over a 24 hour period.

$$P_{sub} + \sum P_{dg} = P_D + \sum P_{RCS} + P_{loss} \tag{3.2}$$

$$Q_{sub} + \sum Q_{dg} = Q_D + \sum Q_{RCS} + Q_{loss} \tag{3.3}$$

$$|V^{min}| \leq |V_n| \leq |V^{max}| \qquad n = 1, 2, ...N_{bus} \tag{3.4}$$

$$P_{dg}^{min} \leq P_{dg} \leq P_{dg}^{max} \tag{3.5}$$

$$P_{dg} \leq P_{dg}^{T,max} < min(P_{n,D}) \tag{3.6}$$

Here, P_{sub} and Q_{sub} are real power and reactive powers of substations respectively. P_D and Q_D are real and reactive power demands in power distribution system. P_{loss} and Q_{loss}

are real power loss and reactive power loss. Here, RCS has real power load (P_{RCS}) and reactive power load (Q_{RCS}). V^{min}, V^{max}, P_{dg}^{min}, and P_{dg}^{max} are lower voltage limit, upper voltage limit, DGs lower real power limit and DGs upper real power limit respectively. $P_{dg}^{T,max}$ is the maximum limit of total active power supplied by all DGs. $P_{n,D}$ is real power demand at n^{th} node of power distribution system.

3.2.1.2 Stage II: Optimal sizing of RCSs

After identifying the optimal locations of RCSs, optimal locations and sizes of DGs, the number of assigned EVs at each RCS calculated in Stage I were considered as input information to Stage II. Based on this, arrival rate was calculated and used in M1/M2/C queuing model for finding the waiting time in queue at RCSs. In stage II, optimal sizing of RCS was done by determining the optimal number of connectors at each RCS location. Installation cost of RCS (*ICRCS*) and waiting time (W_T) in queue at RCSs depend on the number of connectors at RCSs. In Stage II, the optimal number of connectors was determined by minimizing the *ICRCS* and W_T. Eq. (3.7) shows objective function in Stage II, where the feasible number of connectors (C) at each RCS were decision variables.

$$f(C) = min(W_T, ICRCS) \tag{3.7}$$

Eq. (3.8) is supporting the fact that every RCS should have a minimum of one connector, and is used in Stage II while determining the optimal number of connectors at RCS, where $CS_i^{connector}$ is the number of connectors at i^{th} RCS.

$$CS_i^{connector} \geq 1 \qquad i = 1,2,..z(numberofRCS) \tag{3.8}$$

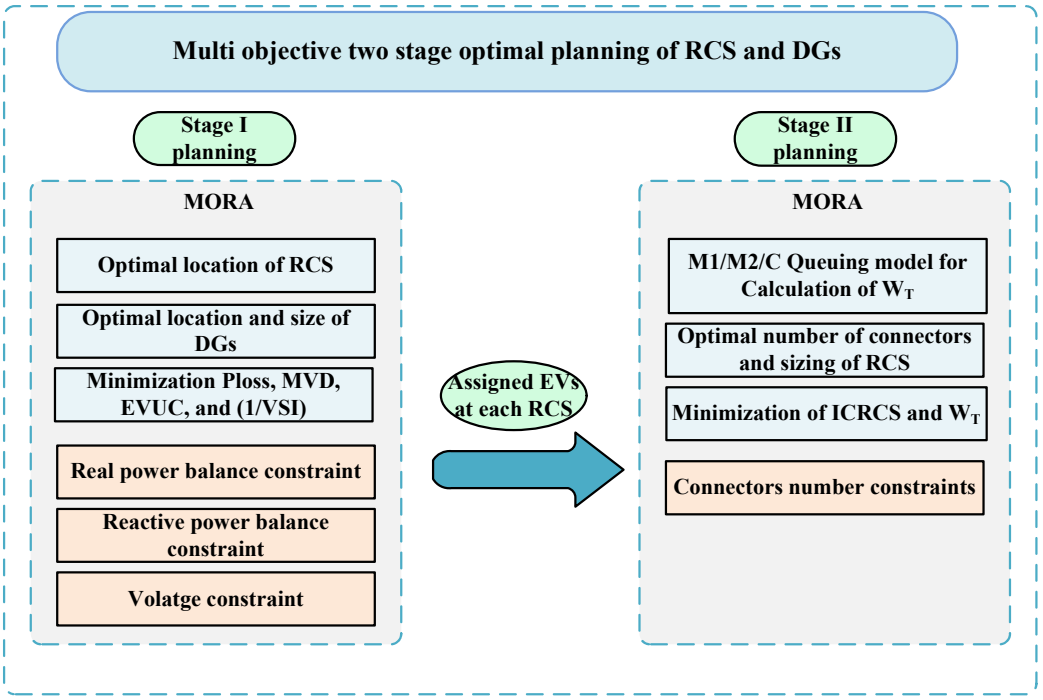

Figure 3.1: Proposed two stage model for optimal planning of RCSs and DGs

3.2.2 DG modelling

Modelling of DGs is necessary for the load flow studies. DGs can be modelled either as PQ mode or PV mode. In this chapter, DG is modelled in PQ mode i.e negative load model. Here, the DG reactive power output is calculated from Eq. (3.9) with known quantities of real power output (P_{dg}) and power factor (pf).

$$Q_{dg} = P_{dg} \times tan(cos^{-1}(pf)) \tag{3.9}$$

3.2.3 RCS modelling

In this work, RCS is modelled as load due to EVs. Real power load (P_i^{RCS}) and reactive power load (Q_i^{RCS}) due to EVs at i^{th} RCS are obtained by Eqs. (3.10) and (3.11) respectively. Eqs. (3.12) and (3.13) are used to determine the connectors and capacity of i^{th} RCS respectively. Here, R_c is the connector capacity, P_{evc} is the charging probability of EVs. P_i^{RCS} depends on the total number of EVs (N_i^{EV}) at i^{th} RCS and rating of EV battery (P_{EV}^{max}). The effective real and reactive power loads ($P_n^{Effload}, Q_n^{Effload}$) at n^{th} bus in power distribution system are calculated using Eq. (3.14) and (3.15) respectively.

It is considered that charging station is operating at 0.95 lag power factor [58].

$$P_i^{RCS} = N_i^{EV} \times P_{EV}^{max} \tag{3.10}$$

$$Q_i^{RCS} = P_i^{RCS} \times tan(cos^{-1}(pf)) \tag{3.11}$$

$$RCS_i^{connectors} = max(P_{evc}) \times N_i^{EV} \tag{3.12}$$

$$RCS_i^{capacity} = RCS_i^{connectors} \times R_c \tag{3.13}$$

$$P_n^{Effload} = P_n^{load} - P_n^{dg} + P_n^{RCS} \tag{3.14}$$

$$Q_n^{Effload} = Q_n^{load} - Q_n^{dg} + Q_n^{RCS} \tag{3.15}$$

3.2.4 Network power loss

RCS integration results in high active power loss as there will be an increase in current flow through the branches. Furthermore, RCS location has a significant impact on power distribution system performance. Power loss can be calculated from the backward forward sweep load flow algorithm. Eq. (3.16) gives the total network power loss at t^{th} hour. Daily power loss was calculated using Eq. (3.17).

$$ploss(t) = \sum_{b=1}^{nb} (i_b)^2 \times (R_b) \tag{3.16}$$

$$Ploss = \sum_{t=1}^{24} ploss(t) \tag{3.17}$$

Where i_b is b^{th} branch current, R_b is b^{th} branch resistance, and nb is the total number of branches. Rapid charging stations (RCSs) impose additional load on the network, resulting in increased power loss and voltage magnitude degradation at the buses.

3.2.5 Voltage Deviation (VD)

Voltage variations beyond the permissible limits are produced by RCSs loading. As a result, the system may become unstable. The voltage stability of the system is achieved by reducing the maximum voltage deviation (MVD) and increasing the voltage stability index (VSI). The load flow algorithm gives the voltage magnitude at each bus. Eq. (3.18) gives the maximum value of voltage deviation ($VD_{max}(t)$) at time t. Maximum

voltage deviation (MVD) over a day can be calculated by Eq. (3.19).

$$VD_{max}(t) = max(1 - v(i), t) \qquad i = 1, 2, 3...N_{distnodes} \tag{3.18}$$

$$MVD = \sum_{t=1}^{24} VD_{max}(t) \tag{3.19}$$

3.2.6 Voltage Stability Index (VSI)

Voltage stability index (Eq. (3.20)) is one of the important factors that gives information about system voltage stability. Utility expects VSI at each bus to be near unity. VSI varies with loading i.e as the loading increases, VSI would reduce. The bus having maximum VSI (≤ 1) is strong, and is capable of taking extra load.

$$VSI_r = 2V_s^2V_r^2 - V_r^4 - 2V_r^2(P_rR(k) + Q_rX(k)) - |z|^2(P_r^2 + Q_r^2) \tag{3.20}$$

Where, VSI_r is VSI at receiving end of a line k, V_r and V_s are receiving end and sending end voltages, P_r and Q_r are real and reactive power at the receiving end of line k, $R(k)$ and $X(k)$ are resistance and reactance of line k.

3.2.7 EV User Cost (EVUC)

When moving from an EV location to RCS, energy is lost. The EV user selects the closest charging station available for charging. The best locations for RCS must take EV user behaviour into account when choosing the RCS to use. Minimization of the user cost of electric vehicles is considered in the objective function while locating RCS.

Consider m ($m \in S$) RCSs dispersed at various sites ($C_1, C_2, ..C_s$). The road transportation network is segmented into Z zones, with electric vehicles assumed to be present at each zone's geometrical center. RCS can be placed at interconnected points of power distribution network and road transportation network in a coupled network. Figure 3.4 shows the test system, in question where each zone and feasible charging station locations were identified by its coordinates i.e (x_{Z_1}, y_{Z_1}) and (x_{C_1}, y_{C_1}) respectively. In a test system, distribution network nodes are the possible locations for RCS placement. So there is a need to find the distance between all zones to selected m charging station locations in optimal planning. Eq. (3.21) can determine the distance between the selected m charging stations and each zone. Information about the distances between all zones and particular charging stations is provided by D matrix Eq. (3.22). Each element in DD

matrix reflects the distance between the nearest RCS among the selected RCS and the corresponding zones and is determined by the minimum value in each row of D matrix using Eq. (3.23). EVs located at the zones are assigned to the nearest RCS.

$$d_{Z_1-C_1} = \sqrt{(x_{Z_1} - x_{C_1})^2 + (y_{Z_1} - y_{C_1})^2} \tag{3.21}$$

$$D = \begin{bmatrix} d_{Z_1-C_1} & d_{Z_1-C_2} & .. & d_{Z_1-C_m} \\ d_{Z_2-C_1} & d_{Z_2-C_2} & .. & d_{Z_2-C_m} \\ . & . & . & . \\ . & . & . & . \\ d_{Z_z-C_1} & d_{Z_z-C_2} & .. & d_{Z_z-C_m} \end{bmatrix} \tag{3.22}$$

$$DD = \begin{bmatrix} min(d_{Z_1-C_1} & d_{Z_1-C_2} & .. & d_{Z_1-C_m}) \\ min(d_{Z_2-C_1} & d_{Z_2-C_2} & .. & d_{Z_2-C_m}) \\ min(. & . & . & .) \\ min(. & . & . & .) \\ min(d_{Z_z-C_1} & d_{Z_z-C_2} & .. & d_{Z_z-C_m}) \end{bmatrix} \tag{3.23}$$

$$EV_{usercost} = \sum_{n=1}^{z} DD(i) \times N_i^{EV} \times E_c \times P_e \tag{3.24}$$

Eq. (3.24) gives the Electric vehicle user cost. Here N_i^{EV} is the number of EVs getting charged from i^{th} RCS, E_c is the average energy consumption of EVs and P_e is the cost of electricity.

3.2.8 Installation Cost of RCSs (ICRCS)

The installation cost of an RCS is important from a charging station owner perspective. ICRCS depends on the number of connectors ($RCS_i^{connectors}$) at RCS, and is computed using Eq. (3.25).

$$ICRCS(i) = C_{init} + 25 \times C_{land} \times RCS_i^{connectors} + C_{con}(RCS_i^{connectors} - 1) \times Pc \tag{3.25}$$

Where, C_{init} is initial investment cost, C_{land} is land cost, $RCS_i^{connectors}$ is the number of connectors at i^{th} RCS, C_{con} is connector cost, and P_c is connector rating.

3.2.9 RCS connector operation Model

The M1/M2/C queuing model is taken into account in this study to describe the serviceability of charging stations [82]. M1 denotes the rate of EV arrivals per hour, M2 is the rate of RCS connector service per hour, and C denotes the number of service points at the charging station. Electric Vehicles (EVs) often drive up to a charging station to charge their batteries. They arrive at a rate of $\lambda/hour$ on average. It is modelled as a non-homogeneous Poisson process as it is time-dependent. Connectors are available in the RCS to charge the EV. These connectors perform the role of servers and charge the EVs at a service rate of $\mu/hour$. In this case, the waiting line for EVs is assumed to be infinitely long. To ensure service to all EVs in the RCS, the arrival rate must always be lower than the service rate (Eq. (3.27)).

$$\lambda(t) = N_{ev}^{iCS} \times P_{evc} \tag{3.26}$$

$$\rho = \frac{\lambda(t)}{C\mu_t} < 1 \tag{3.27}$$

The probability of number of EVs charging at each RCS simultaneously is modelled using Eq. (3.28).

$$p_t(n) = \frac{(C\rho)^n}{n!} \times p_t(0) \qquad\qquad n = 1,2,3,...,C \tag{3.28}$$

$$p_t(0) = \left[\sum_{s=0}^{C-1} \frac{(C\rho)^s}{s!} + \frac{(C\rho)^C}{C!} \frac{1}{(1-\rho)} \right]^{-1} \tag{3.29}$$

Where, $p_t(0)$ as expressed in above equations is the probability of no EV getting charged.

According to Little's equations, Eq. (3.30) gives the expected number of EV users waiting at the RCS at t^{th} hour.

$$E_t[n] = p_t(0) \left[\frac{1}{(C-1)!} \left(\frac{\lambda_t}{\mu_t} \right)^C \frac{\lambda_t \mu_t}{(C\mu_t - \lambda_t)^2} \right] \tag{3.30}$$

Waiting time in queue of EV at t^{th} hour can be calculated using Eq. (3.31). Total waiting time in a 24 hours period at all RCS is calculated using Eq. (3.32)

$$W(t) = \frac{E_t[n]}{\lambda(t)} \tag{3.31}$$

$$W_T = \sum_{i=1}^{m} \sum_{t=1}^{24} W(t) \tag{3.32}$$

It is necessary to calculate the minimum and maximum limit for connectors at each RCS to satisfy Eq. (3.27). The arrival rate at RCS is calculated using Eq. (3.26). Eq. (3.12) can be used to calculate the maximum number of connectors (C^{max}) at RCS, while Eq. (3.33) can be used to get the minimum number of connectors (C^{min}).

$$\frac{\lambda^{max}}{\mu} < C^{min} \qquad \lambda^{max} \in \lambda(t) \tag{3.33}$$

3.3 Multi-Objective Optimization Algorithms

Multi-objective optimization is preferable to identify the best solution for achieving multiple goals. Multiple-objective issues can be resolved using scalarization techniques and Pareto-based approaches. The weighted sum strategy is used in scalarization approaches to combine all the objectives into a single objective function. Here, a single objective is the sum of individual objectives, multiplied by weights according to their priority. However, this approach is not optimal for multi-objective problems with conflicting objectives. In this case, pareto dominance based multi-objective approaches provide the most efficient solutions.

3.3.1 Non dominated Sorting Genetic Algorithm (NSGA II)

A multi objective optimization problem with conflicting objectives can be solved using NSGA II, proposed by Kalyan Deb in [4]. To achieve optimal pareto fronts, crowding distance, and dominance principle are used. Since the objectives are inherently conflicting, the best compromise solution is selected using a fuzzy min-max decision-making method. The flowchart of NSGA II algorithm is shown in Figure 3.2.

3.3.2 Multi Objective Rao 3 Algorithm (MORA)

Dominance principle and crowding distance analysis must be used to determine pareto optimal solutions in a system with multiple objectives that are in conflict with each other. In this study, Multi objective Rao Algorithm (MORA) proposed by Rao in 2021 [5] was used to find the best solution. Fewer algorithmic parameters (population size and maximum iterations) make MORA simpler to understand and use.

The population of a feasible decision variable (P_o) with size (N) is initially generated at random. The rank and crowding distance were used to determine the best and worst solutions after evaluating the fitness function. New solutions (P_n) were determined using Eq. (3.34). A set of solutions of size (N) was chosen from a set ($P_o U P_n$) based on rank and crowding distance after the evaluation of the fitness function for the new solution.

$$\begin{aligned} X^{'}_{i,j,k} = X_{i,j,k} + r1_{j,k}(X_{j,best,k} - |(X_{j,worst,k})|) \\ + r2_{j,k}((|X_{i,j,k} or X_{r,j,k}|) - (X_{r,j,k} or X_{i,j,k})) \end{aligned} \tag{3.34}$$

Here $X^{'}_{i,j,k}$ is the new solution of i^{th} candidate, j^{th} variable in k^{th} iteration. $X_{i,j,k}$ is the old solution of i^{th} candidate, j^{th} variable in k^{th} iteration, $r1, r2$ are random values between [0,1]. $X_{j,best,k}$ is the best value of j^{th} variable of X in k^{th} iteration. $X_{j,worst,k}$ is the worst value of j^{th} variable of X in k^{th} iteration. $X_{r,j,k}$ randomly selected r^{th} candidate, j^{th} variable in k^{th} iteration. The flowchart of MORA for optimal planning is shown in Figure 3.3.

3.3.3 Implementation of Multi Objective Rao 3 Algorithm (MORA) for optimal planning of RCS and DGs

Step 1: Read the test system data and initialize the algorithm parameters (population size and maximum iterations).
Step 2: Randomly initialize the population and determine the respective fitness values.

- $Pop_{stage1} = [l_{RCS}, l_{DG}, S_{DG}]$ for Stage 1
- $Pop_{stage2} = [C]$ for Stage 2.
  (l_{RCS} is location of RCS, l_{DG} is location of DG, S_{DG} is size of DG, and C is number of connectors).

Step 3: Set gen = 1.
Step 4: Perform the non dominated sorting and calculate the crowding distance.
Step 5: Obtain best and worst solutions based on the non dominated sorting and crowding distance.
Step 6: Update the candidate solutions based on the update equation (3.34) and find the updated fitness value.
Step 7: Combine both old and modified solutions and perform non dominated sorting and crowding distance.

Step 8: Select best population of size (N) from combined solutions of size 2N.
Step 9: Set Iter=Iter+1.
Step 10: Terminate the process, if ($Iter > Iter_{max}$) and save the pareto optimal front data otherwise continue from step 4 to step 10.
Step 11: Perform the fuzzy min max decision making technique to select the compromised optimal solution optimal front and print the results.

Table 3.1: Parameters of EV

Parameters	Values
EV battery capacity	27.69 kWh
No of EVs	600
Avg. power consumption	0.142 kWh/km
Connector rating (P_c)	96 kW

Table 3.2: Cost coefficients of land

Coefficients	Costs
C_{init}	70000 $
C_{land}	240\$/m^2
C_{con}	280.33\$/kW

Table 3.3: Classification of connected loads in IEEE 33 bus RDS

Residential loads	Commercial loads	Industrial loads
2,3,5,6,7,8	4,11,12,18	22,26,27,28
9,10,13,14,15	19	29,30,31,32
16,17,20,23,24	–	33

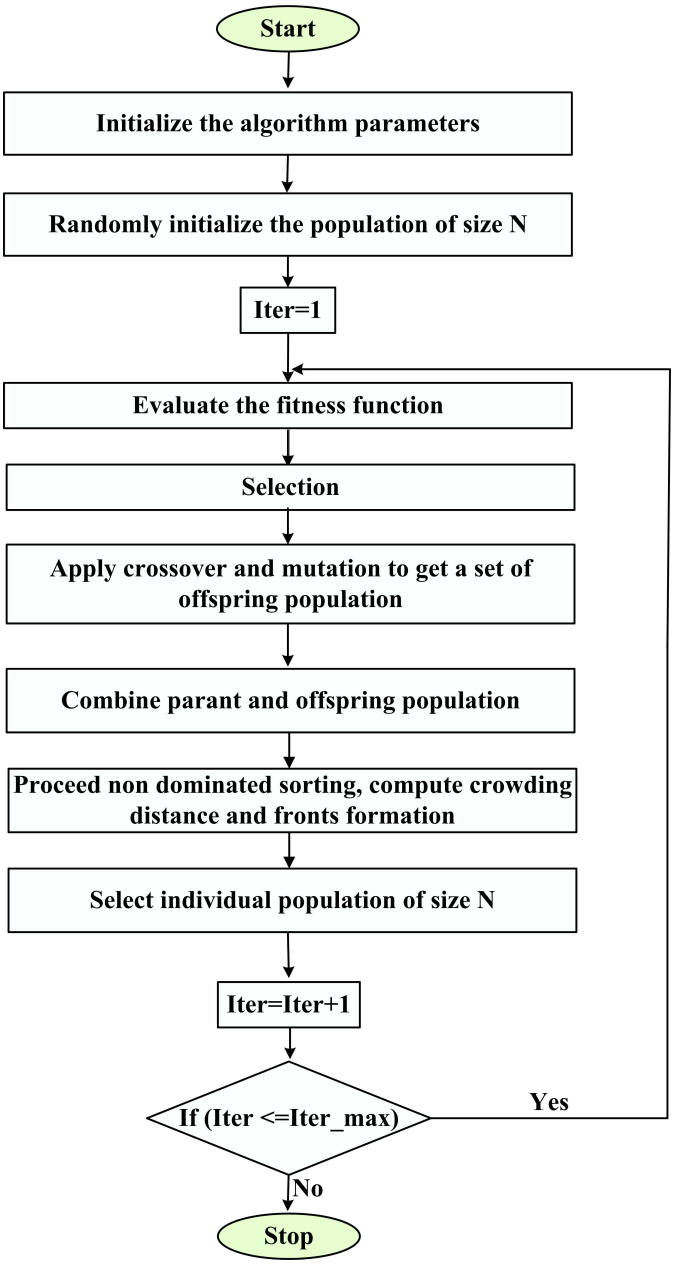

Figure 3.2: Flowchart of NSGA II [4] for the proposed problem.

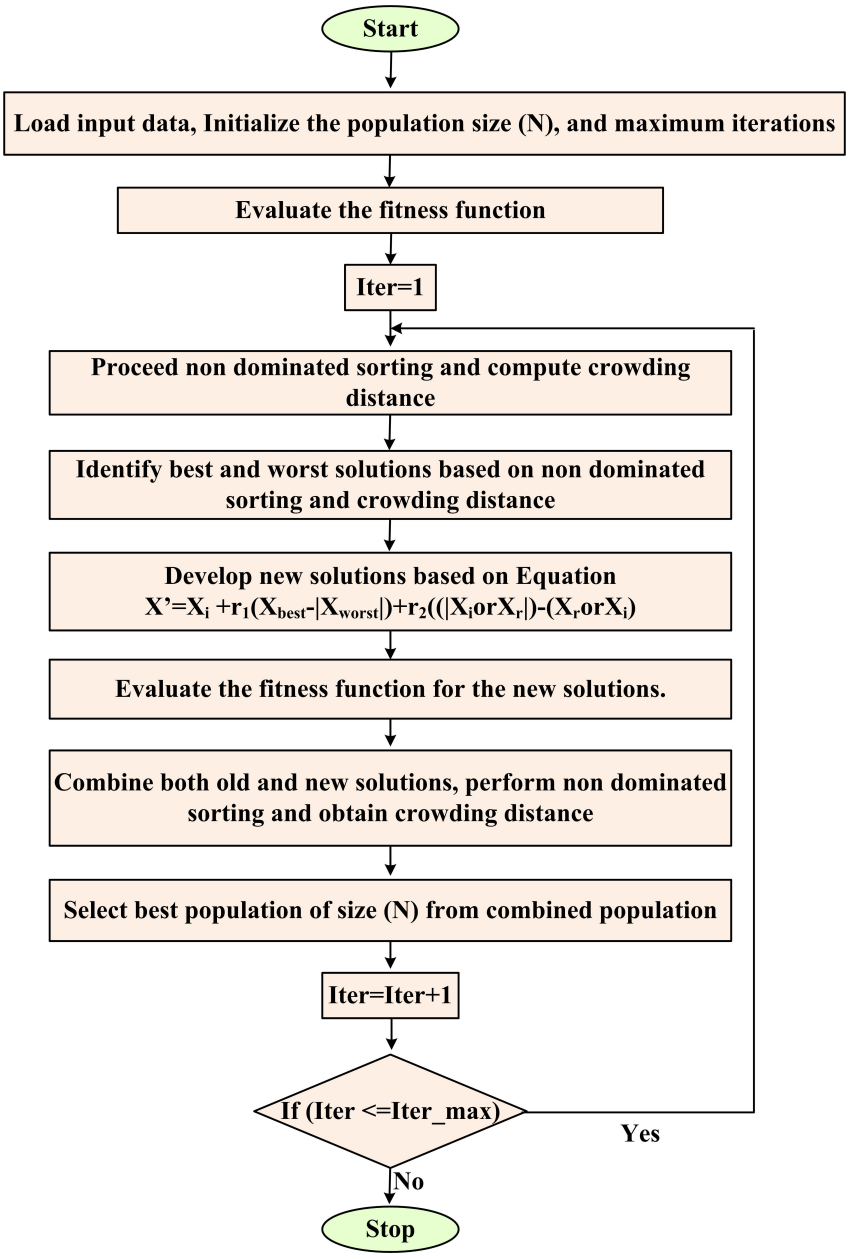

Figure 3.3: Flowchart of MORA [5] for the proposed problem.

3.4 Simulation Results and Discussion

The effectiveness of the proposed method for RCS and DG optimal planning in coupled networks was evaluated on the proposed test system. The proposed test system is a coupled network of IEEE 33 bus power distribution system superimposed on a 20×38 km^2 road transportation area. The transportation area in chosen test system is divided into 190 zones with each zone having an area of $2 \times 2km^2$. It is considered that EVs are

located at the geometrical center of each zone, and the distribution of 600 EVs throughout 190 zones in the transportation area is represented in Table 3.4. In the first stage, the best location for RCS and the best location and size for DGs were determined simultaneously. Queuing theory was employed in the second Stage to size RCS properly. In both stages, multi-objective Rao 3 algorithm (MORA) was used to solve optimization problems with a population size of 30 and 100 iterations respectively. The optimal results obtained by MORA were compared with the results obtained by NSGA II algorithm. The parameters considered for NSGA II in optimization population size of 30, maximum generation of 100, crossover probability of 0.8, and mutation probability of 0.33.

Table 3.4: Assumed Number of Electric Vehicles assigned to each of the 190 zones of Transportation system

1	4	3	1	5	1	1	2	3	4	4	5	5	4	2	5	3	3	4
3	4	2	4	1	3	3	1	5	5	4	4	2	1	2	4	5	1	4
3	5	4	1	1	5	4	5	4	4	3	1	3	3	5	2	5	5	2
4	1	2	2	5	2	2	4	4	4	5	4	2	3	5	2	2	5	1
4	3	4	4	4	5	4	1	4	3	4	4	4	1	2	1	5	3	4
2	4	5	3	3	4	2	3	3	5	3	4	3	3	1	5	4	2	1
5	5	4	2	2	2	4	4	5	5	2	5	4	2	2	3	3	3	2
5	5	4	2	4	4	3	5	5	4	1	1	1	5	3	4	3	3	3
1	4	3	1	1	1	4	2	1	3	5	4	4	2	2	1	4	3	3
4	1	1	1	5	1	4	3	5	2	1	2	4	3	5	4	1	5	4

Figure 3.5 shows the probability of EVs charging at RCS. Observations show that EVs do not charge before 5:00 am and after 9:00 pm. The line and load data for IEEE 33 bus system were taken from [102]. There are 33 buses and 32 lines in the test system. Of the 33 buses, 17 carry residential loads, 9 carry industrial loads, and 5 carry commercial loads (Table 3.3). In this study, the variation in load was also taken into account. Figure 3.6 depicts the load demand variation over 24 hours. Simulations were carried out in MATLAB 2014b software with PC specification of Intel core i3 processor and 4 GB RAM.

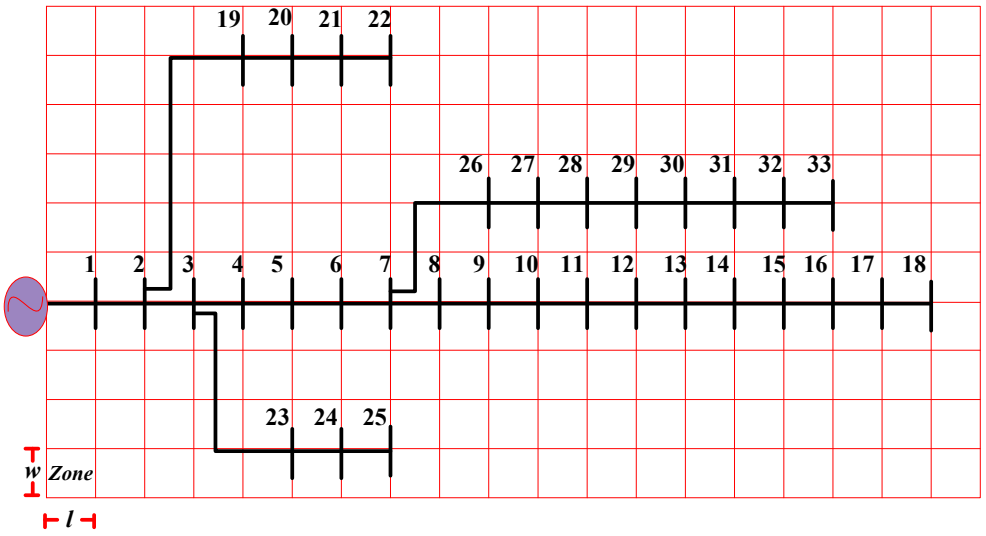

Figure 3.4: Test system (Coupled network of Road transportation network and IEEE 33 Bus Power distribution network)

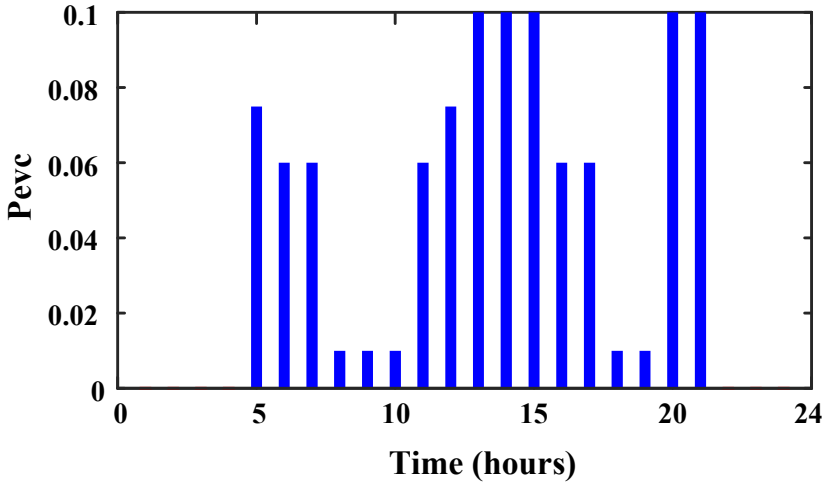

Figure 3.5: Electric Vehicle charging probability

3.4.1 Base case

The analysis of test system was done without integrating RCSs and DGs in Base case. Backward forward sweep algorithm was employed to analyse the network, because the test system consists of IEEE 33 bus power distribution system, which has high R/X

ratio. It reported a Base case active power loss of 2811 kW, maximum voltage deviation of 1.5816 (p.u.), and voltage stability index (VSI_{min}) of 0.6479. Figure 3.7 shows a plot of voltage profiles of IEEE 33 bus RDS for 24 hours at each bus. It is observed from Figure 3.7 that at 17^{th} hour the system's minimum voltage is 0.8968 (p.u.) at the 18^{th} bus of IEEE 33 Bus RDS.

3.4.2 Stage 1: Optimal location of RCSs and optimal location and sizing of DGs

MORA was used to find the optimal locations for RCSs and optimal locations and sizes for DGs in the first stage. Two scenarios, with three cases in each, were used to analyse the optimal planning.

3.4.2.1 Scenario 1: Optimal planning of RCS in coupled network

In this scenario, the analysis of network was done by integrating RCSs. In scenario 1 three cases were considered to analyse the network for optimal planning of RCSs. MORA algorithm was applied in each case to get the optimal fronts.
Case 1: *Optimal planning of RCSs by minimizing Ploss, MVD, and EVUC.*
Case 2: *Optimal planning of RCSs by minimizing Ploss, 1/VSI$_{min}$, and EVUC.*
Case 3: *Optimal planning of RCSs by minimizing Ploss, MVD, 1/VSI$_{min}$, and EVUC.*

Table 3.5: Optimal locations of RCSs and the number of EVs assigned to RCSs in Scenario 1 by NSGA II and MORA for different cases

Case No.	NSGA II		MORA	
	RCSs location	Number of EVs	RCSs location	Number of EVs
Case 1	2, 23, 27	150, 69, 381	2, 19, 27	134, 70, 396
Case 2	2, 22, 27	165, 77, 358	2, 19, 24	103, 198, 299
Case 3	2, 19, 23	102, 235, 263	2, 19, 22	171, 57, 372

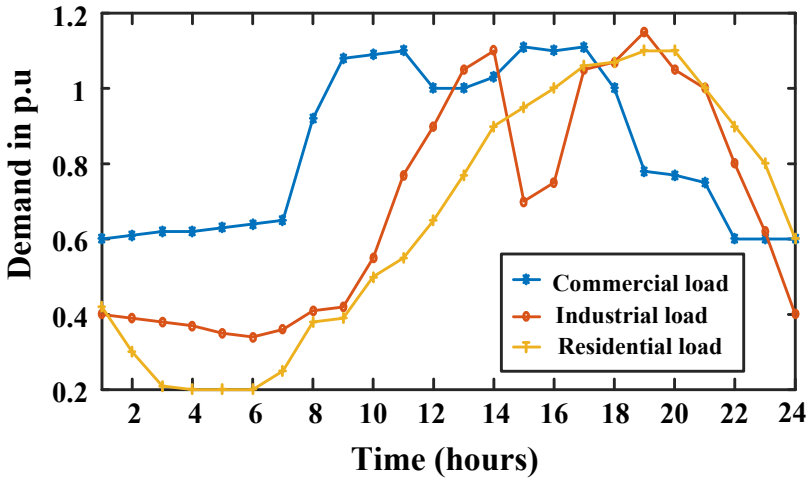

Figure 3.6: Plot of load demands of various types of loads

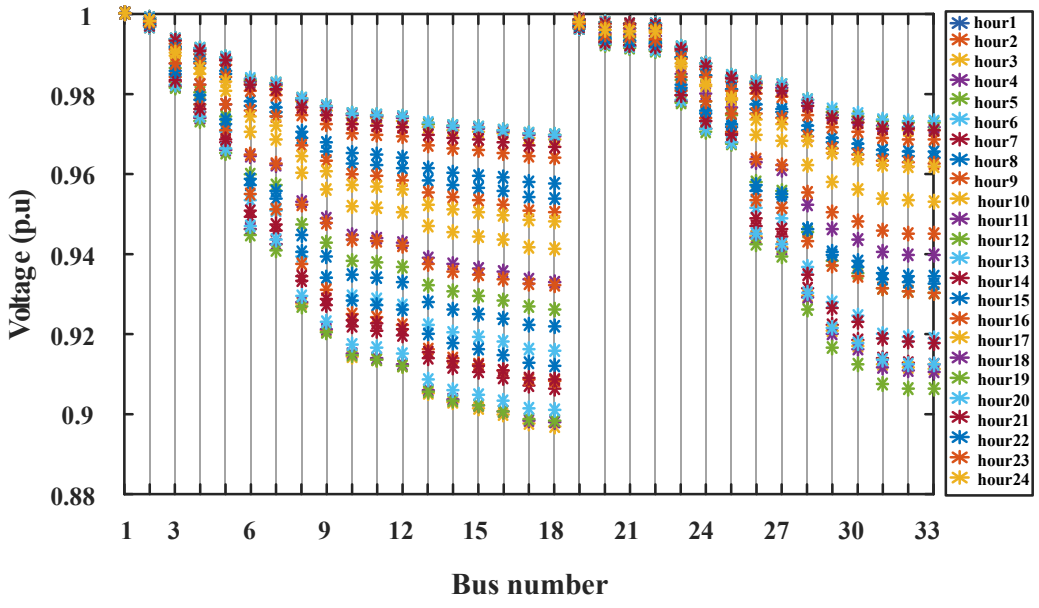

Figure 3.7: Plot of Voltage profiles at each bus of IEEE 33 Bus RDS for 24 hours with out the integration of RCSs and DGs

Fuzzy min max decision making technique was employed to achieve the compromised optimal solution. The optimal pareto front in Case 3 by MORA is shown in Figure

3.13. Optimal locations of RCSs and the corresponding objective function parameters are given in Table 3.5 and Table 3.6 respectively.

Table 3.6: Objective function parameters in Scenario 1 by NSGA II and MORA for different Cases

Case No.	NSGA II				MORA			
	Ploss (kW)	MVD (p.u)	VSI_{min}	EVUC ($)	Ploss (kW)	MVD (p.u)	VSI_{min}	EVUC ($)
Case 1	3572.8	1.7223	0.6182	60.7222	3560.3	1.7217	0.6182	60.0221
Case 2	3499.8	1.7093	0.6219	60.9249	3124.5	1.6124	0.6424	88.6718
Case 3	3026	1.6093	0.6430	94.2015	2977.1	1.5898	0.6464	86.7004

From Table 3.6, it is observed that MORA algorithm yielded better objective parameters compared to NSGA II with Ploss of 3560.3 kW, MVD of 1.7217 (p.u), VSI_{min} of 0.6182, and EVUC of 60.0221 $ in Case 1. The maximization of VSI in place of MVD resulted in improvement of voltage profile in Case 2. Better values of Ploss, MVD, and VSI_{min} were obtained by MORA in Case 2. However the highest EVUC was encountered by MORA (EVUC 88.6718 $) compared to NSGA II (EVUC 60.9249 $). The consideration of VSI maximization along with minimization of Ploss, MVD, and EVUC resulted in better voltage profile (MVD, VSI) and Ploss in Case 3 compared to all cases in Scenario 1. In Case 3, MORA yielded Ploss of 2997.1 kW, MVD of 1.5898 (p.u), VSI_{min} of 0.6464, and EVUC 86.7004 $. From Figure 3.8 and Figure 3.9, it is observed that the presence of RCSs in the test system resulted in reduction of minimum voltage of the system to 0.8963 (p.u) and 0.8951 (p.u) at 18^{th} bus in 17^{th} hour by MORA and NSGA II algorithms, respectively compared to Base case (0.8968 (p.u)). From Scenario 1, it is clear that though the RCSs are placed at appropriate locations in the distribution network, it resulted in increased power loss i.e 1.07 % of Base case (Ploss) and deteriorated voltage profile.

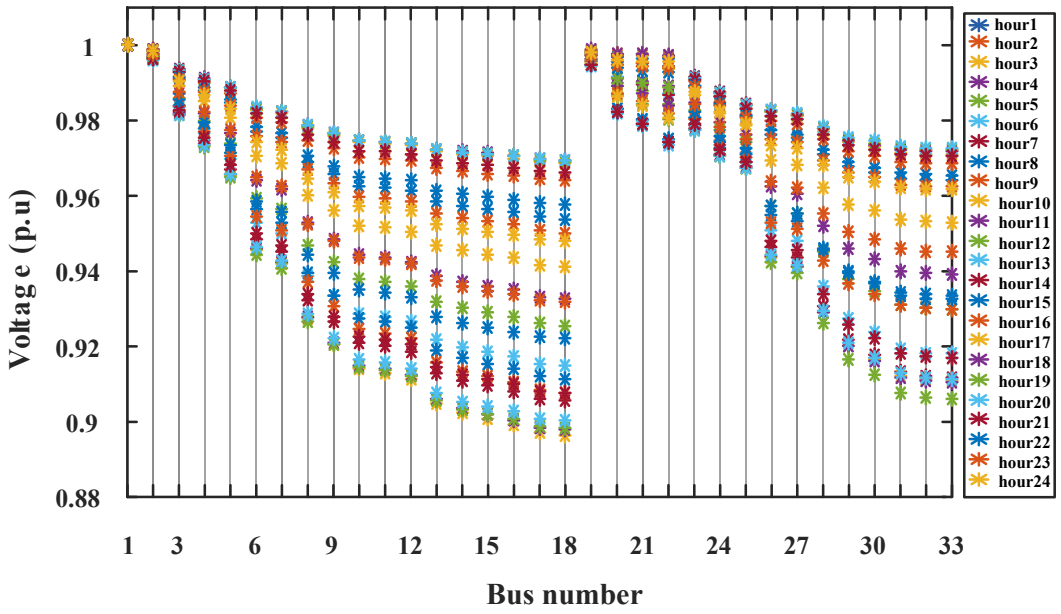

Figure 3.8: Plot of Voltage profiles at each bus of IEEE 33 Bus RDS for 24 hours with the integration of RCSs by MORA in Case 3

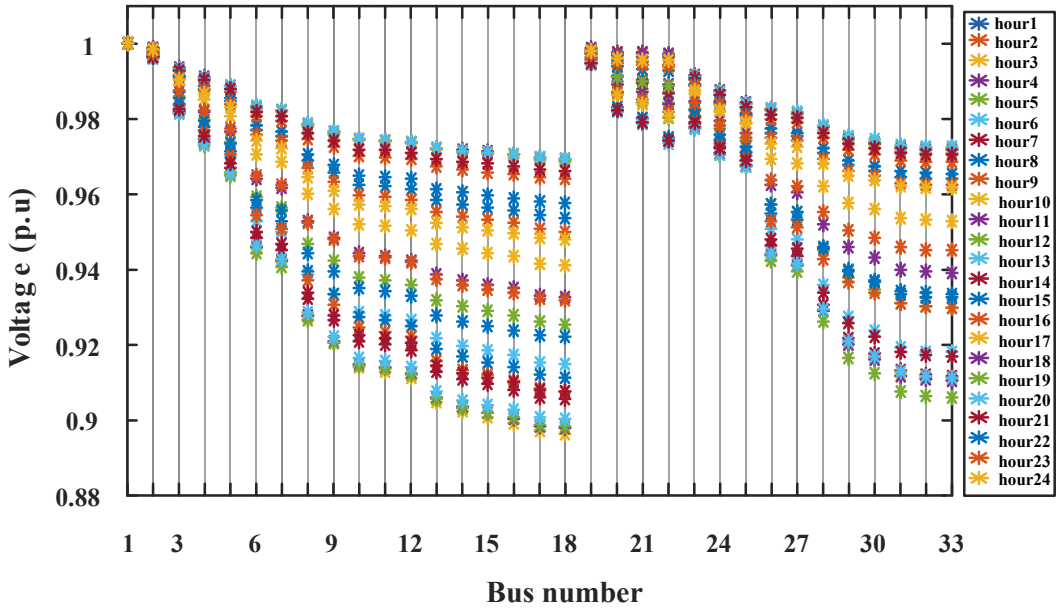

Figure 3.9: Plot of Voltage profiles at each bus of IEEE 33 Bus RDS for 24 hours with the integration of RCSs by NSGA II in Case 3

3.4.2.2 Scenario 2: Concurrent optimal planning of RCSs and DGs.

Though the RCSs were located at optimal places, loading due to RCSs would reduce the performance of the power distribution system. To solve the above issue, Renewable type DGs of size 5 kW-1 MW placement in power distribution system was adopted in this chapter in Scenario 2. The power distribution system has a minimum active power demand of 1420 kW at 4^{th} hour (Figure 3.10). To prevent reverse power flow, the total active power supplied by DGs is limited to less than or equal to 1400 kW. Three cases were considered in this scenario to analyse the network.

Case 4: *Concurrent optimal planning of RCSs and DGs in coupled network by minimizing the Ploss, EVUC, and MVD.*

Case 5: *Concurrent optimal planning of RCSs and DGs in coupled network by minimizing the Ploss, EVUC, and $1/VSI_{min}$.*

Case 6: *Concurrent optimal planning of RCSs and DGs in coupled network by minimizing the Ploss, EVUC, $1/VSI_{min}$, and MVD.*

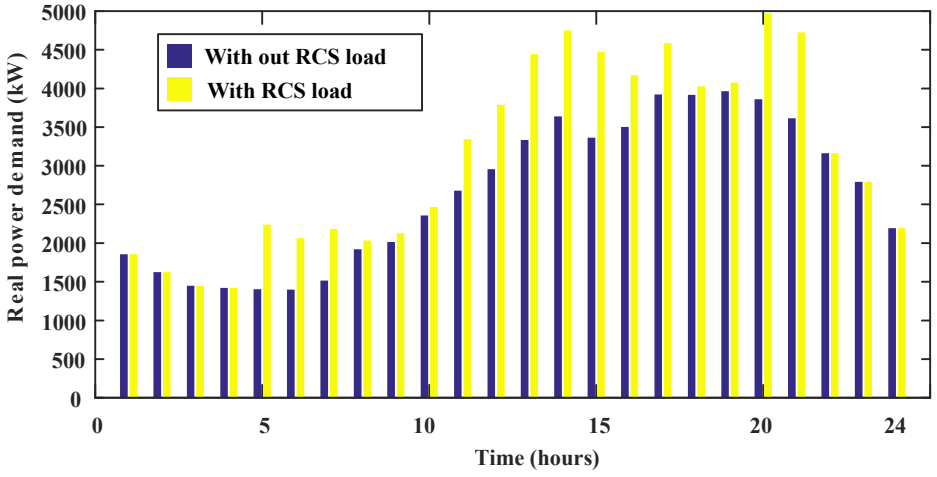

Figure 3.10: Daily Real power demand with and without RCSs load

MORA and NSGA-II algorithms were applied on the test system to obtain optimal locations and sizes of RCSs and DGs. Fuzzy min max decision making was employed to obtain the best compromised solution from optimal fronts. The optimal front by MORA is shown in Figure 3.14. The optimal locations of RCSs and assigned EVs at RCSs obtained by MORA and NSGA II algorithms are mentioned in Table 3.7. Optimal locations and sizes of DGs obtained by MORA and NSGA II are given in Table 3.8.

Objective parameters obtained in various cases by MORA and NSGA II algorithms in Scenario 2 are listed in Table 3.9.

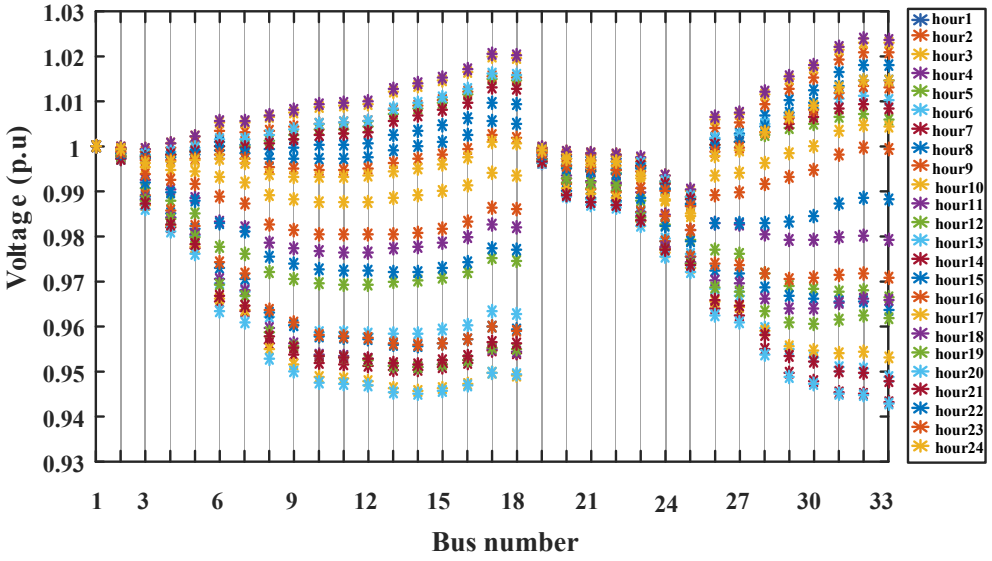

Figure 3.11: Plot of Voltage profiles at each bus of IEEE 33 Bus RDS for 24 hours with the integration of RCSs and DGs by MORA in Case 6

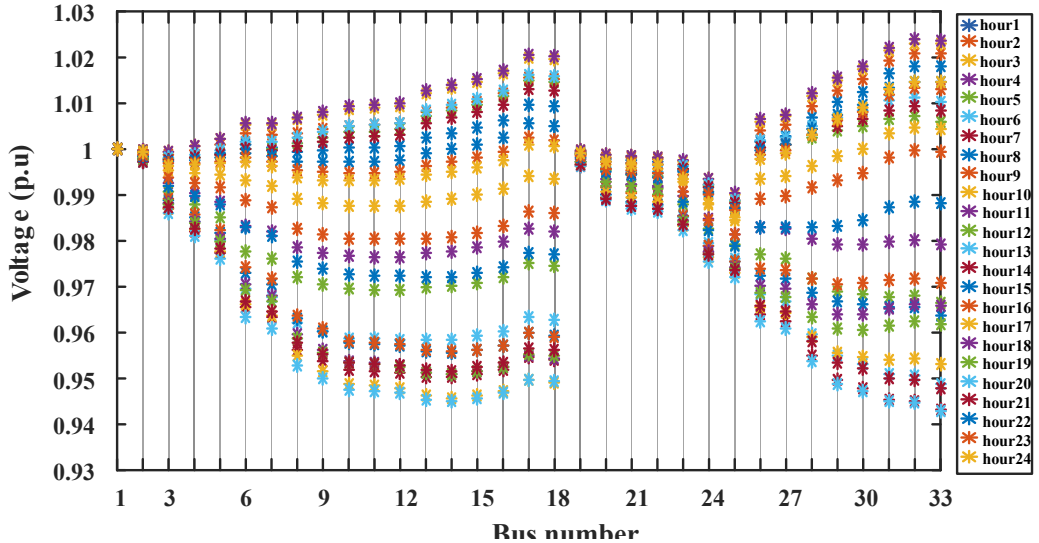

Figure 3.12: Plot of Voltage profile at each bus of IEEE 33 Bus RDS for 24 hours with the integration of RCSs and DGs by NSGA II in Case 6

Table 3.9 shows that the integration of DG reduced power loss, MVD, and improved VSI

of power distribution system compared to Scenario 1. In Case 4, MORA algorithm led to lower power loss (1228.1 kW), MVD (0.6955 (p.u), and EVUC (52.5431 $) compared to NSGA II. However, better VSI_{min} (0.7870) was obtained by NSGA II.

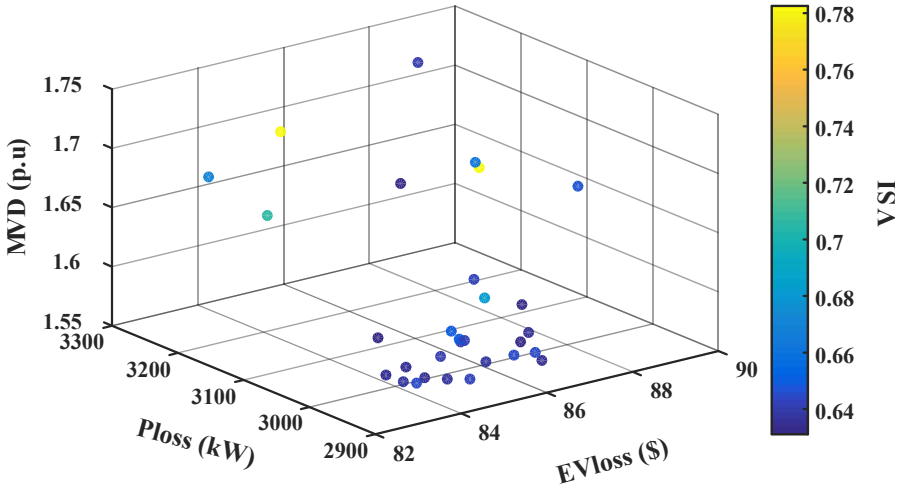

Figure 3.13: Optimal pareto-front of Ploss, MVD, VSI, and EVUC by MORA in Case 3

Table 3.7: Optimal locations of RCSs and the number of EVs assigned to RCSs in Scenario 2 by NSGA II and MORA for different cases

Case No.	NSGA II		MORA	
	RCSs location	Number of EVs	RCSs location	Number of EVs
Case 4	2, 21, 32	178, 138, 284	2, 22, 32	196, 135, 269
Case 5	2, 21, 30	167, 107, 326	2, 21, 29	163, 33, 338
Case 6	2, 21, 33	183, 157, 260	2, 22, 33	201, 151, 248

Table 3.8: Optimal locations and sizes of DGs in Scenario 2 by NSGA II and MORA for different cases

Case No.	NSGA II		MORA	
	DG location	DG size	DG location	DG size
Case 4	18, 30, 33	383, 246, 748	9, 18, 33	280, 300, 804
Case 5	15, 18, 33	708, 226, 443	11, 17, 32	280, 250, 854
Case 6	17, 30, 32	383, 276, 718	14, 30, 32	483, 103, 804

In Case 5, lower Ploss (1274.2 kW), MVD (0.7035 (p.u)), and better VSI_{min} (0.7797) were obtained by MORA compared to NSGA II. Furthermore, the maximization of VSI along with the minimization of Ploss and EVUC resulted in better values of VSI_{min} (0.7797) in Case 5 compared to Case 4 (VSI_{min} (0.7785)) by MORA. Collective consideration of Ploss, MVD, VSI_{min} and EVUC parameters in objective function resulted in lowest Ploss (1182.3 kW), MVD (0.6864 (p.u)), and better value of VSI_{min} of 0.7946 and EVUC of 53.4033 $ in Case 6 by MORA. The minimum voltage of system is 0.9432 (p.u) in Case 6, at bus 33 in 17^{th} hour (Figure 3.11). It was more compared to 0.9428 (p,u) by NSGA-II in Case 6 (Figure 3.12). The voltage at 18^{th} bus 17^{th} hour improved to 0.9461 (p.u) compared to base case (0.8968 (p.u)).

Table 3.10: Comparison of objective function parameters in Base case, Case 3, and Case 6

Case No.	Ploss (kW)	MVD (p.u)	VSI_{min}	EVUC ($)
Base case	2811	1.5816	0.6479	–
Case 3	2977.1	1.5898	0.6464	86.7004
Case 6	1182.3	0.6864	0.7946	53.4033

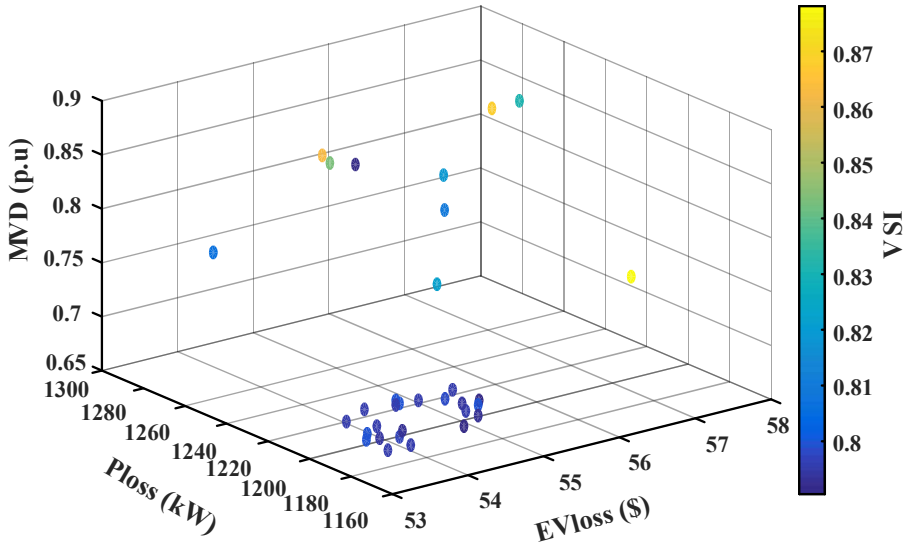

Figure 3.14: Optimal pareto-front of Ploss, MVD, VSI, and EVUC by MORA in Case 6

The objective function parameters of best cases from scenario 1 (Case 3), scenario 2 (Case 6) and Base case are listed in Table 3.10. Table 3.10 shows concurrent optimal planning of RCSs and DGs (Case 6) solved the issues caused by the integration of RCSs (Case 3). Ploss was 42 % of base case in Case 6 while it was 107 % in Case 3. MVD was 43.17 % of Base case MVD in Case 6 while it was 100.6 % in Case 3.

Maximum value of VSI_{min} was obtained in Case 6 compared to Base case and Case 3. Furthermore, lowest EVUC (53.4033 $) was obtained in Case 6 compared to Case 3. Therefore, the proposed method of integration of DGs along with RCSs is a viable method to optimally locate RCSs without losing power distribution system performance. Furthermore, selecting optimal number of connectors at each RCS is necessary to minimize the installation cost of RCSs and waiting time in queue at RCSs. This would benefit the RCS owner financially. To achieve this goal, the optimal number of connectors was calculated in Stage 2.

3.4.3 Stage 2: Optimal sizing of RCSs

The number of connectors at RCS decides its size, cost, and waiting time for EVs to be charged at RCS. In the literature, Eqs. (3.12) and (3.13) were used to calculate the connectors at RCSs and RCS capacity. However, Eq. (3.12) gives maximum connectors at RCS. Consideration of maximum connectors at RCS results in high installation cost and low waiting time in queue. However, it is not feasible. Hence, it is necessary to determine the optimal number of connectors.

Table 3.11: Comparison of results in traditional and proposed approach in stage 2

Parameter	Traditional approach	Proposed approach	
		NSGA II	MORA
Optimal no of connectors	20, 15, 25	9, 13, 15	10, 8, 14
RCS capacity (kW)	1920, 1440, 2400	864, 1248, 1440	960, 768, 1344
ICRCS ($)	3.15×10^6	2.01×10^6	1.75×10^6
W_T (min)	0.0088	35.5202	27.9801

From Stage 1, it is observed that in Case 6, better objective parameters are obtained by MORA. In Case 6, three RCSs were optimally located at 2^{nd}, 22^{nd}, and 33^{rd} buses of distributions system with each assigned EVs of 201, 151, and 248 respectively.

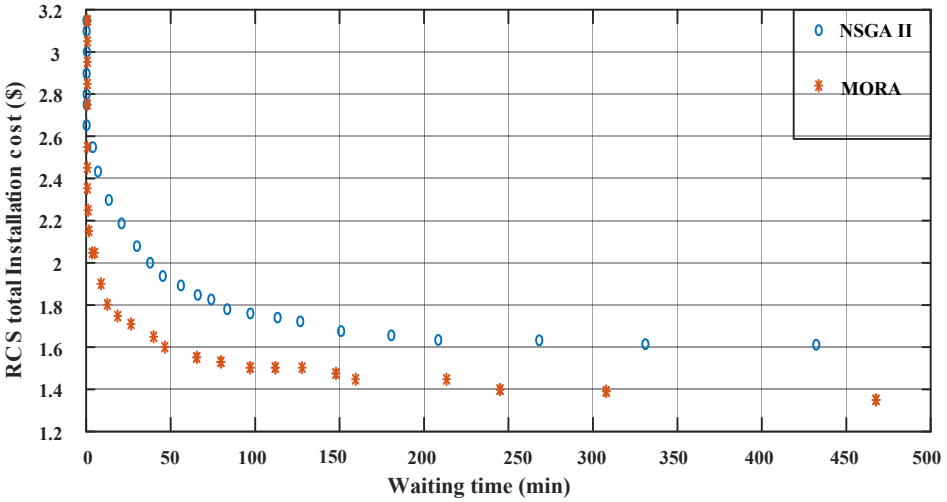

Figure 3.15: Plot of Waiting time and RCSs total installation cost by MORA and NSGA II

To employ queue theory, arrival rate ($\lambda(t)$) at each RCS and, the service rate of connector is required. Here, Arrival rate ($\lambda(t)$) at RCS is time dependent, and is obtained by Eq. (3.26). EV battery takes 22 minutes to get 85% charge [82]. Hence service rate μ/hr of $2.73/hr$ was considered in this chapter. Here the number of connectors (C) at each RCS is a variable, its minimum (C^{min}) and maximum (C^{max}) limits are calculated according to Eqs. (3.33) and (3.27) respectively. NSGA II and MORA algorithms were applied to obtain the compromised optimal feasible solution for sizing of RCS with C limits of C^{min} =[8, 6, 10] and C^{max} = [20, 15, 25]. Fuzzy min max decision making was used to find the best solution among solutions from pareto fronts.

Table 3.11 shows that, traditionally 20, 15, and 25 connectors were installed at RCS 1, RCS 2, and RCS 3 respectively. This resulted in maximum installation cost of 3.15×10^6\$ and minimum waiting time in queue of 0.0088 minutes i.e no waiting time in queue. However, it is not economical for the owner of RCS because of which waiting time was considered in the proposed approach. Using the proposed approach, NSGA II yielded 2.01×10^6\$ installation cost and 36.96 minutes of waiting time in queue for 9, 13, and 15 connectors at RCS 1, RCS 2, and RCS 3 respectively. Best compromised objective parameters of 1.75×10^6\$ installation cost and 27.9801 minutes of waiting time in queue were obtained with 10, 8, and 14 connectors by MORA. The optimal

connectors decided the size of RCS 1 as 960 kW, RCS 2 as 768 kW, and RCS 3 as 1344 kW by MORA. The plot between waiting time in queue and installation cost by NSGA II and MORA (Figure 3.11) shows the effectiveness of MORA in achieving optimal results.

3.5 Summary

The proposed two stage approach considered the distribution network operational parameters, EV user behaviour, and charging station owner perspectives in optimal planning of RCS, which was validated on coupled road transportation network and power distribution network. In the planning, M1/M2/C queuing model was used for finding the waiting in queue at RCS. During the analysis, the load demand variation of various types of load and variation of EV charging probability was considered.

The formulation of placement problem as multi objective problem and solved through the pareto based Multi objective Rao algorithm (MORA) yielded better locations and capacities that favoured optimal performance of power distribution system in Stage 1. Optimal number of connectors obtained in Stage 2 at each RCS favoured EV user by reducing waiting time and RCS owner by reducing RCS installation cost. This work can be further extended by integrating the D-STATCOM along with RCS and DGs to enhace the performance of power distribution system.

Table 3.9: Objective function parameters in scenario 2 by NSGA II and MORA for different cases

Case No.	NSGA II				MORA			
	Ploss (kW)	MVD (p.u)	VSI_{min}	EVUC ($)	Ploss (kW)	MVD (p.u)	VSI_{min}	EVUC ($)
Case 4	1272.4	0.7003	0.7870	53.2199	1228.1	0.6955	0.7785	52.5431
Case 5	1408.3	0.7267	0.7619	53.3290	1274.2	0.7035	0.7797	54.7130
Case 6	1218.2	0.6964	0.7933	54.4474	1182.3	0.6864	0.7946	53.4033

Chapter 4
Optimal planning of RCSs, DGs, and D-STATCOMs in coupled network

4.1 Introduction

Two stage approach proposed in the previous chapter improved the performance of power distribution system. However, the integration of D-STATCOMs along with RCSs and DGs would result in better performance. This chapter proposes a two stage methodology for optimal planning of RCSs, D-STATCOMs, and DGs in a coupled power distribution and road transportation network. Best optimal positions of RCSs and optimal positions and capacities of DGs and D-STATCOMs are identified in Stage 1 by considering the minimization of power loss, voltage deviation, EV user cost, and maximization of voltage stability index. In Stage 2, optimal connectors count is identified by considering the minimization of installation cost of RCSs and waiting time in queue at RCSs.

4.2 Problem formulation

4.2.1 Distributed Generator modelling

Distributed generators (DG) can be modelled either in PV mode or PQ mode. PQ mode is a negative load model, implying that the output of the DG is simulated as a negative load. In this chapter, PQ load modelling is considered, hence reactive power output (Q_{dg}) is computed using known values of real power output (P_{dg}) and DG operational power factor (pf_{dg}) using Eq. (4.1).

$$Q_{dg} = P_{dg} \times tan(cos^{-1}(pf_{dg})) \tag{4.1}$$

4.2.2 D-STATCOM modelling

D-STATCOM is a power electronic device consisting of a voltage source converter supported by a DC source. It injects/absorb reactive power into/from a power distribution system. D-STATCOM can mitigate the issues like voltage fluctuations, low power factor, power loss, and reliability. In the thesis D-STATCOM is used as reactive power

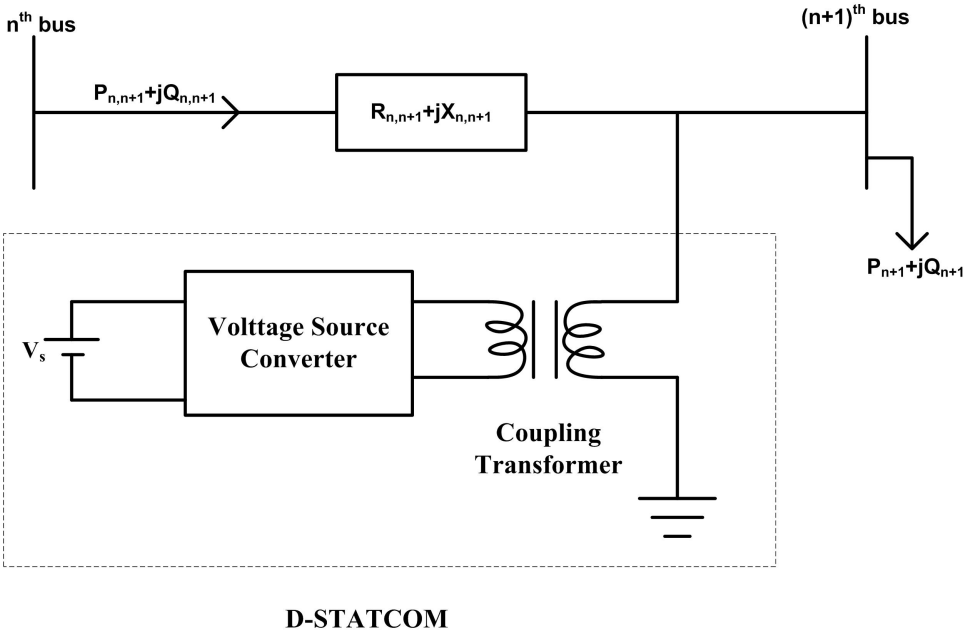

Figure 4.1: Single line diagram of Radial distribution system with D-STATCOM

compensating device to support RDS by injecting reactive power at connected node. It is modelled in negative load (PQ) mode [56]. The single line diagram of radial distribution system connected with D-STATCOM is shown in Fig. 4.1. Integration of D-STATCOM at n^{th} bus of power distribution network could change the net reactive power; it is computed using Eq. (4.2), where, Q_n^{new} is the new demand after adding D-STATCOM at n^{th} bus. Q_n^{base} is the base reactive power demand at n^{th} bus and Q_n^{DS} is the reactive power output of D-STATCOM at n^{th} bus. Eq. (4.3) and Eq. (4.4) gives power loss after the placement of D-STATCOM and Eq. (4.5) gives loss reduction due to D-STATCOM integration.

$$Q_n^{new} = Q_n^{base} - Q_n^{DS} \tag{4.2}$$

$$P_{loss}(n,n+1) = \frac{P_{n+1}^2 + (Q_{n+1}^{base} - Q_{n+1}^{DS})^2}{|V|^2} R_{n,n+1} \tag{4.3}$$

$$P_{loss}(n,n+1) = \frac{P_{n+1}^2 + Q_{n+1}^{2,base}}{|V|^2} R_{n,n+1} + \frac{Q_{n+1}^{2DS} - 2Q_{n+1}^{DS} Q_{n+1}^{base}}{|V|^2} R_{n,n+1} \tag{4.4}$$

$$\Delta P_{loss}^{DS} = \frac{Q_{n+1}^{2DS} - 2Q_{n+1}^{DS} Q_{n+1}^{base}}{|V|^2} R_{n,n+1} \tag{4.5}$$

4.2.3 Rapid Charging Stations (RCSs)

Rapid charging stations are needed to charge Electric Vehicle (EVs) batteries. These RCSs acts as bulk load on the power distribution system. RCS works at lagging power factor (0.95), so it has the real power load and reactive power load [58]. The real power load (P^{RCS}) due to i^{th} RCS depends on the number of EVs getting charged and the rating of EV battery $P^{max}_{EV,B}$ from a particular RCS, it is calculated using Eq. (4.6). Reactive power load (Q^{RCS}) due to i^{th} RCS is calculated using Eq. (4.7).

$$P^{RCS}(i) = N^{iRCS}_{EV} \times P^{max}_{EV,B} \tag{4.6}$$

$$Q^{RCS}(i) = P^{RCS}(i) \times tan(cos^{-1}(pf_{EV})) \tag{4.7}$$

4.2.4 Objective function

Optimal planning of DGs and D-STATCOMs along with RCSs is done in two stages. In Stage 1, the most suitable locations for RCSs, D-STATCOMs, and DGs, and capacities of DGs and D-STATCOMs are determined by considering minimization of active power loss (Ploss), maximum voltage deviation (MVD), EV user cost (EVUC), and maximizing of voltage stability index (VSI). Eq. (4.8) shows the objective function considered in Stage 1, where the location of RCS (l_{RCS}), location of DG (l_{DG}), size of DG (S_{DG}), location of D-STATCOM (l_{DST}), and size of D-STATCOM (S_{DST}) are the decision variables.

$$f(l_{RCS}, l_{DG}, l_{DST}, S_{DG}, S_{DST}) = min(Ploss, MVD, EVUC, 1/VSI) \tag{4.8}$$

Number of EVs that are taking energy from a particular RCS is calculated in Stage 1, and it is utilised in Stage 2 for determining the waiting time at the corresponding RCS. Minimization of building cost of RCS (ICRCS) and waiting time (W_T) at RCS are considered in Stage 2 for determining the optimal capacity of RCS. The objective function taken into account in Stage 2 is shown in Eq. (4.9), where the decision variable is the connectors count (C) at each RCS.

$$f(C) = min(ICRCS, W_T) \tag{4.9}$$

4.2.5 Active power loss (Ploss)

Power flow through the lines cause power loss in power distribution system. Extra load on the system could cause more power loss and voltage deviation. Backward Forward Sweep load flow algorithm is applied to get branch flows, node voltages, and the corresponding angles. Active power loss is calculated using Eq. (4.10), where $i(b)$ is current through b^{th} branch, having a resistance of $R(b)$. P_{loss} is the daily active power loss in kW.

$$Ploss = \sum_{t=1}^{24} \sum_{b=1}^{nb} i^2(b) \times R(b) \tag{4.10}$$

4.2.6 Maximum Voltage Deviation (MVD)

The loading of the distribution network resulted in deviation of voltage from its base values. Maximum Voltage Deviation (MVD) is the sum of maximum voltage deviation values in 24 hours period. It is calculated using Eq. (4.11), where $v_t(i)$ is the voltage at i^{th} bus in t^{th} hour.

$$MVD = \sum_{t=1}^{24} \sum_{i=1}^{nb} max(1 - v_t(i)) \tag{4.11}$$

4.2.7 Voltage Stability Index (VSI)

The VSI and voltage deviation both have a role in the stability of the distribution network. VSI at the receiving end of a line k (VSI_r) was calculated using Eq. (4.12), where V_r and V_s are the voltages at the receiving and sending ends of the line, P_r and Q_r are the real and reactive power at the receiving end of the line, and R(k) and X(k) are the resistance and reactance of the line k, respectively.

$$VSI_r = 2V_s^2V_r^2 - V_r^4 - 2V_r^2(P_rR(k) + Q_rX(k)) - |z|^2(P_r^2 + Q_r^2) \tag{4.12}$$

4.2.8 EV User Cost (EVUC)

EV user cost is the cost of electrical energy lost in travelling towards RCS location from EV position. EVUC depends on the distance between RCS and the current location of EV. An EV user expects the charging station to be located in proximity to his location.

The EV user behaviour is included in the optimal planning of RCS by adding the minimization of EVUC as an objective in optimization. In this chapter, coupled distribution network with road transportation network is considered for optimal planning. In test system, distribution nodes are superimposed on transportation area as shown in Figure 4.2. Distribution nodes are the possible locations for placing the RCS. Each distribution node and transportation zone has x and y coordinates on the coordinate plane. The distance between each zone to RCS can be calculated using Eq. (4.13), where $d_{Z_z-C_m}$ is the distance between z^{th} zone and m^{th} RCS. Where, x_Z and y_Z are x and y coordinates of zone, x_C and y_C are x and y coordinates of RCS.

$$d_{Z_z-C_m} = \sqrt{(x_{Z_z} - x_{C_m})^2 + (y_{Z_z} - y_{C_m})^2} \tag{4.13}$$

EVUC can be calculated using Eq. (4.14). Where P_E is the electricity price while SEC is the specific energy consumption of EV. DD is a matrix consisting of distance between each zone to the nearest RCS. DD matrix consists of the minimum distance between each zone to all RCSs (Eq. (4.15)).

$$EVUC = \sum_{z=1}^{nz} DD(z) \times N^{EV}(z) \times SEC \times P_E \tag{4.14}$$

$$DD = \begin{bmatrix} min(d_{Z_1-C_1} & d_{Z_1-C_2} & .. & d_{Z_1-C_m}) \\ min(d_{Z_2-C_1} & d_{Z_2-C_2} & .. & d_{Z_2-C_m}) \\ min(. & . & . & .) \\ min(. & . & . & .) \\ min(d_{Z_z-C_1} & d_{Z_z-C_2} & .. & d_{Z_z-C_m}) \end{bmatrix} \tag{4.15}$$

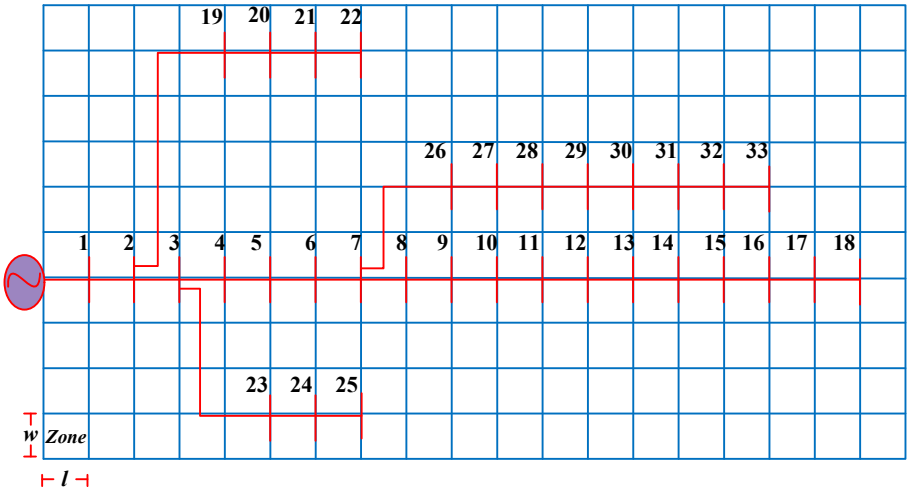

Figure 4.2: IEEE 33 Bus Power distribution network coupled with Road transportation network (Test system)

4.2.9 RCS building cost (ICRCS)

From the standpoint of an RCS owner, ICRCS is the key consideration. The RCS owner expects low installation cost so as to install more RCSs. It also helps EV user as more RCS would provide RCS to charge EVs. ICRCS mainly depends on the number of connectors at i^{th} RCS ($N.C_i^{RCS}$), and is calculated using Eq. (4.16). The number of connectors determines the RCS's capacity, which is computed using Eq. (4.17), where C_{init} (7000\$) is the initial investment cost, C_{land} (240 \$/m^2) is the land cost, C_{con} (280.33 \$/kW) is the connector cost, and P_c is connector rating.

$$ICRCS(i) = C_{init} + 25 \times C_{land} \times N.C_i^{RCS} + C_{con}(N.C_i^{RCS} - 1) \times Pc \tag{4.16}$$

$$RCS(i)_{cap} = N.C_i^{RCS} \times P_c \tag{4.17}$$

4.2.10 Waiting time (WT)

In this study the serviceability of charging stations is described using M1/M2/C queuing model [82]. Here, M1 denotes arrivals rate per hour, M2 denotes service rate per hour, and C denotes the number of service points. Electric vehicles (EVs) frequently arrive at charging station at the rate of $\lambda/hour$ to fuel their batteries. Here, arrival rate is time-dependent, and is calculated using Eq. (4.18). The connectors at each RCS charge EVs at a service rate of $\mu/hour$. Though there exists a waiting line of EVs at RCS,

connectors must guarantee a service to all EVs in the RCS, and this factor is governed by Eq. (4.19).

$$\lambda(t) = N_{EV}^{iRCS} \times P_{evc} \tag{4.18}$$

$$\rho = \frac{\lambda(t)}{C\mu_t} < 1 \tag{4.19}$$

Total time taken in queue at RCSs can be calculated using (Eq. 4.20), where $wt(t)$ is the average waiting time of EVs at t^{th} hour (Eq. 4.21). The anticipated count of EV users waiting in t^{th} hour at RCSs can be calculated using Eq. (4.22). The probability of no EV getting charged can be calculated using Eq. (4.23).

$$WT = \sum_{i=1}^{m} \sum_{t=1}^{24} wt(t) \tag{4.20}$$

$$wt(t) = \frac{E_t[n]}{\lambda(t)} \tag{4.21}$$

$$E_t[n] = p_t(0) \left[\frac{1}{(C-1)!} \left(\frac{\lambda_t}{\mu_t} \right)^C \frac{\lambda_t \mu_t}{(C\mu_t - \lambda_t)^2} \right] \tag{4.22}$$

$$p_t(0) = \left[\sum_{s=0}^{C-1} \frac{(C\rho)^s}{s!} + \frac{(C\rho)^C}{C!} \frac{1}{(1-\rho)} \right]^{-1} \tag{4.23}$$

In order to calculate optimal connectors count using optimization technique, it is required to calculate limits of connectors count at RCSs. Eq. (4.24) gives the most count of connectors (C^{max}) at RCS, while Eq. (4.25) gives least count of connectors (C^{min}).

$$C^{max} = max(P_{evc}) \times N_{EV}^{iRCS} \tag{4.24}$$

$$\frac{\lambda^{max}}{\mu} < C^{min} \qquad \lambda^{max} \in \lambda(t) \tag{4.25}$$

4.2.11 Constraints

A few equality and inequality constraints must be taken into account during optimisation to guarantee system stability. Eq. (4.26) and Eq. (4.27) are the equality constraints of real and reactive power in a considered system. Eq. (4.28) is used to maintain voltage of each bus within limits (V^{min}, V^{max}). DG's minimum and maximum active power limits

(P_{dg}^{min}, P_{dg}^{max}) are imposed by Eq. (4.29) in the optimization. However, the output of all DGs has to be limited to minimum real power load at any time on the system to avoid reverse power flow (Eq. (4.30)).

$$P_{sub} + \sum P_{DG} = P_D + \sum P_{RCS} + P_{loss} \tag{4.26}$$

$$Q_{sub} + \sum Q_{DG} + \sum Q_{DST} = Q_D + \sum Q_{RCS} + Q_{loss} \tag{4.27}$$

$$|V^{min}| \leq |V_n| \leq |V^{max}| \qquad n = 1, 2, ...N_{bus} \tag{4.28}$$

$$P_{dg}^{min} \leq P_{dg} \leq P_{dg}^{max} \tag{4.29}$$

$$P_{dg} \leq P_{dg}^{T,max} < min(P_D) \tag{4.30}$$

Here P_{sub}, P_{DG}, P_D, P_{loss}, and P_{RCS} are substation real power, real power output of DG, base real power demand on system, real power loss, and real power load due to RCS. Q_{sub}, Q_{DG}, Q_D, Q_{loss}, and Q_{RCS} are substation reactive power, reactive power output of DG, base reactive power demand on system, reactive power loss, and reactive power load due to RCS. Q_{DST} is the reactive power output of D-STATCOMs. The maximum amount of active power that can be delivered by all DGs is $P_{dg}^{T,max}$.

4.3 Multi-objective algorithms

Majority of the problems are complex in nature and there is a need to consider more than one goal in finding optimal solution. There are mainly two approaches for solving multi objective problems. The first is the weighted sum strategy, in which many objectives are combined into a single objective by adding their respective weights together. Here, the sum of all weights is equal to 1. Second is pareto based technique, it consist of dominance principle, which is preferred when at least one objective is in conflict with other objectives. In pareto based approaches, decision making techniques are deployed to pick up best solution from pareto front.

4.3.1 Multi objective Rao 3 Algorithm (MORA)

Multi objective Rao 3 algorithm was proposed in 2021 by Rao et.al to solve constrained and unconstrained multi objective problems having conflicting objectives [5]. It has no algorithm specific parameters and searching process involves the interaction of best, worst and random solutions. It is less complex and easier to understand. Dominance principle and crowding distance evaluation are used in deciding the best and worst so-

lution. New solution is generated using Eq. (4.31) shown below:

$$X_p^{'} = X_p + r_1 \times (X_b - |X_w|) + r_2 \times (|(X_p or X_r)| - (X_r or X_p)) \tag{4.31}$$

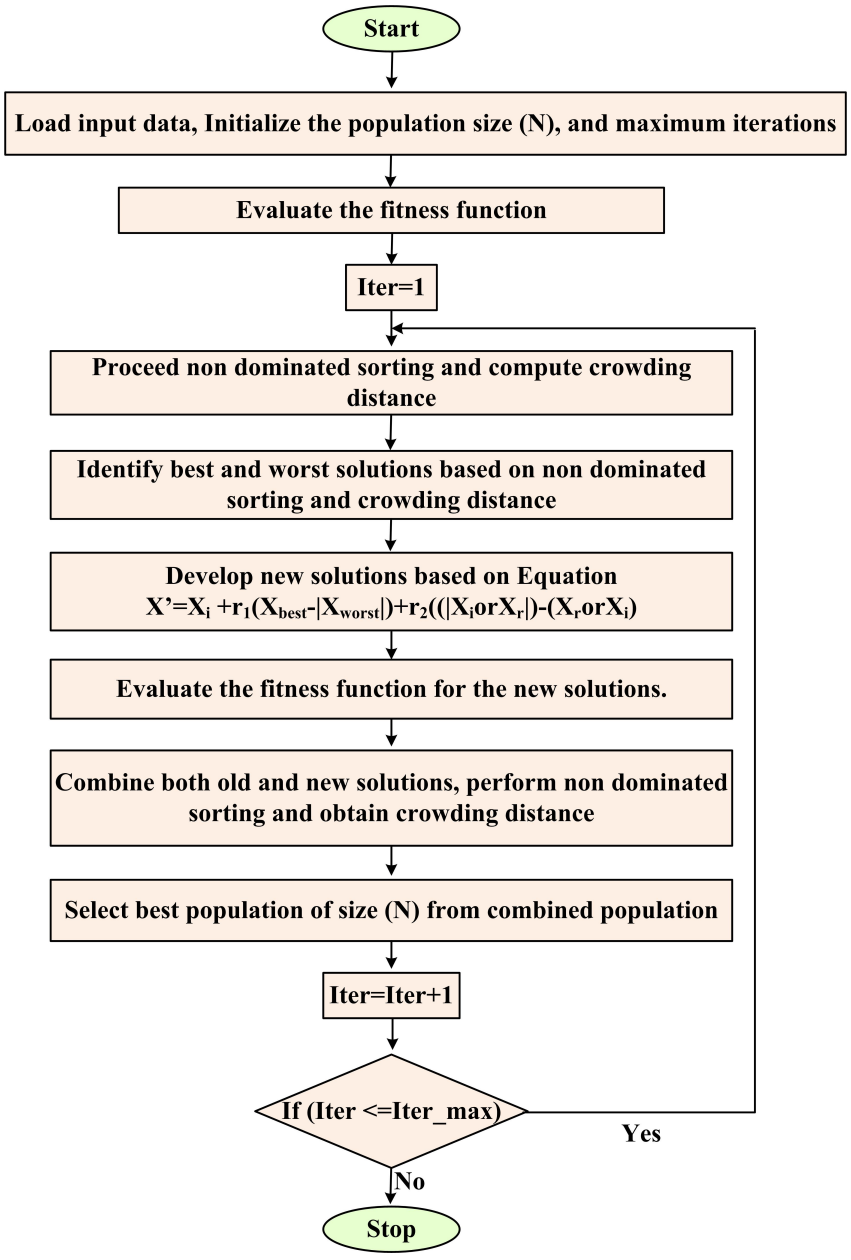

Figure 4.3: Flow chart of MORA algorithm [5]

Here, $X_p^{'}$ is new solution, X_p is present solution, X_b is best solution, X_w is worst solution, r_1 and r_2 are random values between 0 and 1. X_r is randomly selected solution for multi objective problems.

4.3.2 Non dominated Sorting Genetic Algorithm II (NSGA II)

NSGA-II was proposed by Deb in 2002 for solving constrained and unconstrained multi-objective problems [4]. It has significance in finding solutions to problems with conflicting objectives. It is fast and elitist in nature and uses non dominating sorting approach. It involves non dominated sorting, crowding distance, cross over and mutation processes in finding the best optimal solutions.

4.3.3 Implementation of Multi Objective Rao Algorithm (MORA) for optimal planning of RCSs, DGs, and D-STATCOMs

Step 1: Read the test system data and initialize the algorithm parameters (population size and maximum iterations).
Step 2: Randomly initialize the population and determine the respective fitness values.

- $Pop_{stage1} = [l_{RCS}, l_{DG}, l_{DST}, S_{DG}, S_{DST}]$ for Stage 1
- $Pop_{stage2} = [C]$ for Stage 2.
  (l_{RCS} is location of RCS, l_{DG} is location of DG, l_{DST} is location of D-STATCOM, S_{DG} is size of DG, S_{DST} is size of D-STATCOM, and C is number of connectors).

Step 3: Set iter = 1.
Step 4: Perform the non dominated sorting and calculate the crowding distance.
Step 5: Obtain best and worst solutions based on the non dominated sorting and crowding distance.
Step 6: Update the candidate solutions based on the update equation (4.31) and find the updated fitness value.
Step 7: Combine both old and modified solutions and perform non dominated sorting and crowding distance.
Step 8: Select best population of size (N) from combined solutions of size 2N.
Step 9: Set Iter=Iter+1.
Step 10: Terminate the process, if ($Iter > Iter_{max}$) and save the pareto optimal front data otherwise continue from step 4 to step 10.
Step 11: Perform the fuzzy min max decision making technique to select the compromised optimal solution optimal front and print the results.

Table 4.1: Parameters of EV

Parameters	Values
P_{EVB}^{max}	27.69 kWh
N_T^{EV}	600
SEC	0.142 kWh/km
P_c	96 kW

Table 4.2: Bus groups of connected loads in power distribution network

Residential loads	Commercial loads	Industrial loads
2,3,5,6,7,8	4,11,12,18	22,26,27,28
9,10,13,14,15	19	29,30,31,32
16,17,20,23,24	–	33

Table 4.3: Assumed Number of Electric Vehicles at the 190 zones of Transportation system

1	4	3	1	5	1	1	2	3	4	4	5	5	4	2	5	3	3	4
3	4	2	4	1	3	3	1	5	5	4	4	2	1	2	4	5	1	4
3	5	4	1	1	5	4	5	4	4	3	1	3	3	5	2	5	5	2
4	1	2	2	5	2	2	4	4	4	5	4	2	3	5	2	2	5	1
4	3	4	4	4	5	4	1	4	3	4	4	4	1	2	1	5	3	4
2	4	5	3	3	4	2	3	3	5	3	4	3	3	1	5	4	2	1
5	5	4	2	2	2	4	4	5	5	2	5	4	2	2	3	3	3	2
5	5	4	2	4	4	3	5	5	4	1	1	1	5	3	4	3	3	3
1	4	3	1	1	1	4	2	1	3	5	4	4	2	2	1	4	3	3
4	1	1	1	5	1	4	3	5	2	1	2	4	3	5	4	1	5	4

4.4 Simulation Results and discussion

In this chapter, coupled Power distribution network and Road transportation network is considered as test system. It is assumed that the road transportation network of test system has an area of 20×38 km^2. There are 190 zones, each with a 4 km^2 area. It is assumed that SOC of each EV arrived is 20% SOC and charge up to 85% SOC. In [82], EV battery characteristics were shown, where EV battery is charged up to 85% SOC in

22 minutes. The load data and line data of IEEE 33 bus power distribution network are taken from [102]. The simulations were run on a computer with an Intel I3 processor and 4GB of RAM using MATLAB 2014b software.

The buses of power distribution network are classified into residential type, commercial type, and industrial type loads. Buses of various types of loads are shown in Table 4.2. Each type of load varies with respect to time and the variation of load demand in p.u of the above stated loads is shown in Figure 4.4. Figure 4.5 depicts the variation in EV charging probability during a 24-hour period.

The optimal planning of RCSs along with the DGs and D-STATCOMs was done through the following four cases.

- Base case : Test system without the integration of RCSs, DGs, and D-STATCOMs.
- Case 1 : Integration of RCSs into the coupled network.
- Case 2 : Integration of RCSs along with DGs into the coupled network.
- Case 3 : Integration of RCSs along with the DGs and D-STATCOMs into the coupled network.

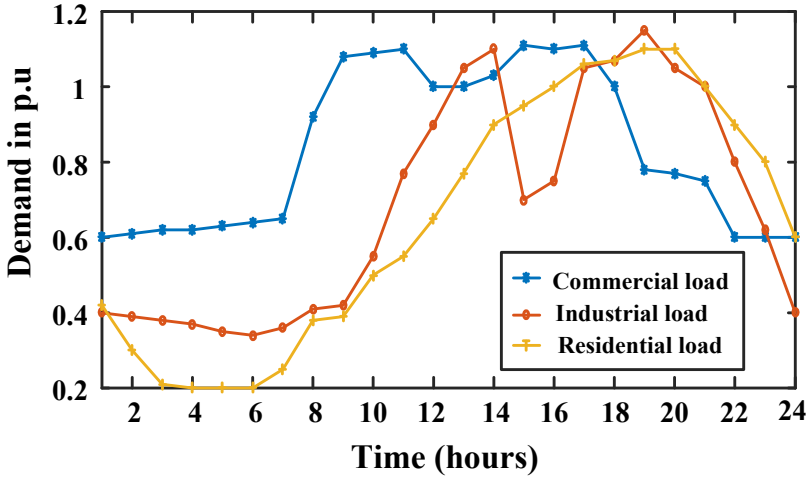

Figure 4.4: Plot of various types of loads demand

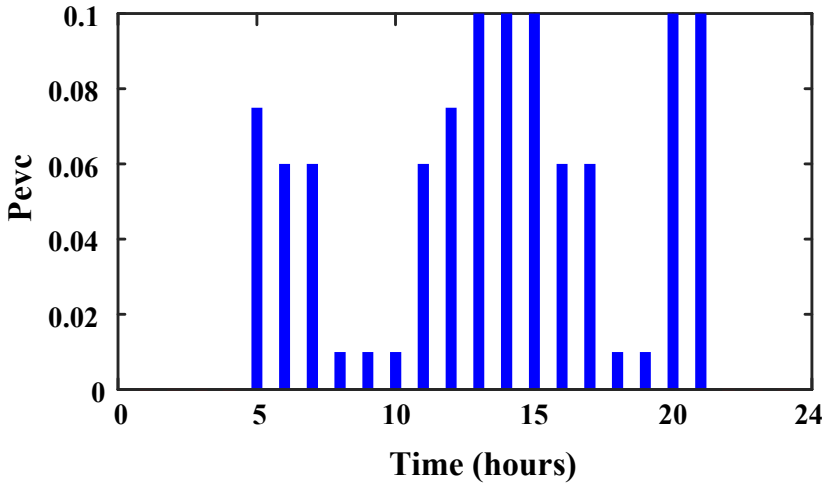

Figure 4.5: Hourly probability of Electric Vehicle charging

4.4.1 Base case

In Base case RCSs, DGs, and D-STATCOMs were not integrated into the coupled network. The variation of load demand for various loads was considered in the analysis. This consideration results in total active power demand and reactive power demand of 63,868 kW and 39,236 kVAr respectively. Backward forward sweep load flow analysis was performed and found that total active power loss is 2811 kW. Though the RCSs were not installed, poor results for MVD (1.5816 p.u), and VSI (0.6479) were observed. The variation of voltage profile in Base case is shown in Figure 4.6. From the figure, it is observed that the system experienced a minimum voltage (0.8968 p.u) at 18^{th} bus in 17^{th} hour.

4.4.2 Case 1 : Integration of RCSs into the coupled network

Impact of RCS integration into the power distribution system is analysed in Case 1. MORA is employed to solve the optimization problem by following the above mentioned constraints. Optimal front corresponding to Case 1 by MORA algorithm is shown in Figure 4.8. The best compromised solution is chosen using fuzzy min max technique.

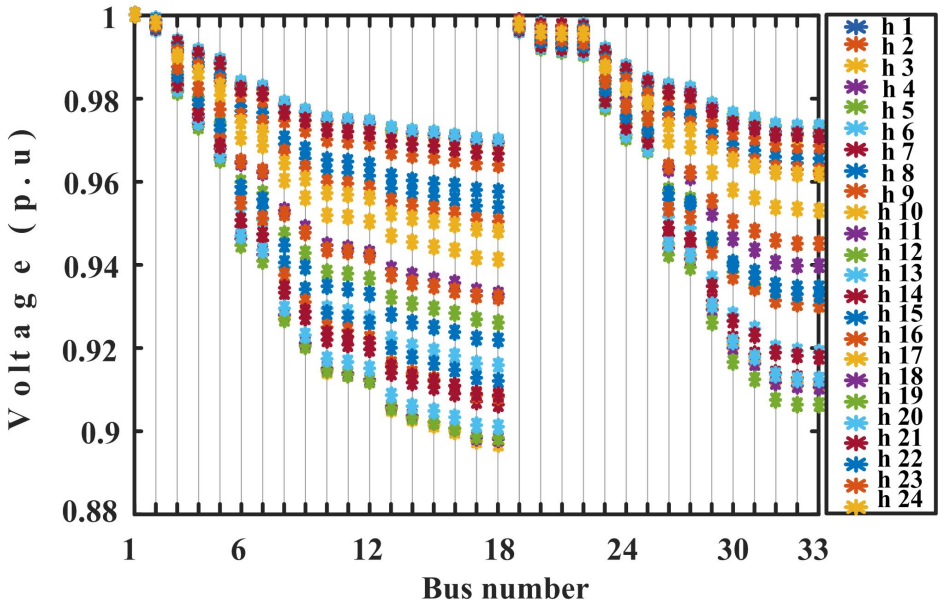

Figure 4.6: Voltage profile of IEEE 33 bus power distribution network in Base case

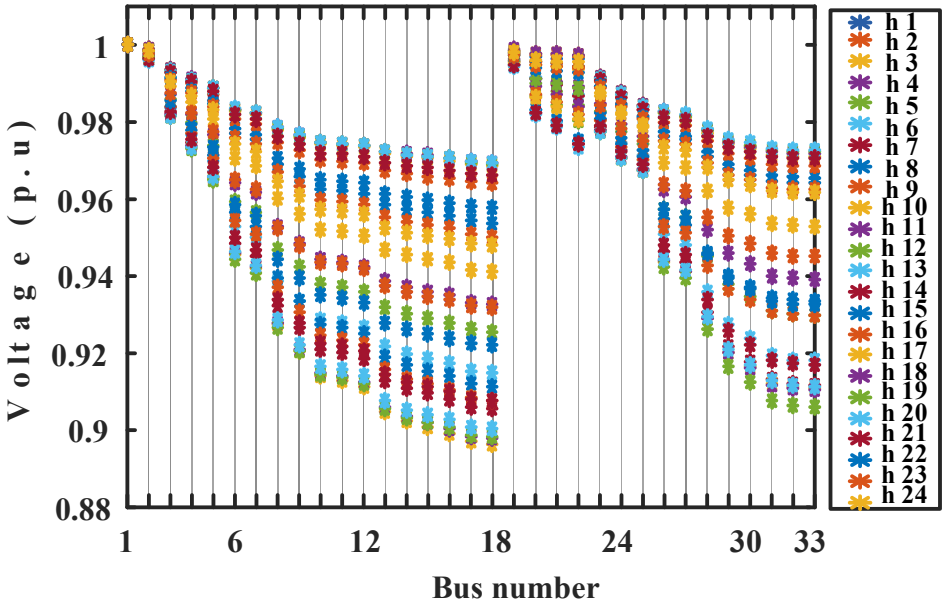

Figure 4.7: Voltage profile of IEEE 33 bus power distribution network in Case 1

Table 4.4 shows the optimal locations of RCSs and various objective parameters consid-

ered in Stage 1 by both algorithms. From Table 4.4 it is noticed that MORA outperforms NSGA-II in all four objective parameters. Integration of RCSs resulted in increased Ploss (2977.1 kW) and MVD (1.5818 p.u). VSI_{min} (0.6464) is reduced compared to base case values. EV user cost is minimum for locations obtained by MORA (86.7004 $) compared to NSGA-II outcomes. It is expected that the system always maintains voltage within the limits. However, Figure 4.7 shows that the integration of RCSs resulted in system minimum voltage of 0.8951 p.u by MORA, which is lower compared to base case value of 0.8968 p.u.

Table 4.4: Optimal RCSs locations and objective parameters obtained in Stage 1 of Case 1 by MORA and NSGA-II algorithms

Optimal results	NSGA II	MORA
RCSs location	2, 19, 23	2, 19, 22
EVs at RCSs	102, 235, 263	171, 57, 372
Ploss (kW)	3026	2977.1
MVD (p.u)	1.6093	1.5818
VSI_{min}	0.6430	0.6464
EVUC ($)	94.2015	86.7004

Table 4.5: Optimal RCSs sizes and objective parameters obtained in Stage 2 of Case 1 by MORA and NSGA-II algorithms

Optimal results	NSGA II	MORA
RCSs connectors	5, 10, 20	10, 3, 22
Wt (min)	94.8866	81.2981
ICRCS ($)	1.91×10^6	1.9×10^6
RCSs size	480, 960, 1920	960, 288, 2112

Table 4.5 shows various optimal results achieved in Stage 2. The connector count at every RCS was decided optimally by considering minimization of waiting time at RCSs and ICRCS in Stage 2. Both service rate (μ) and arrival rate (λ) were required to calculate waiting time. Here, charging time of 22 minutes for an EV battery showed that a connector could serve 2.73 EVs per hour i.e connector service rate (μ) is 2.73/hr [82]. Arrival rate can be obtained from the number of EVs assigned to a particular RCS and EVs charging probability (Eq. (4.18)). From Stage 1 (Table 4.4), it is known that

charging stations were located at 2^{nd}, 19^{th}, and 22^{nd} bus locations with allocated EVs of 171, 57, and 372 by MORA.

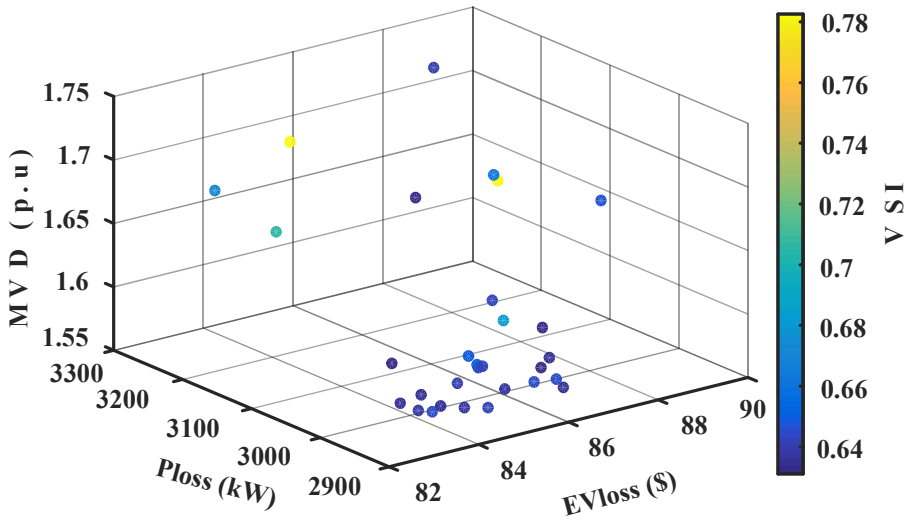

Figure 4.8: Optimal pareto fronts in Stage 1 of Case 1 by MORA

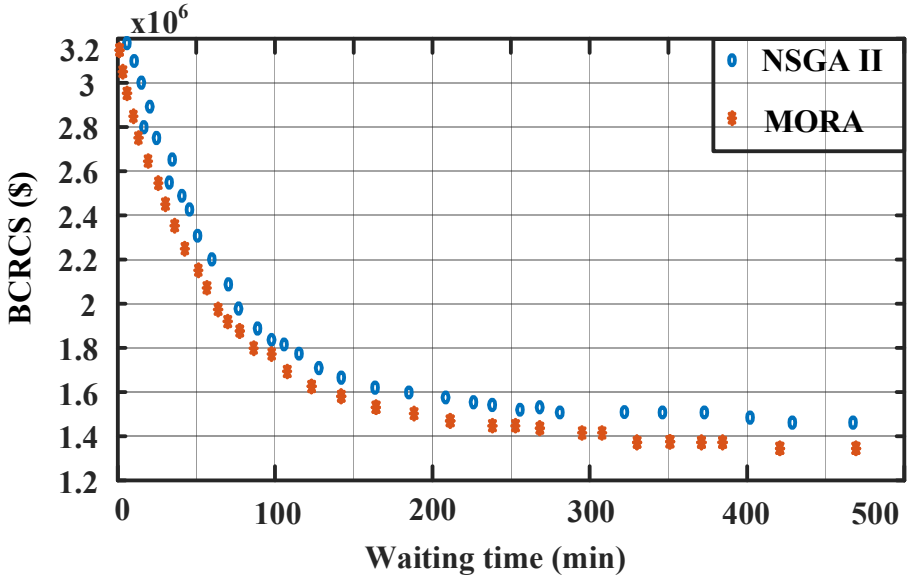

Figure 4.9: Optimal pareto fronts in Stage 2 of Case 1 by both algorithms

From the allocated EVs at each RCS, minimum connectors (C^{min}=[7 3 14]) and maxi-

mum connectors (C^{max} [17 6 37]) were calculated using Eqs. (4.25) and (4.19) respectively. In the same way C^{min}=[4 9 10] and C^{max}=[10 24 26] were obtained for NSGA II from Stage 1. Both algorithms were applied to obtain optimal connectors count at every RCS. Optimal front yielded in Stage 2 of Case 1 by MORA is shown in Figure 4.9. From Table 4.5 it is observed that lower waiting time at RCS of 81.2981 (min) and ICRCS of 1.9×10^6 \$ were achieved by MORA. Optimal connectors of 10, 3, and 22 were placed at RCS1, RCS2, and RCS3 respectively with corresponding sizes of 960 kW, 288 kW, and 2112 kW respectively.

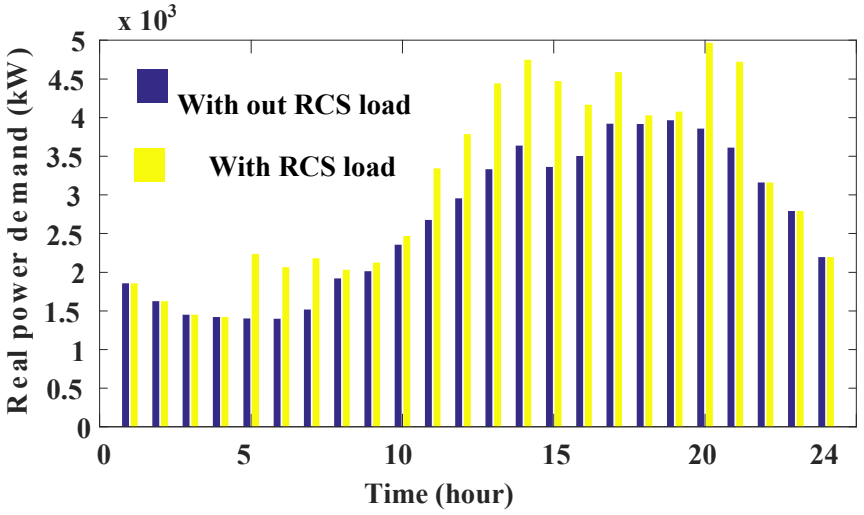

Figure 4.10: Daily real power demand including and excluding with RCS load.

4.4.3 Case 2 : Integration of RCSs along with DGs into the coupled network

From Case 1 it is observed that the integration of RCSs caused escalation of Ploss, MVD, and reduction of VSI_{min}. In this context, 5 kW to 1 MW size DGs were considered for installation with 0.95 lag power factor. From Figure 4.10 it is noticed that, at 4^{th} hour, the system experienced lowest real power demand of 1420 kW. The combined real power share by all DGs was bounded to less than or equal to 1400 kW to avoid reverse power flow. Both algorithms were applied to find optimal locations and capacities of RCSs and DGs. Figure 4.13 shows the optimal front of objectives considered in Stage 1 of Case 2 yielded by MORA. Fuzzy min max technique was used to identify the best solution from optimal front. From Table 4.6, it is observed that DG integration resulted

in better values of objective parameters compared to Case 1. Rapid charging stations were located at 2^{nd}, 22^{nd}, and 33^{rd} buses of RDS. DGs were located at 14^{th}, 30^{th}, 32^{nd} buses of RDS with DG sizes of 483 kW, 103 kW, and 804 kW respectively by MORA algorithm. MORA offered lowest Ploss of 1182.3 kW while NSGA II yielded 1218.2 kW power loss. Better voltage profile was achieved through lower values of MVD at 0.6864 p.u and VSI_{min} of 0.7946 by MORA algorithm.

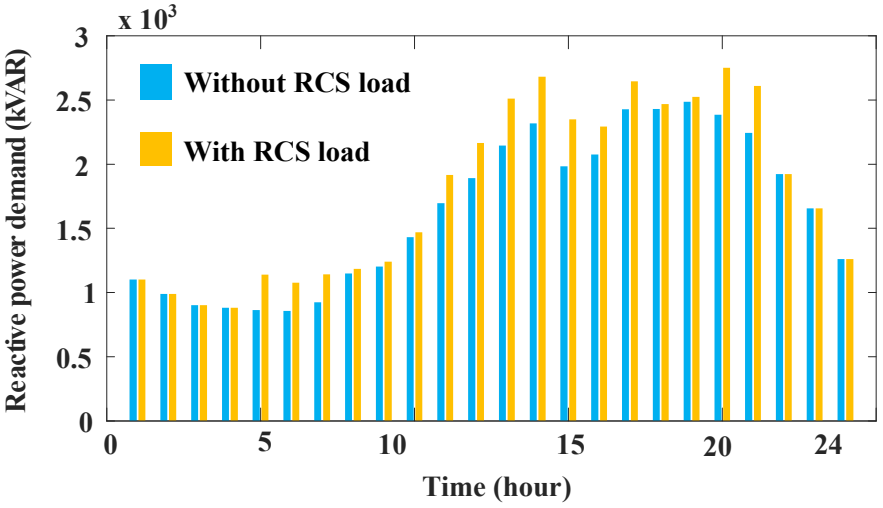

Figure 4.11: Daily reactive power demand including and excluding with RCSs load.

Table 4.6: Optimal RCSs locations and objective parameters obtained in Stage 1 of Case 2 by MORA and NSGA II algorithms

Optimal results	NSGA II	MORA
RCSs location	2, 21, 33	2, 22, 33
EVs at RCSs	183, 157, 260	201, 151, 248
Location of DGs	17, 30, 32	14, 30, 32
DG size(kW)	383, 276, 718	483, 103, 804
Ploss (kW)	1218.2	1182.3
MVD (p.u)	0.6964	0.6864
VSI_{min}	0.7933	0.7946
EVUC ($)	54.4474	53.4033

Table 4.7: Optimal RCSs sizes and objective parameters obtained in Stage 2 of Case 2 by MORA and NSGA II algorithms

Optimal results	NSGA II	MORA
RCSs connectors	11,7,15	10, 8, 14
W_T (min)	56.1041	27.9801
ICRCS ($)	1.8×10^6	1.75×10^6
RCSs size	1056, 762, 1440	960, 768, 1344

Integration of DGs allows RCSs to settle at optimal locations to reduce EVUC. The optimal locations of RCSs by MORA algorithm yielded an EVUC value of 53.4033 $ while NSGA II resulted in 54.4474 $ of EVUC. Figure 4.12 shows the voltage profile of power distribution network with the inclusion of DGs along with RCSs at locations achieved by MORA. From this figure it is observed that the presence of DG in power distribution network resulted in better system lowest voltage (0.9432 (p.u)) compared to Case 1 and Base case. When compared to base case scenario (0.8968 p.u), the voltage at 18^{th} buses in 17^{th} hours improved to 0.9461 p.u.

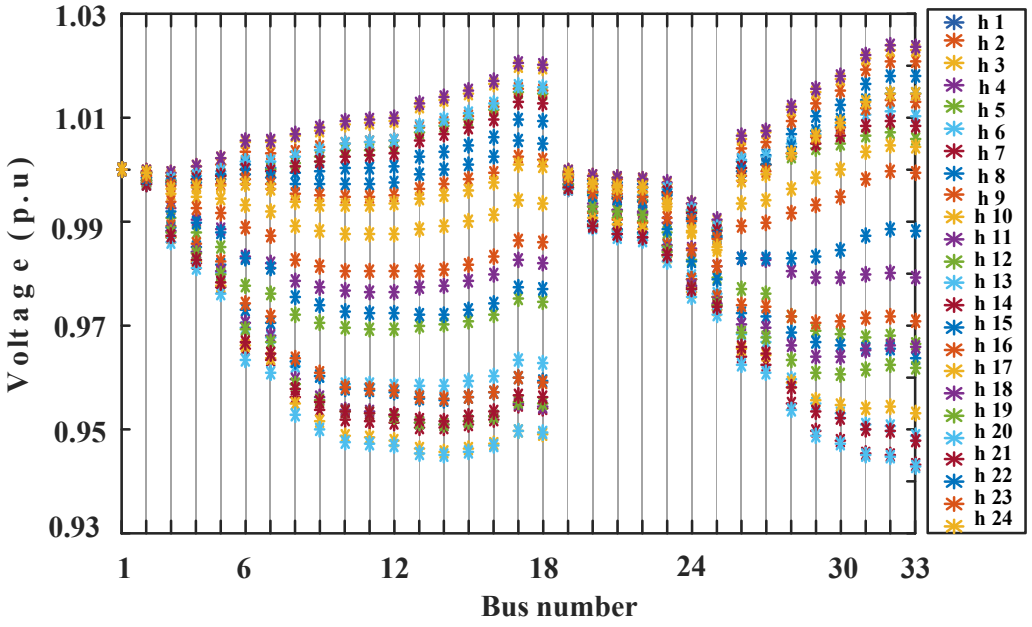

Figure 4.12: Voltage profile in IEEE 33 bus power distribution network in Case 2

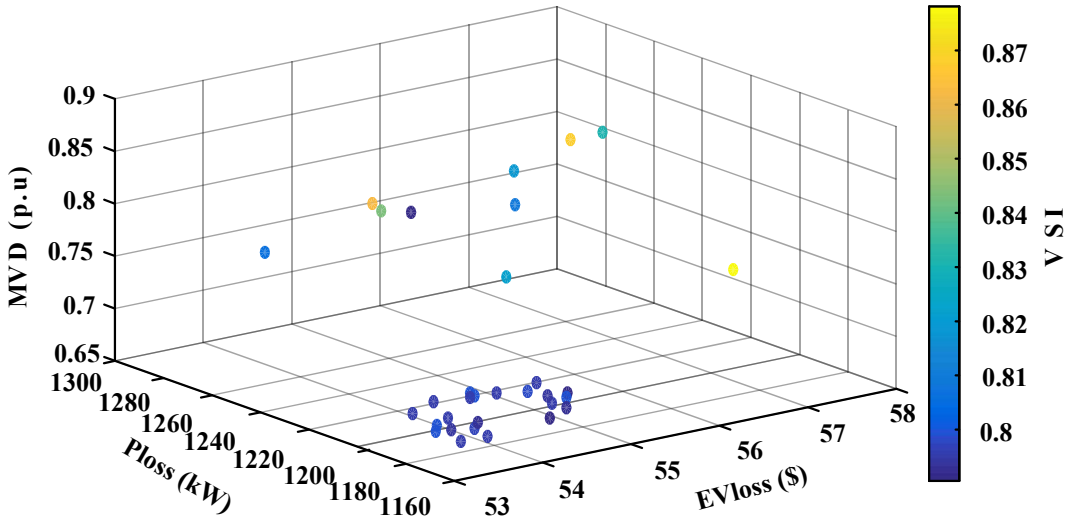

Figure 4.13: Optimal pareto fronts in Stage 1 of Case 2 by MORA.

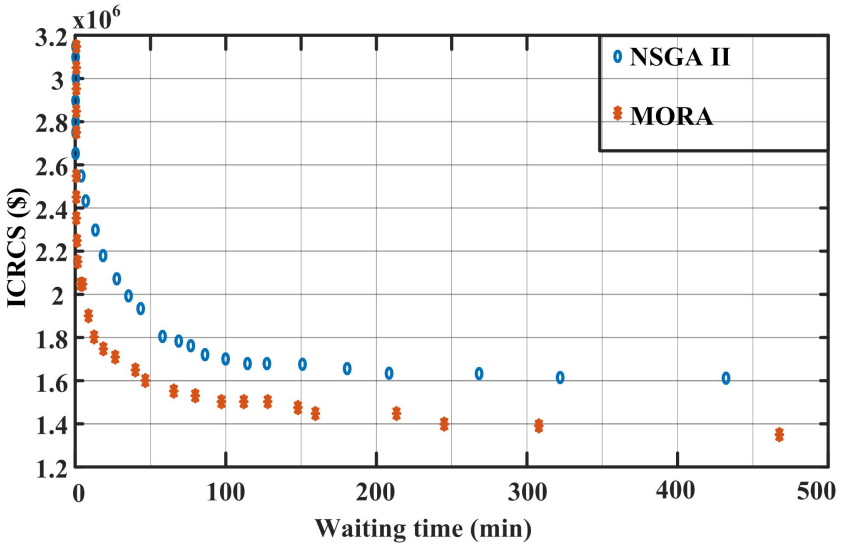

Figure 4.14: Optimal pareto fronts in Stage 2 of Case 2 by MORA.

Both algorithms were applied to obtain the optimal number of connectors in Stage 2. MORA yielded 10, 8, and 14 connectors at the respective charging stations; NSGA II led to 11, 7, and 15 connectors at the corresponding RCSs. The optimal front of Stage 2 achieved by MORA in Case 2 is shown in Figure 4.14. Fuzzy min max technique was used to identify better solution. Minimum waiting time at RCSs was 27.9801 minutes and a lower installation cost of 1.75 $\times 10^6$ \$ was yielded by MORA algorithm.

4.4.4 Case 3 : Integration of RCSs along with the DGs and D-STATCOMs into the coupled network

Providing Reactive power support could improve the performance of power distribution network. Hence, simultaneous integration of DGs and D-STATCOMs is done along with RCSs in Case 3 by both algorithms. Figure 4.11 shows that the systems minimum reactive power requirement is 882 kVAr. However, DGs have the capability to supply 460 kVAr reactive power. So the total Reactive power supplied by all D-STATCOMs is limited to 420 kVAr in optimal planning.

Figure 4.15 shows pareto front in Stage 1 of Case 3 yielded by MORA. Fuzzy min max technique was used to identify better results. Table 4.8 shows that charging stations were located at 2^{nd}, 21^{st}, and 32^{nd} buses of RDS along with DGs located at 15^{th}, 29^{th}, 33^{rd} buses of RDS with the sizes of 391 kW, 303 kW, and 704 kW respectively. Here D-STATCOMs are located at 13^{th}, 17^{th}, and 31^{st} buses of RDS with sizes of 30 kVAr, 87 kVAr, and 302 kVAr, as determined by MORA algorithm. Locations and sizes of DGs, D-STATCOMs and RCSs obtained by NSGA II are shown in Table 4.8. Minimum power loss of 990.34 kW resulted in Case 3 by MORA compared to 1092.8 kW power loss by NSGA II. Better voltage profile was observed with the inclusion of D-STATCOMs along with DGs. Lower MVD of 0.5934 p.u and higher VSI_{min} of 0.8195 were yielded by MORA algorithm. The better spreading of charging stations in a coupled network resulted in lower value of EVUC in Case 3. Lowest EVUC of 53.2199 $ was achieved for RCSs locations obtained by MORA algorithm. Figure 4.17 shows the integration of D-STATCOMs and DGs which resulted in improved system lowest voltage of 0.9521 (p.u), which is the best value among all cases considered in this study.

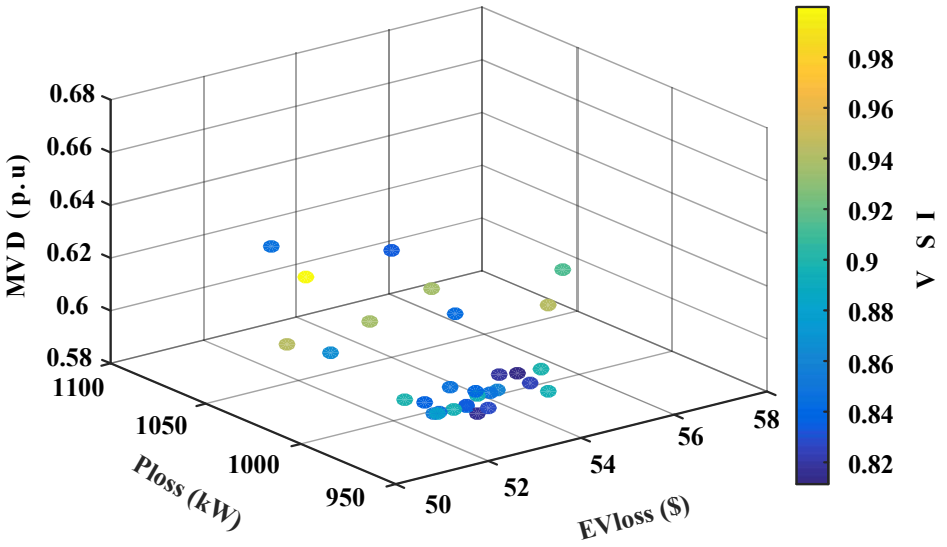

Figure 4.15: Optimal pareto fronts in Stage 1 of Case 3 by MORA.

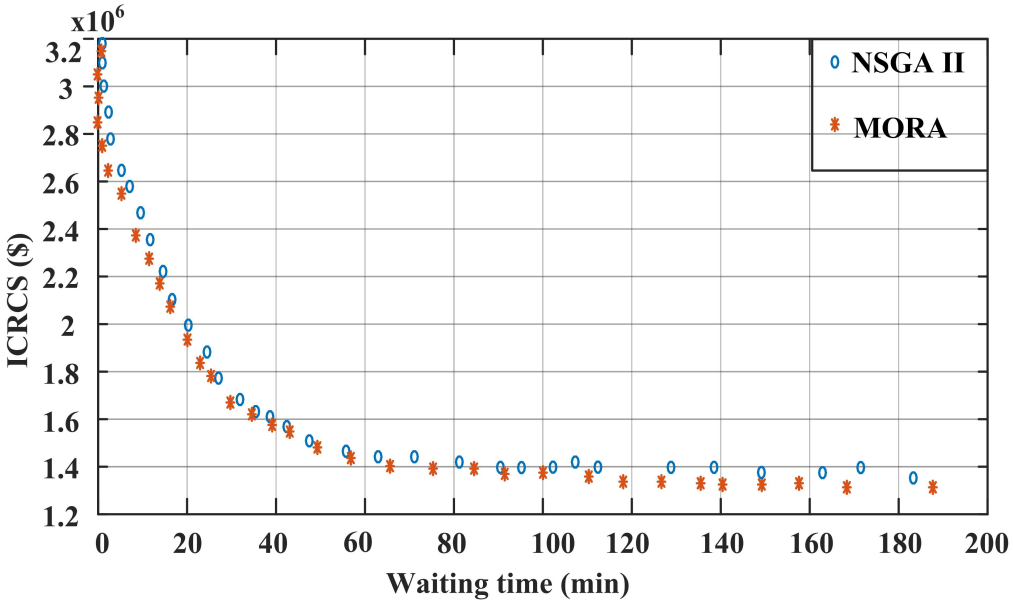

Figure 4.16: Optimal pareto fronts in Stage 2 of Case 3 by MORA.

Table 4.8: Optimal RCSs locations and objective parameters obtained in Stage 1 of Case 2 by both algorithms

Optimal results	NSGA II	MORA
RCSs locations	3, 21, 33	2, 21, 32
EVs at RCSs	206, 134, 260	178, 138, 284
DG locations	2, 16, 31	15, 29, 33
DG size (kW)	110, 407, 853	391, 303, 704
D-STATCOMs locations	14, 18, 32	13, 17, 31
D-STATCOMs size (kVAr)	28, 35, 354	30, 87, 302
Ploss (kW)	1092.8	990.34
MVD (p.u)	0.6412	0.5934
VSI_{min}	0.8094	0.8195
EVUC ($)	53.2344	53.2199

Optimal pareto front in Stage 2 is shown in Figure 4.16. Fuzzy min max technique is used to obtain better solutions and are shown in Table 4.10. Table 4.10 demonstrates the superiority of the MORA algorithm in reaching the optimal number of connectors. Lowest waiting time at RCSs of 28.4217 (min) and lowest ICRCS of 1.7×10^6 $ were observed for connectors of 9, 8, and 14 at the respective charging stations by MORA algorithm.

Table 4.9: Comparison of various objective in all cases

Case	Ploss (kW)	MVD (p.u)	VSI_{min}	EVUC ($)	Wt (min)	ICRCS ($)
Base case	2811	1.5816	0.6479	–	–	–
Case 1	2977.1	1.5818	0.6464	86.7004	81.2981	1.9×10^6
Case 2	1182.3	0.6864	0.7946	53.4033	27.9801	1.75×10^6
Case 3	990.34	0.5934	0.8195	53.2199	28.4217	1.7×10^6

Table 4.10: Optimal RCSs sizes and objective parameters obtained in Stage 2 of Case 2 by MORA and NSGA-II algorithms

Optimal results	NSGA II	MORA
RCSs connectors	10, 10, 12	9, 8, 14
Wt (min)	32.9638	28.4217
ICRCS ($)	1.72×10^6	1.7×10^6
RCSs size	960, 960, 1152	864, 768, 1344

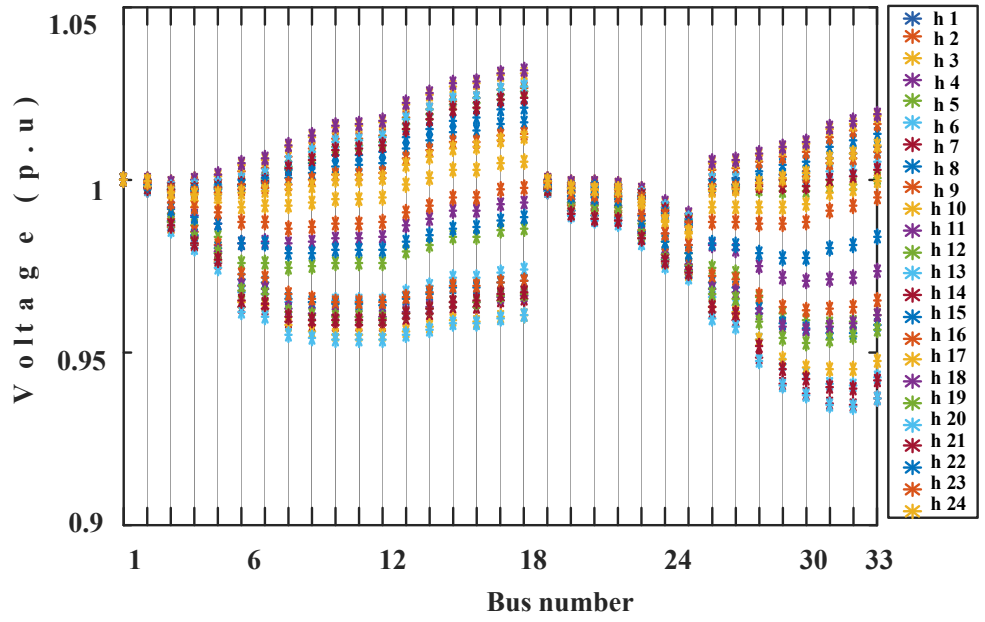

Figure 4.17: Voltage profile in IEEE 33 bus power distribution network in Case 3

Table 4.9 shows better objective values achieved in various cases. From this it can be concluded that the optimal planning of RCSs, DGs, and D-STATCOMs reduced Ploss by 64.8 % and MVD by 62.4 % compared to base case values. For better voltage stability, VSI_{min} should be near unity (≤ 1); it improved by 26.5 % in Case 3 when compared to Base case. Integration of D-STATCOMs and DGs made the RCSs spread over the test system, which resulted in low EVUC in Case 3. Optimal connectors count in Stage 2 of Case 3 resulted in low ICRCS of 1.7×10^6 $ and waiting time at RCSs of 28.4217 minutes. Thus, it can be concluded that simultaneous optimal planning of RCSs, DGs and D-STATCOMs offers better performance for power distribution system and EV user convenience (low EVUC). Furthermore it also favours RCS owner by lowering building cost and waiting time at RCSs.

4.5 Summary

A two stage approach is proposed for optimal placement and sizing of RCSs, DGs, and D-STATCOMs in coupled network. Stage 1 dealt with the minimization of active power loss, voltage deviation, EV user cost, and improvement of voltage stability index. Queue theory has been utilized in stage 2 and an optimal number of connectors obtained at each RCS for low waiting time and RCS installation cost. During the simulation, hourly load demand variation at various bus types and the hourly probability of EVs charging are considered. The placement problem is solved using novel metaphor less pareto based Multi objective Rao algorithm. The simultaneous integration of D-STATCOMs along with RCSs and DGs resulted in better voltage profile, lower power loss, and lower EV user cost. The performance of distribution network can be further enhanced through the employment of network reconfiguration technique.

Chapter 5

Network reconfiguration and optimal planning of RCSs, DGs, and D-STATCOMs in coupled network

5.1 Introduction

The integration of Rapid charging stations (RCSs) increases voltage deviation and power losses. If RCS located at wrong location it harms the power distribution system further. As the EV load increases, the existing distribution network may not operate at optimum level, where network reconfiguration plays a vital role. This chapter proposes a multi objective two-stage approach that includes both optimal planning of RCSs, DGs, and D-STATCOMs and network reconfiguration. Pareto based multi objective Rao 3 algorithm and queue theory were used in optimal planning. The proposed approach yielded optimal locations, capacities and optimal network for a reduced values of active power loss, voltage deviations, EV user cost, waiting time, RCS installation cost and improved voltage stability index.

5.2 Problem formulation

5.2.1 Distributed Generator

Distributed Generator (DG) modelling can be carried out in either PV mode or PQ mode. In this chapter, PQ mode is considered to model DG. Real power output (P_{dg}) and operating power factor (pf_{dg}) are known values in PQ mode, which is a negative load model. Using Eq. (5.1), reactive power output (Q_{dg}) is calculated from known values.

$$Q_{dg} = P_{dg} \times tan(cos^{-1}(pf_{dg})) \tag{5.1}$$

5.2.2 D-STATCOM

Reactive power is compensated by D-STATCOM to support the power distribution system. The output of D-STATCOM (Q_n^{DST}) is represented with a negative value at the

appropriate bus because it is modelled in PQ mode. The net reactive power (Q_n^{net}) after adding D-STATCOM at n^{th} bus is calculated using Eq. (5.2).

$$Q_n^{net} = Q_n^{base} - Q_n^{DST} \tag{5.2}$$

5.2.3 Rapid Charging Stations (RCSs)

Electric vehicles (EVs) are charged quickly at rapid charging stations. The count of EVs consuming energy determines the burden caused by RCSs. As RCS operate at 0.95 power factor lagging, there are demands from both active and reactive power from the utility. Eqs. (5.3) and Eq. (5.4) provide real power demand and reactive power demands (P_i^{RCS} and Q_i^{RCS}) caused by RCS, where N_i^{EV} and P_{EB}^{max} are the number of EVs at i^{th} station and EV battery capacity respectively

$$P_i^{RCS} = N_i^{EV} \times P_{EB}^{max} \tag{5.3}$$

$$Q_i^{RCS} = P_i^{RCS} \times tan(cos^{-1}(pf_{RCS})) \tag{5.4}$$

5.2.4 Objective function

Optimal planning of RCSs, DGS, and D-STATCOMs along with network reconfiguration has been done in two stages. In Stage 1, active power loss, voltage deviation, and EV user cost were minimized while improving voltage stability index. Stage 1 yields the locations of RCSs, locations and capacities of DGs and D-STATCOMs. Information regarding the EV count that is allocated to each RCS was used in Stage 2 for calculating waiting time. The optimal connector count at each RCS was determined in Stage 2 by considering RCS building cost and waiting time. Eq. (5.8) shows the objective function considered in Stage 1, where, ts, L, and S (Eq. (5.5) - Eq. (5.7)) are the matrices which consist of tie line switches, locations of RCS, DG, D-STATCOM (L_{RCS}, L_{DG}, L_{DST}), and sizes of DG and D-STATCOM (S_{DG}, S_{DST}) as decision variables. Eq. (5.9) shows the objective function considered in Stage 2, where C is the connector count and it is a

decision variable in Stage 2.

$$ts = [ts_1, ts_2, .., ts_n] \tag{5.5}$$

$$L = [L_{RCS}, L_{DG}, L_{DST}] \tag{5.6}$$

$$S = [S_{DG}, S_{DST}] \tag{5.7}$$

$$f(ts, L, S) = min(Ploss, MVD, EVUC, 1/VSI) \tag{5.8}$$

$$f(C) = min(ICRCS, W_T) \tag{5.9}$$

5.2.5 Power loss (Ploss)

Power loss results from power flow across power distribution network lines. The voltages and associated angles of power distribution network buses were obtained using the backward-forward sweep load flow technique. Power loss, voltage variation, and VSI were computed using the load flow algorithm's output. The active power loss of power distribution network over a day was calculated using Eq. (5.10), where, i is the current flowing through branch 'b' with resistance R.

$$Ploss = \sum_{t=1}^{24} \sum_{b=1}^{nb} i^2 \times R(b) \tag{5.10}$$

5.2.6 Maximum Voltage Deviation (MVD)

Voltage variations at the buses would be caused by the loading of power distribution network. But voltage deviation should be as minimal as possible for power distribution network to operate efficiently. The Maximum Voltage Deviation (MVD) in power distribution network was calculated using Eq. (5.11). It is always anticipated that power distribution networks should have a minimum MVD, Where $v_t(i)$ is the voltage of i^{th} bus at t^{th} hour in a day.

$$MVD = \sum_{t=1}^{24} \sum_{i=1}^{nb} max(1 - v_t(i)) \tag{5.11}$$

5.2.7 Voltage Stability Index (VSI)

Along with voltage deviation, VSI affects voltage stability. Here, power distribution network must always operate at its highest VSI (≤ 1). Eq. (5.12) can be used to deter-

mine VSI at the receiving end line of k. Where, k^{th} line has the sending end voltage of V_s and receiving end voltage of V_r. P_r and Q_r are the real and reactive demands at the receiving end of line k.

$$VSI_r = 2V_s^2V_r^2 - V_r^4 - 2V_r^2(P_rR(k) + Q_rX(k)) - |z|^2(P_r^2 + Q_r^2) \tag{5.12}$$

5.2.8 EV User Cost (EVUC)

The cost associated with energy loss incurred during a trip to RCS is the EV user cost. When deciding the best location, it is necessary to determine the distance between RCS and EVs. Eq. (5.13) is used to find the distance between two points. Here (x_Z y_Z) is a point on the coordinate plane where the EV user is present and (x_C y_C) is a point on the coordinate plane where RCS is present. Charging Station (CS) at a location close to EV user is an economical choice from the user perspective. DD matrix (Eq. (5.14)) consists of distance between each zone (EV location) to the nearest RCS. EVUC is calculated using Eq. (5.15), and depends on factors like distance between charging station and EV user location, number of EVs being charged at the charging station (N^{EV}), specific energy consumption of the EV (SEC), and price of electricity (E_p).

$$d_{Z_z-C_m} = \sqrt{(x_{Z_z} - x_{C_m})^2 + (y_{Z_z} - y_{C_m})^2} \tag{5.13}$$

$$DD = \begin{bmatrix} min(d_{Z_1-C_1} & d_{Z_1-C_2} & .. & d_{Z_1-C_m}) \\ min(d_{Z_2-C_1} & d_{Z_2-C_2} & .. & d_{Z_2-C_m}) \\ min(. & . & . & .) \\ min(. & . & . & .) \\ min(d_{Z_z-C_1} & d_{Z_z-C_2} & .. & d_{Z_z-C_m}) \end{bmatrix} \tag{5.14}$$

$$EVUC = \sum_{z=1}^{nz} DD(z) \times N^{EV}(z) \times SEC \times P_E \tag{5.15}$$

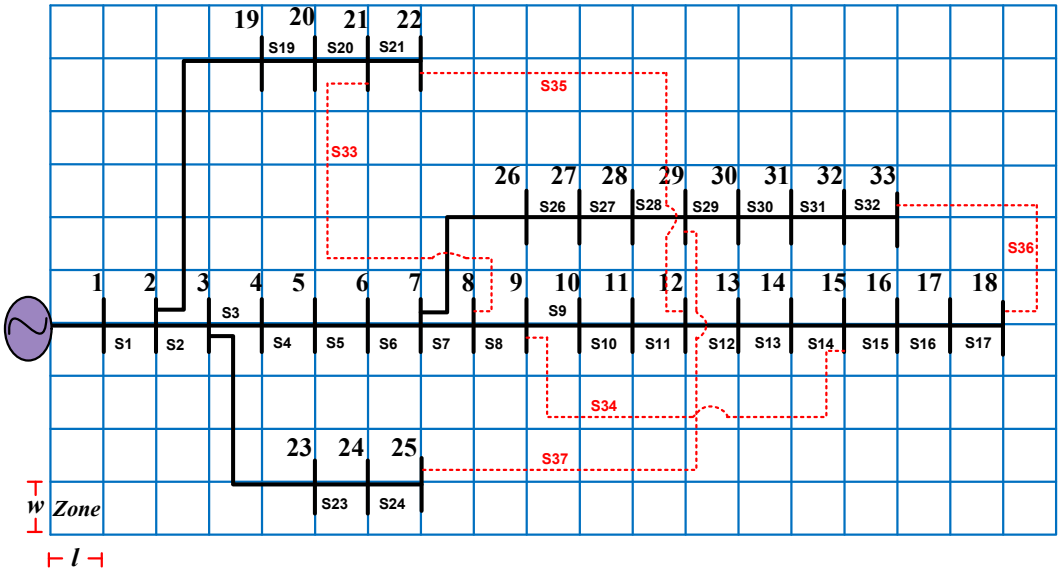

Figure 5.1: IEEE 33 Bus Power distribution network coupled with Road transportation network (Test system)

5.2.9 RCS building cost (ICRCS)

The owner of an RCS always tries to bring down the installation cost. ICRCS is generally affected by several factors, but it mostly depends on the connector count ($N.C_i^{RCS}$) that are installed there. It can be observed that ICRCS would increase as the number of connectors increases, but there would be reduction in waiting time in queue at RCSs. Eq. (5.16) can be used to calculate ICRCS, where C_{inv} (70000 \$) is initial investment, C_{land} (240 \$/m2) is the cost of land, C_{con} (280.33 \$/kW) is the cost of each connector, and Pc is the connector rating (96 kW). Also the capacity of RCS depends on the connector count. It is calculated using Eq. (5.17).

$$ICRCS(i) = C_{init} + 25 \times C_{land} \times N.C_i^{RCS} + C_{con}(N.C_i^{RCS} - 1) \times Pc \tag{5.16}$$

$$RCS(i)_{cap} = N.C_i^{RCS} \times P_c \tag{5.17}$$

5.2.10 Waiting time (W_T)

EVs may have to wait a while before getting energy from RCS. The number of connectors (C) at RCS typically affects waiting time. In order to determine the waiting time, M1/M2/C queuing model is taken into account [82]. In considered queuing model, Eq.

(5.18) gives the total waiting time at all queues of all RCSs in a day. The hourly waiting time is provided by Eq. (5.19), which depends on the estimated number of EV users waiting in queue at RCS ($E_t[n]$ Eq. (5.20)) and arrival rate ($\lambda(t)$ Eq. (5.22)). The probability that no EVs will be charged by connectors at RCS is given by Eq. (5.21). Every RCS must typically serve every EV that arrives, which means that each connector's service rate must be higher than the connector's arrival rate. This requirement is taken into account by optimization Eq. (5.23). The optimal number of connectors must be established within the constraints of minimum and maximum numbers. Here, Eq. (5.24) provides the maximum number of connectors (C^{max}), whereas Eq. (5.25) determines the least number of connectors C^{min}.

$$W_T = \sum_{i=1}^{m} \sum_{t=1}^{24} W(t) \tag{5.18}$$

$$W(t) = \frac{E_t[n]}{\lambda(t)} \tag{5.19}$$

$$E_t[n] = p_t(0) \left[\frac{1}{(C-1)!} \left(\frac{\lambda_t}{\mu_t} \right)^C \frac{\lambda_t \mu_t}{(C\mu_t - \lambda_t)^2} \right] \tag{5.20}$$

$$p_t(0) = \left[\sum_{s=0}^{C-1} \frac{(C\rho)^s}{s!} + \frac{(C\rho)^C}{C!} \frac{1}{(1-\rho)} \right]^{-1} \tag{5.21}$$

$$\lambda(t) = N_{EV}^{iRCS} \times P_{evc} \tag{5.22}$$

$$\rho = \frac{\lambda(t)}{C\mu_t} < 1 \tag{5.23}$$

$$C^{max} = max(P_{evc}) \times N_{EV}^{iRCS} \tag{5.24}$$

$$\frac{\lambda^{max}}{\mu} < C^{min} \qquad \lambda^{max} \in \lambda(t) \tag{5.25}$$

5.2.11 Constraints

In the optimization, real and reactive power balances are included using Eq. (5.26) and Eq. (5.27). The loading on power distribution network results in the deterioration of voltages at the buses. To maintain the voltage within limits, Eq. (5.28) is included.

Every DG has their minimum and maximum generation limits, and these are handled by Eq. (5.29). Eq. (5.30) shows that the combined contribution of all DGs must be limited by the minimum load on the system.

$$P_{sub} + \sum P_{dg} = P_D + \sum P_{RCS} + P_{loss} \tag{5.26}$$

$$Q_{sub} + \sum Q_{dg} + \sum Q_{DST} = Q_D + \sum Q_{RCS} + Q_{loss} \tag{5.27}$$

$$|V^{min}| \leq |V_n| \leq |V^{max}| \qquad n = 1, 2, ...N_{bus} \tag{5.28}$$

$$P_{dg}^{min} \leq P_{dg} \leq P_{dg}^{max} \tag{5.29}$$

$$P_{dg} \leq P_{dg}^{T,max} < min(P_{n,D}) \tag{5.30}$$

Here P_{sub} and Q_{sub} are real power and reactive powers of substations respectively. P_D and Q_D are real and reactive power demands in power distribution system. P_{loss} and Q_{loss} are real power loss and reactive power loss. Here, RCSs have real power loads (P_{RCS}) and reactive power load (Q_{RCS}). Q_{DST} is the reactive power output of D-STATCOMs. V^{min}, V^{max}, P_{dg}^{min}, and P_{dg}^{max} are the lower voltage limit, upper voltage limit, DGs lower real power limit and DGs upper real power limit respectively. $P_{dg}^{T,max}$ is the maximum limit of total active power supplied by all DGs. $P_{n,D}$ is real power demand at n^{th} node of power distribution system.

5.3 Algorithm

5.3.1 Multi objective Rao Algorithm (MORA)

Generally, optimization of complex problems considers more than two objectives. These type of problems are solved through multi objective approach. Multi objective complex problems are solved through heuristic methods due to the advantages on offer by such methods. Mainly, these types of problems are solved through weighted sum approach or Pareto based methods. If the objectives are conflicting in nature, Pareto based methods offer better optimal solutions. Multi objective Rao algorithm is a pareto based optimization algorithm. It was proposed by Rao in 2021 for solving constrained and unconstrained complex optimization problems [5]. It is metaphor less and has no algorithm specific parameters. It has the ability of random interaction among the candidate solutions and moves the candidate solution towards the best solution and away from the worst solution. Eq. (5.31) was used to obtain a new solution in the optimization process.

Figure 5.2 shows the flow chart of implementation of MORA in the optimal planning considered in the present study.

$$X_p^{'} = X_p + r_1 \times (X_b - |X_w|) + r_2 \times (|(X_p or X_r)| - (X_r or X_p)) \tag{5.31}$$

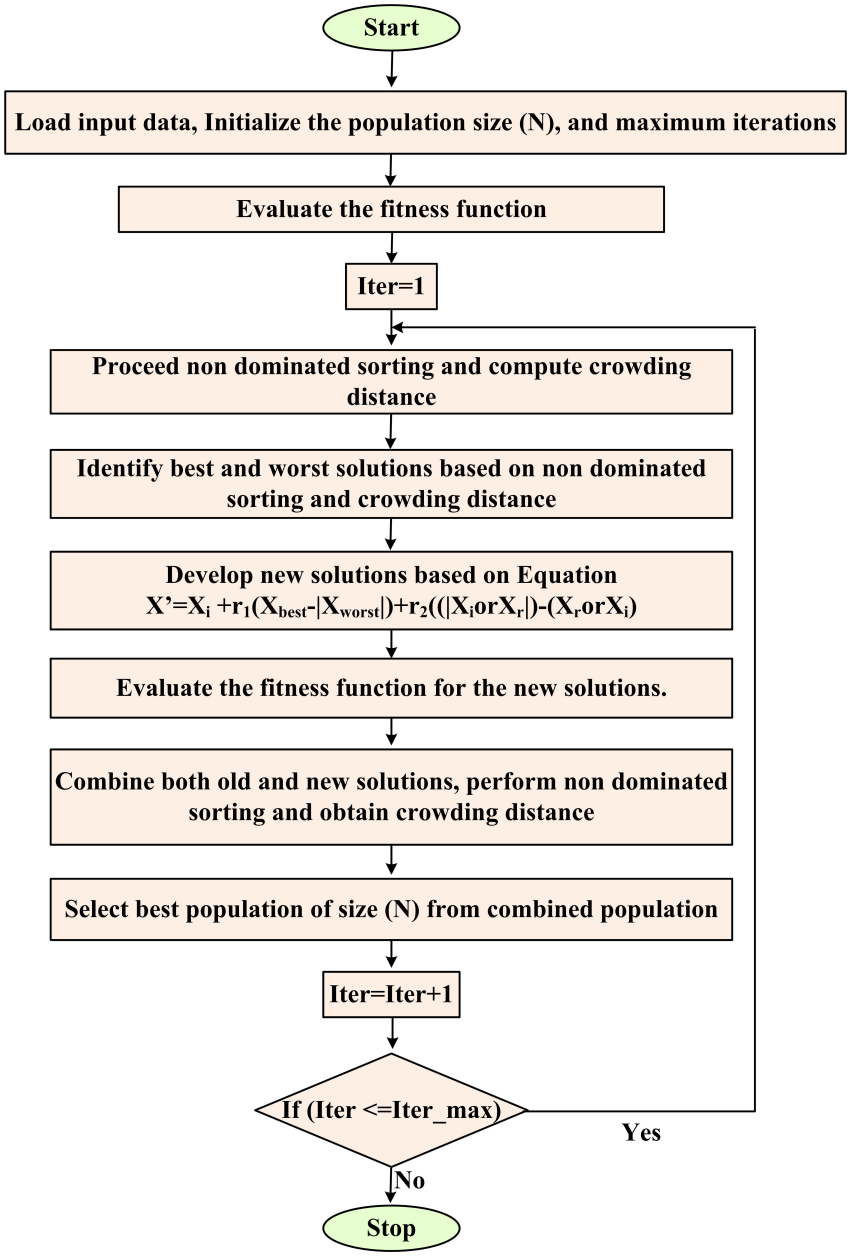

Figure 5.2: Flow chart of MORA algorithm [5]

Here, $X_p^{'}$ is new solution, X_p is present solution, X_b is best solution, X_w is worst solution,

r_1 and r_2 are random values between 0 and 1. X_r is randomly selected solution for multi objective problems.

5.3.2 Non dominated Sorting Genetic Algorithm II (NSGA II)

NSGA II was proposed by Deb in 2002 for solving multi objective problems. The optimization consists of selection stage, cross over stage, and mutation stage [4]. Non dominated sorting and formation of pareto fronts lead to better solution.

5.3.3 Implementation of Multi Objective Rao Algorithm (MORA) for optimal planning of RCSs, DGs, and D-STATCOMs considering network reconfiguration

Step 1: Read the test system data and initialize the algorithm parameters (population size and maximum iterations).
Step 2: Randomly initialize the population (according to section 5.2.4) and determine the respective fitness values.

- $Pop_{stage1} = [ts, L_{RCS}, L_{DG}, L_{DST}, S_{DG}, S_{DST}]$ for stage 1.
- $Pop_{stage2} = [C]$ for stage 2
  (ts is a set of tie line switches, L_{RCS} is location of RCS, L_{DG} is location of DG, L_{DST} is location of D-STATCOM S_{DG} is size of DG, S_{DST} is size of D-STACOM, and C is number of connectors).

Step 3: Set Iter = 1.
Step 4: Perform the non dominated sorting and calculate the crowding distance.
Step 5: Obtain best and worst solutions based on non dominated sorting and crowding distance.
Step 6: Update candidate solutions based on update equation (5.31) and find the updated fitness value.
Step 7: Combine both old and modified solutions and perform non dominated sorting and crowding distance.
Step 8: Select best population of size (N) from combined solutions of size 2N.
Step 9: Set Iter=Iter+1.
Step 10: Terminate the process, if ($Iter > Iter_{max}$) and save the pareto optimal front data otherwise continue from step 4 to step 10.

Step 11: Perform the fuzzy min max decision making technique to select the compromised optimal solution optimal front and print the results.

Table 5.1: Parameters of EV

Parameters	Values
P_{EVB}^{max}	27.69 kWh
N_T^{EV}	600
SEC	0.142 kWh/km
P_c	96 kW

Table 5.2: Bus groups of connected loads in power distribution network

Residential loads	Commercial loads	Industrial loads
2,3,5,6,7,8	4,11,12,18	22,26,27,28
9,10,13,14,15	19	29,30,31,32
16,17,20,23,24	–	33

Table 5.3: Assumed Number of Electric Vehicles at the 190 zones of Transportation system

1	4	3	1	5	1	1	2	3	4	4	5	5	4	2	5	3	3	4
3	4	2	4	1	3	3	1	5	5	4	4	2	1	2	4	5	1	4
3	5	4	1	1	5	4	5	4	4	3	1	3	3	5	2	5	5	2
4	1	2	2	5	2	2	4	4	4	5	4	2	3	5	2	2	5	1
4	3	4	4	4	5	4	1	4	3	4	4	4	1	2	1	5	3	4
2	4	5	3	3	4	2	3	3	5	3	4	3	3	1	5	4	2	1
5	5	4	2	2	2	4	4	5	5	2	5	4	2	2	3	3	3	2
5	5	4	2	4	4	3	5	5	4	1	1	1	5	3	4	3	3	3
1	4	3	1	1	1	4	2	1	3	5	4	4	2	2	1	4	3	3
4	1	1	1	5	1	4	3	5	2	1	2	4	3	5	4	1	5	4

5.4 Simulation Results and discussion

Coupled network of IEEE 33 bus Power distribution network and Road transportation network has been taken for the analysis of the proposed approach. It is shown in Figure 5.1, where transportation area of 20×38 km^2 was divided into 190 zones with each zone of area 2×2 km^2. Table 5.3 shows the assumed number of EVs in each zone of transportation area. It is assumed that EVs are located at the geometrical centre of the respective zones. The loads of power distribution network are categorized into industrial

loads, residential loads, and commercial loads. Table 5.2 shows the bus numbers where various types of loads are connected. The demand variation of various types of loads (Figure 5.3) and hourly charging probability of EVs (Figure 5.4) were considered in the simulation. In the recommended approach, the test system was analysed with Base case, Case 1, Case 2, and Case 3.

- Base case: Analysis of system without including RCSs, DGs, D-STATCOMs, and Network Reconfiguration in a coupled network.
- Case 1: Simultaneous optimal planning of RCSs, DGs, and D-STATCOMs without Network Reconfiguration in coupled network.
- Case 2 : Network reconfiguration of power distribution network in the presence of previous RCSs load, DGs, D-STATCOMs obtained from Case 1.
- Case 3: Simultaneous optimal planning of Network Reconfiguration and RCSs, DGs, and D-STATCOMs in coupled network.

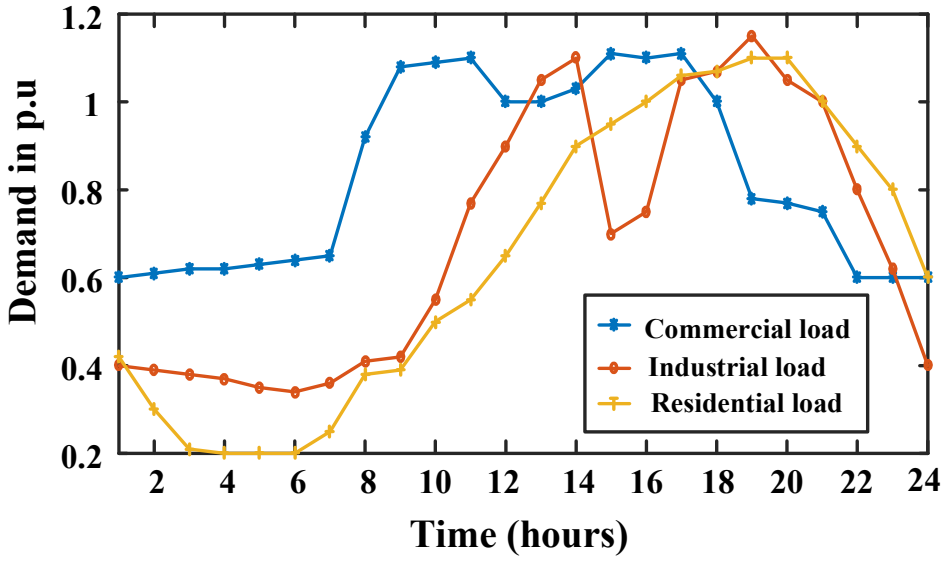

Figure 5.3: Demand variation of various types of loads

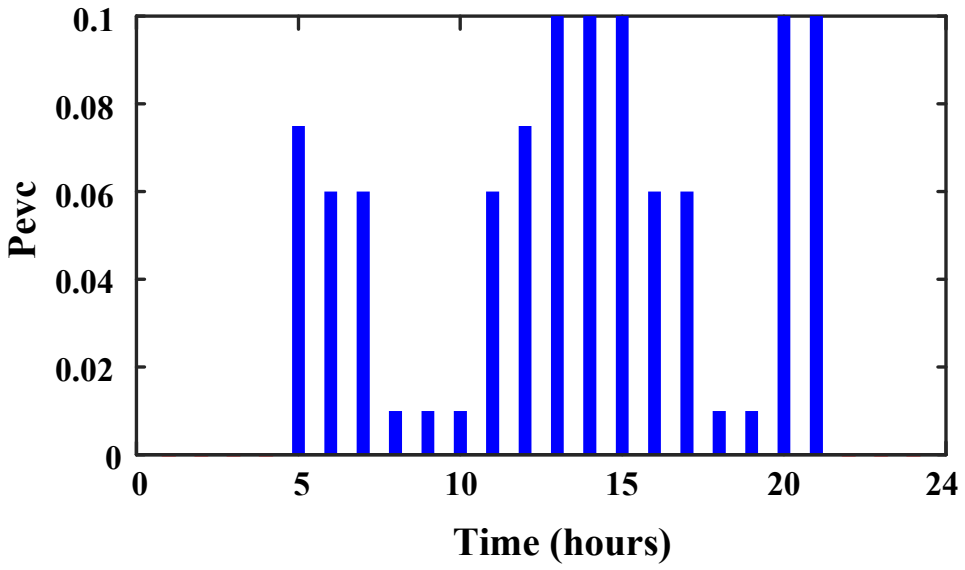

Figure 5.4: Hourly charging probability of Electric Vehicles

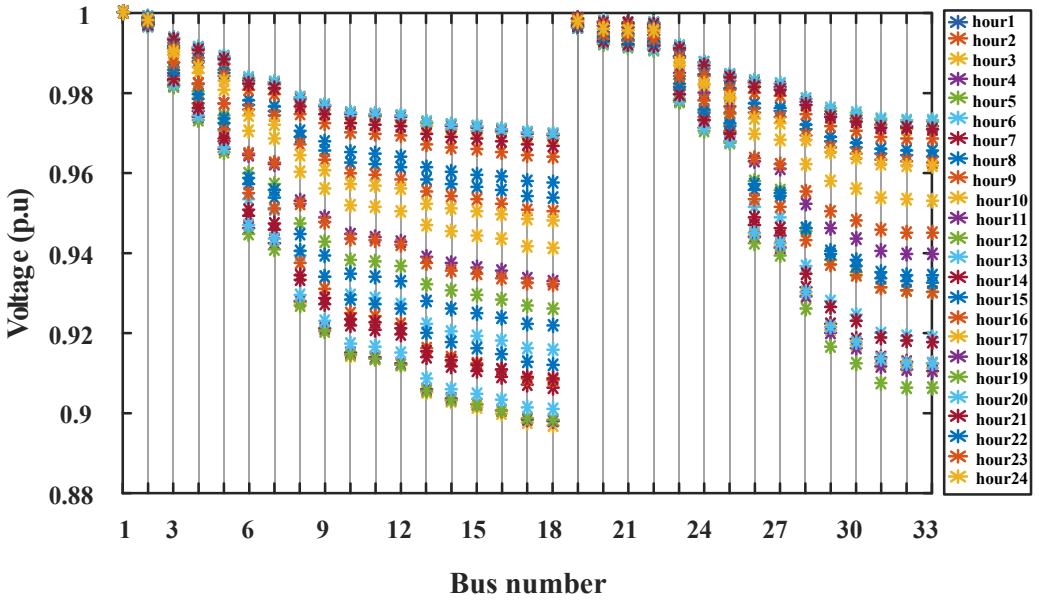

Figure 5.5: Hourly voltage profile of IEEE power distribution network in Base case

5.4.1 Base case

In Base case, the system was analysed without including either RCSs or DGs and D-STATCOMs. Backward forward sweep load flow algorithm was used to perform the load flow study. The state variables of voltage and angles were used to calculate the objective functions that affect the power distribution system. Base case simulation resulted in power loss of 2811 kW, lowest VSI value of 0.6479, and maximum voltage deviation of 1.5816 p.u. The system experienced a minimum voltage of 0.8968 p.u at 18^{th} bus (Figure (5.5)).

5.4.2 Case 1: Simultaneous optimal planning of RCSs, DGs, and D-STATCOMs without Network Reconfiguration in coupled network

In this case, RCSs, distributed generator and distributed static compensators were optimally planned on a coupled network. In planning, the total contribution of all DGs and D-STATCOMs was determined by observing the hourly real power demand (Figure (5.6)) and hourly reactive power demand (Figure (5.7)) on the power distribution system. Here, 1420 kW and 882 kVAr were the minimum real and reactive power demands on the system. The DGs were able to support power distribution network by supplying a reactive power of 460 kVAr. To maintain the system stability, total output power of DGs was limited to 1400 kW and total reactive power output of D-STATCOMs was limited to 420 kVAr.

Figure (5.8) shows the pareto front in Case 1 by MORA algorithm. Here, fuzzy min max decision making technique was employed to select better solution. Table 5.4 shows the placements and sizes of DGs, D-STATCOMs, and RCSs. RCSs were located at 2^{nd}, 21^{st}, 32^{nd} buses while DGs were located at 15^{th}, 29^{th}, 33^{rd} buses with capacities of 391 kW, 303 kW, and 704 kW respectively. D-STATCOMs were placed at 13^{th}, 17^{th}, and 31^{st} buses of power distribution network with capacities of 30 kVAr, 87 kVAr, and 302 kVAr respectively. The above locations and capacities were obtained by MORA algorithm. The technical objectives caused by these locations with out reconfiguration technique are shown in Table 5.5. The integration of DGs, D-STATCOMs and RCSs in power distribution network resulted in lower values of active power loss (990.34 kW), MVD (0.5934 p.u), and EVUC(53.2199 $) in comparison with NSGA II results. The minimum value of VSI should be near unity. Here, the VSI_{min} value is better for the location of MORA (0.8195) compared to NSGA II (0.8094) value. Figure 5.9 shows the

variation of voltage magnitude over 24 hours in a day by MORA algorithm. This figure shows that the system's minimum voltage increased to 0.9521 p.u with the inclusion of RCSs, D-STATCOMs and DGs compared to Base Case.

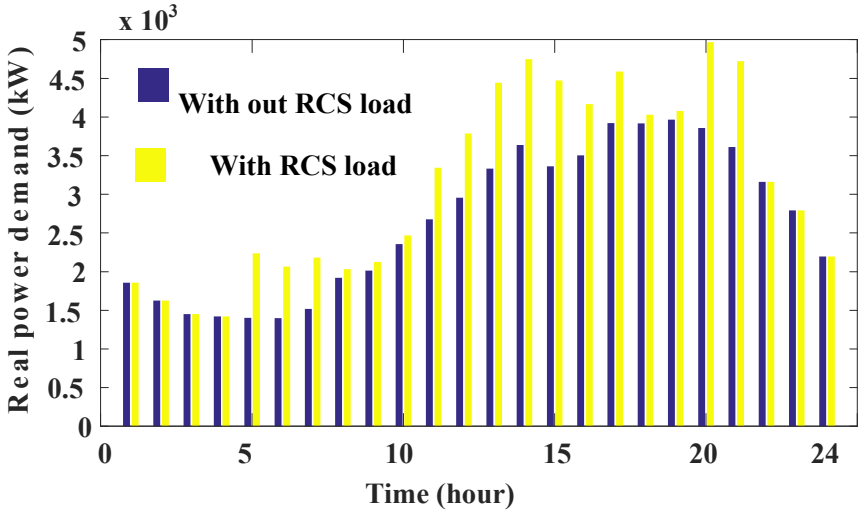

Figure 5.6: Hourly real power demand on the IEEE 33 power distribution system

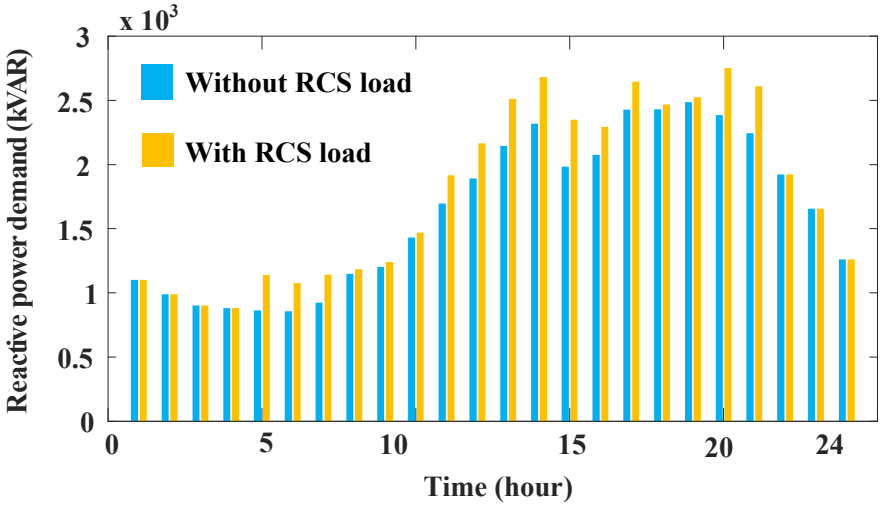

Figure 5.7: Hourly reactive power demand on the IEEE 33 power distribution system

In Stage 2, the optimal count of connectors was decided by employing MORA and NSGA II algorithms. Here, fuzzy min max decision making was employed to select

Table 5.4: Optimal locations and capacities obtained in Stage 1 of Case 1 by both algorithms

Optimal locations and capacities	NSGA II	MORA
RCSs locations	3, 21, 33	2, 21, 32
EVs at RCSs	206, 134, 260	178, 138, 284
DG locations	2, 16, 31	15, 29, 33
DG size (kW)	110, 407, 853	391, 303, 704
D-STATCOMs locations	14, 18, 32	13, 17, 31
D-STATCOMs size (kVAR)	28, 35, 354	30, 87, 302

Table 5.5: Optimal Tie switches and objective parameters obtained in Stage 1 of Case 1 by both algorithms

Optimal results	NSGA II	MORA
Tie switches	34,35,36,37,38	34,35,36,37,38
Ploss (kW)	1092.8	990.34
MVD (p.u)	0.6412	0.5934
VSI_{min}	0.8094	0.8195
EVUC ($)	53.2344	53.2199

optimal solution from the optimal front (Figure (5.10)). In this stage, queue theory was used for determining waiting time. Table 5.6 shows that MORA performed better in achieving better count of connectors that offered low waiting time (28.4217 min) and low building cost of RCS (1.7×10^6 $) compared to NSGA II.

Table 5.6: Optimal RCSs sizes and objective parameters obtained in Stage 2 of Case 1 by both algorithms

Optimal results	NSGA II	MORA
RCSs connectors	10, 10, 12	9, 8, 14
Wt (min)	32.9638	28.4217
ICRCS ($)	1.72×10^6	1.7×10^6
RCSs size (kW)	960, 960, 1152	864, 768, 1344

Table 5.7 shows the the effect of EV load increment on the operational parameters of power distribution system, i.e as the EV load increases, power loss, voltage deviation, system minimum voltage were decreased, while voltage stability index reached worst value. In this context, network reconfiguration is adopted to improve the system performance.

Table 5.7: Effect of EV demand on various objective functions in Case 1 for MORA outcomes

EV demand factor	Ploss	MVD	VSImin	Vmin
1	990	0.5934	0.8195	0.9521
1.1	1020	0.6094	0.8100	0.9493
1.2	1052	0.6255	0.8005	0.9464
1.3	1087	0.6424	0.7910	0.9435
1.4	1124	0.6599	0.7815	0.9406
1.5	1164	0.6778	0.7721	0.9377

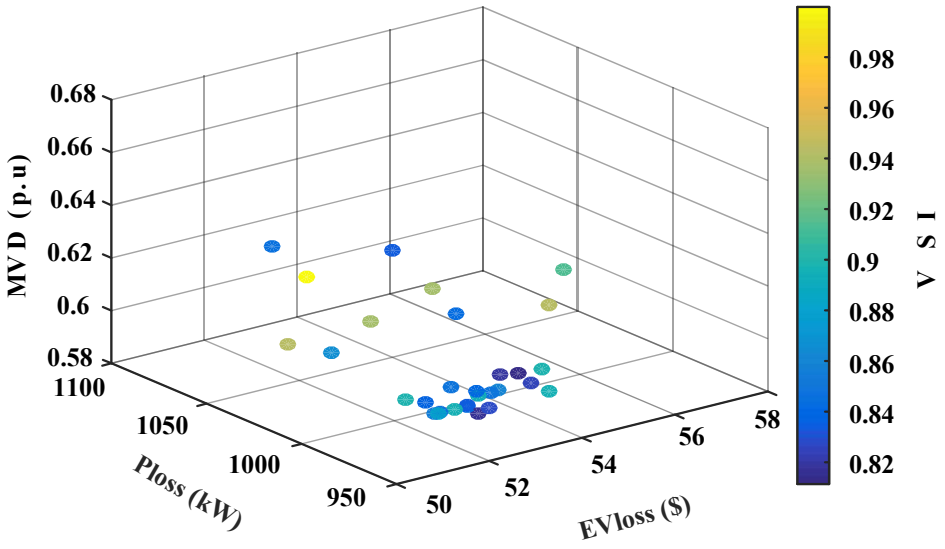

Figure 5.8: Pareto front in Stage 1 of Case 1 by MORA algorithm

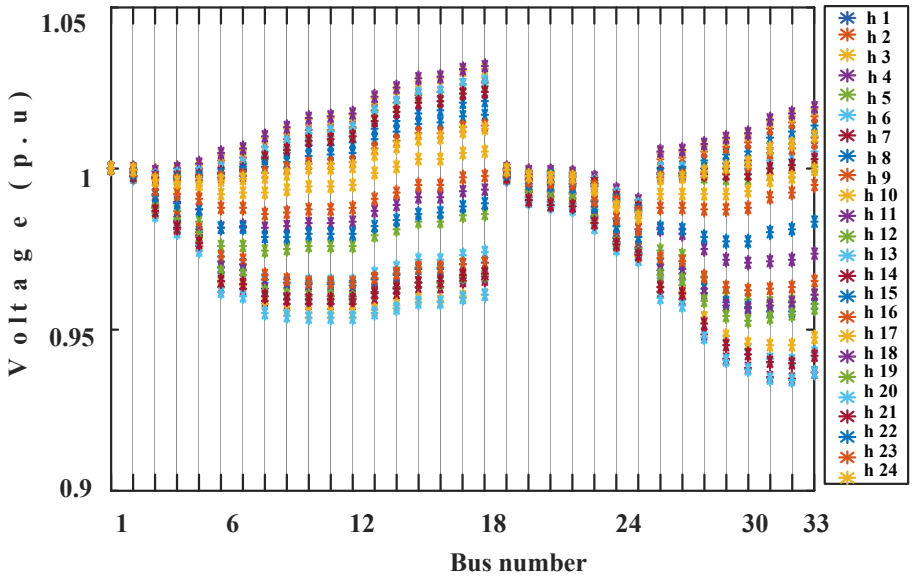

Figure 5.9: Hourly voltage profile of IEEE 33 bus power distribution network in Case 1 by MORA algorithm

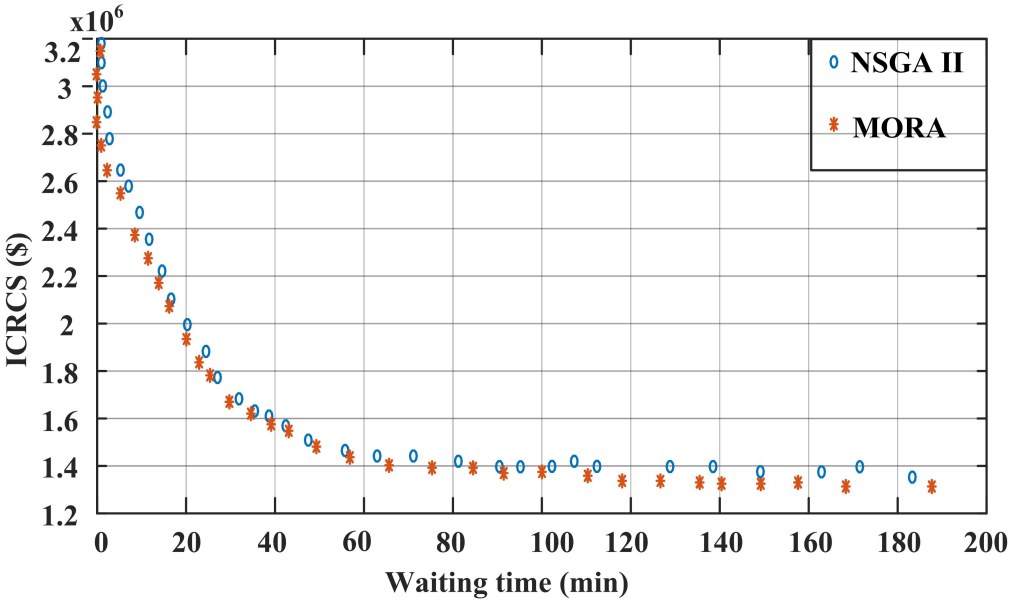

Figure 5.10: Pareto front in Stage 2 of Case 1 by both algorithms

5.4.3 Case 2 : Network reconfiguration of power distribution network after the integration of RCSs, DGs, and D-STATCOMs

In Case 2, Network Reconfiguration Technique (NRT) was employed on the distribution network of coupled network with RCS load, DGs, and D-STATCOMs placed at locations achieved from Case 1.

In network reconfiguration, the opening and closing of sectionalizing switches and tie switches of power distribution system were performed by maintaining radiality to obtain optimal network. Both (MORA and NSGA II) algorithms were applied to obtain optimal tie switches of distribution network. Here, minimization of active power loss, MVD and EV user cost were considered as technical objectives along with improvement of VSI. Table 5.8 shows the tie switches and technical objectives obtained in Case 2 by both algorithms. These were selected by fuzzy min max technique from optimal pareto front (Figure (5.11)). From the table it is observed that tie switches yielded by MORA algorithm resulted in better values of the technical objectives considered compared to NSGA II. From Table 5.5 and Table 5.8, it is noticed that the performance of the distribution network improved after reconfiguration. Active power loss of 791.93 kW resulted after the reconfiguration, which was lower compared to the system before reconfiguration. Better voltage stability was maintained with a low value of MVD (0.4560 p.u) and high value of VSI (0.8381) after NRT compared to Case 1 (0.5934 p.u, 0.8195). However, EVUC was same in both Case 1 and Case 2 as EVUC depends on RCS locations. The reconfiguration of distribution network improved the system's minimum voltage to 0.9544 p.u (Figure (5.12)). Optimal connector count, waiting time, ICRCS, and RCS size were same as Case 1 because RCS locations were same in both cases.

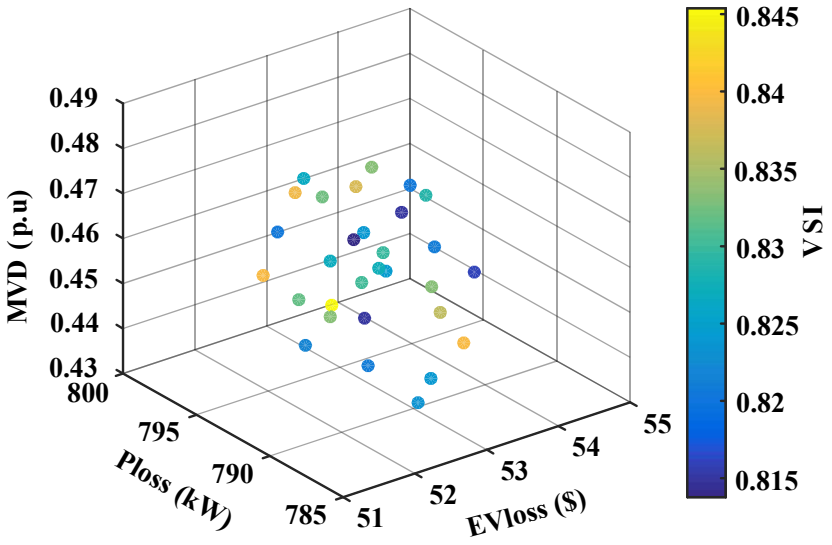

Figure 5.11: Pareto front in Stage 1 of Case 2 by MORA algorithm

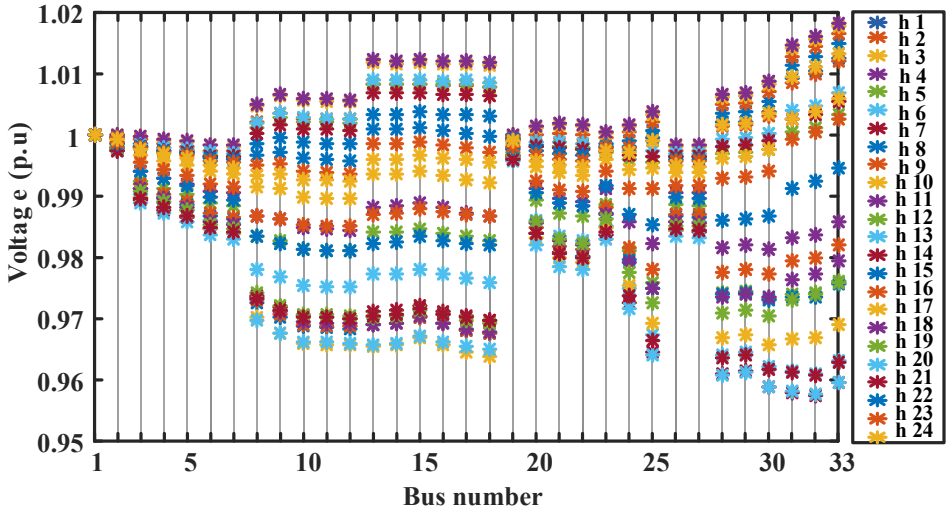

Figure 5.12: Hourly voltage profile of IEEE 33 bus power distribution network in Case 2 by MORA algorithm

From the Table 5.9 and Table 5.7, it is observed that network reconfiguration has resulted in better operational parameters compared to Case 1 .

Table 5.8: Optimal Tie swiches and objective parameters obtained in Stage 1 of Case 2 by both algorithms

Optimal results	NSGA II	MORA
Tie switches	6,8,28,34,36	7,12,27,35,36
Ploss (kW)	921.4615	791.93
MVD (p.u)	0.5145	0.4560
VSI_{min}	0.8385	0.8381
EVUC ($)	53.2344	53.2199

Table 5.9: Effect of EV demand on various objective functions in Case 2 for MORA outcomes

EV demand factor	Ploss	MVD	VSImin	Vmin
1	791.9	0.4560	0.8381	0.9574
1.1	824.23	0.4705	0.8302	0.9551
1.2	858.65	0.4859	0.8223	0.9528
1.3	895.20	0.5018	0.8145	0.9504
1.4	933.9	0.5197	0.8067	0.9480
1.5	974.8	0.5384	0.7988	0.9457

5.4.4 Case 3: Simultaneous Network Reconfiguration and optimal planning of RCSs, DGs, and D-STATCOMs in coupled network

In Case 3, network reconfiguration and optimal planning were done simultaneously. NSGA II and MORA algorithms were applied to achieve optimal tie switches of power distribution network, optimal locations and capacities of RCSs, DGs, and D-STATCOMs.

Optimal pareto front achieved by MORA algorithm is shown in Figure (5.13). The compromised optimal solutions were selected using fuzzy min max decision technique. Table 5.10 shows the optimal results obtained in Stage 1 of Case 3. Both algorithms were implemented to determine the optimal locations and capacities of RCSs, distributed generators, and distributed static compensator. MORA yielded 3^{rd}, 22^{nd}, and 33^{rd} buses for placing RCSs, while NSGA II picked 2^{nd}, 21^{st}, 33^{rd} buses. DGs were located at 14^{th}, 29^{th}, and 32^{nd} buses with capacities of 341 kW, 349 kW, and 703 kW respectively. Here, reactive power compensating was done by installing D-STATCOMs at 17^{th}, 18^{th}, and 31^{st} buses with capacities of 48 kVAr, 107 kVAr, and 262 kVAr.

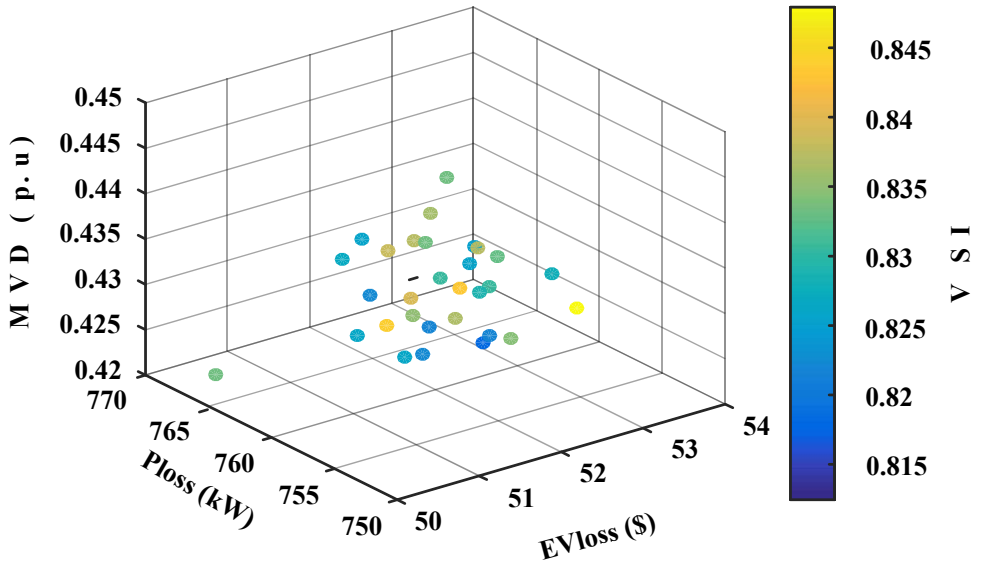

Figure 5.13: Optimal pareto front in Stage 1 of Case 3 by MORA algorithm

Table 5.11 shows tie switches and technical objectives which resulted in Stage 1 by both algorithms. It is observed from this table that tie switches obtained by MORA resulted in better objectives. Active power loss (762.6367 kW) was lower in MORA compared to NSGA II (768.01 kW). MVD of 0.4318 p.u was minimum for MORA while it was 0.4357 p.u by NSGA II. Minimum value of VSI was 0.8357 for MORA, and it was more compared to VSI value yielded by NSGA II. Better locations of RCSs by MORA algorithm resulted in lower value of EVUC (52.2025 $). Figure (5.14) shows the voltage magnitude variations over a day. From the figure it is noticed that the system experienced better voltage profile with minimum voltage of 0.9573 p.u, and had an improved value compared to all cases considered in this chapter.

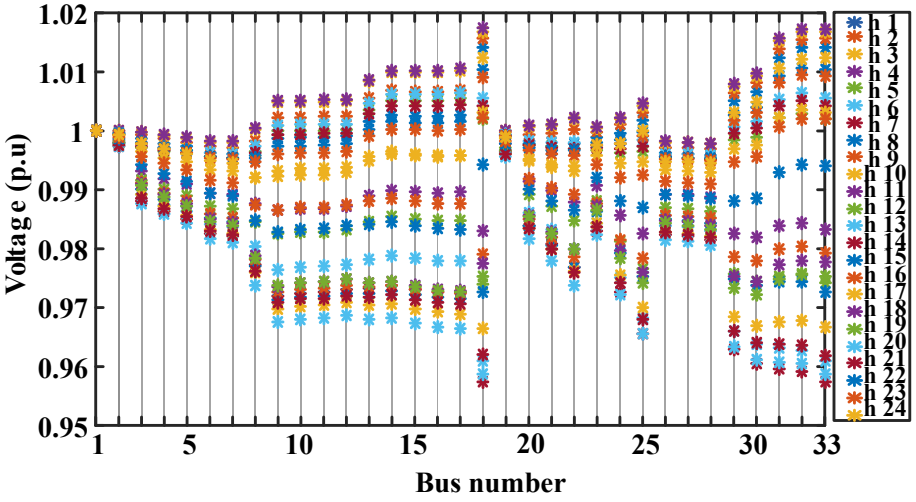

Figure 5.14: Hourly voltage profile of IEEE 33 bus power distribution network in Case 3 by MORA algorithm

Figure (5.15) shows the pareto front obtained in Stage 2 by MORA. Table 5.12 shows the optimal results obtained in Stage 2 of Case 3. MORA yielded 11, 8, and 12 connectors at RCS1, RCS2, and RCS3, respectively, while NSGA II yielded 10, 9 , 12 connectors. The selection of optimal connectors at respective RCS by MORA resulted in lower waiting time of 27.37 min compared to NSGA II (29.37 min) while both algorithms yielded same ICRCS of 1.7×10^6 \$.

Table 5.10: Optimal locations and capacities obtained in Stage 1 of Case 3 by both algorithms

Optimal locations and capacities	NSGA II	MORA
RCSs locations	2, 21, 33	3, 22, 33
EVs at RCSs	183, 157, 260	209, 143, 248
DG locations	14, 28, 32	14, 29, 32
DG size (kW)	386, 290, 723	341, 349, 703
D-STATCOMs locations	3, 18, 31	17, 18, 31
D-STATCOMs size (kVAR)	50, 113, 256	48, 107, 262

Table 5.11: Optimal Tie switches objective parameters obtained in Stage 1 of Case 3 by both algorithms

Optimal results	NSGA II	MORA
Tie switches	7,8,27,34,36	7,8,17,28,34
Ploss (kW)	768.01	762.6367
MVD (p.u)	0.4357	0.4318
VSI_{min}	0.8415	0.8357
EVUC ($)	54.4474	52.2025

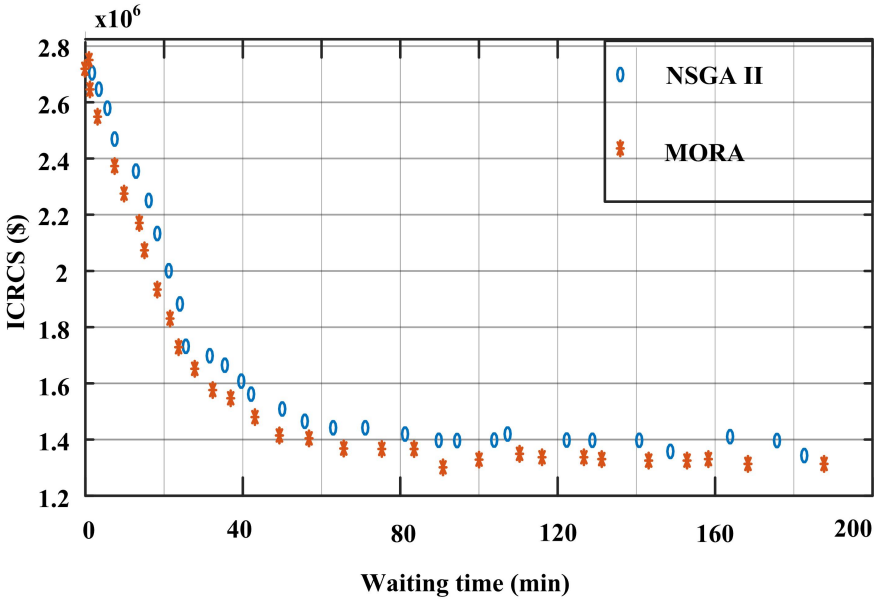

Figure 5.15: Optimal pareto front in Stage 2 of Case 3 by both algorithms

Table 5.13 shows that simultaneous network reconfiguration and optimal planning of RCSs, DGs, and D-STATCOMs in Case 3 has resulted in better values of system operational parameter compared to Case 1 and Case 2.

Table 5.12: Optimal RCSs sizes and objective parameters obtained in Stage 2 of Case 3 by MORA and NSGA-II algorithms

Optimal results	NSGA II	MORA
RCSs connectors	10, 9, 12	11, 8, 12
Wt (min)	29.37	27.37
ICRCS ($)	1.7×10^6	1.7×10^6
RCSs size (kW)	960,864, 1152	1056, 768, 1152

Table 5.13: Effect of EV demand on various objective functions in Case 3 for MORA outcomes

EV demand factor	Ploss	MVD	VSImin	Vmin
1	762.6	0.4318	0.8357	0.9591
1.1	799.04	0.4479	0.8332	0.9550
1.2	837.62	0.4653	0.8302	0.9526
1.3	878.4	0.4834	0.8201	0.9515
1.4	921.39	0.5019	0.8080	0.9507
1.5	966.62	0.5208	0.7982	0.9502

Table 5.14 shows the comparison of objective parameters in Stage 1 of all cases by MORA algorithm. It is noticed from the comparison that, simultaneous network reconfiguration and optimal planning RCSs, DGs, and D-STATCOMs (Case 3) yielded better performance and user comfort. The active power loss was 27.13 % of base power loss in Case 3 while it was 35.23 % and 28.17 % in Case 1 and Case 2 respectively. Better voltage profile with 27.3 % MVD and 28.98 % VSI_{min} was obtained compared to base case. The optimal locations of DGs and D-STATCOMs obtained in Case 3 made the RCSs spread over the network considered and this resulted in lower EVUC of 52.2025 $. Table 5.15 shows the waiting time and RCS building cost in all Cases. From the comparison, it can be observed that Case 3 resulted in lower waiting time of 27.37 min compared to Case 1 and Case 2. The building cost was same in all cases. From the analysis made in all the cases, it can be concluded that simultaneous optimal planning

Table 5.14: Comparison of objective parameters of Stage 1 in all cases by MORA algorithm

Objective parameter	Base Case	Case 1	Case 2	Case 3
Ploss (kW)	2811	990.34	791.93	762.6367
MVD (p.u)	1.5816	0.5934	0.4560	0.4318
VSI_{min}	0.6479	0.8195	0.8381	0.8357
EVUC ($)	–	53.2199	53.2199	52.2025

Table 5.15: Comparison of objective parameters of Stage 2 in all cases by MORA algorithm

Objective parameter	Base Case	Case 1	Case 2	Case 3
Wt (min)	–	28.42	28.42	27.37
ICRCS ($)	–	1.7×10^6	1.7×10^6	1.7×10^6

of RCSs, DGs, and D-STATCOMs along with reconfiguration techniques gives better performance of power distribution network and also offers benefit of low EVUC from EV user perspective.

5.5 Summary

The load due to RCSs reduces the performance of the power distribution system. In this context, optimal planning of RCSs, DGs, and D-STATCOMs along with network reconfiguration was done in a coupled network. Optimal planning was done in two stages. Stage 1 deals with network reconfiguration and optimal planning of RCSs, DGs and D-STATCOMs by considering minimization of active power loss, EV user cost, voltage deviation, and improvement of voltage stability index. In Stage 2, queue model was employed in obtaining optimal connector count at each RCS. Minimization of waiting time and building cost of RCS were considered in Stage 2. In the simulation, variation of various load types and EV charging was considered. Analyses included optimal planning of RCSs, DG, and D-STATCOMs without network reconfiguration as Case 1, applying network reconfiguration of power distribution network with the location obtained and sizes of RCSs, DGs, and D-STATCOMs from Case 1 as Case 2, and simultaneous optimal planning and network reconfiguration as Case 3. The reduction of 72.86 % active power loss, 72.69 % of MVD, and improvement of VSI_{min} from 0.6479 to 0.8357 in Case 3 (compared to base case) by MORA algorithm showed that simultaneous optimal planning of RCSs, DGs, and D-STATCOMs along with network reconfiguration offers better performance of the power distribution network. Here, the ability of random interactions among candidate solutions and moving the candidate solution toward the best and away from the worst solution yielded better solutions than NSGA II algorithm.

Chapter 6
Conclusion

6.1 General

In order to reduce greenhouse gas emissions, transportation system must be electrified. Adopting electric vehicles for road transport is a feasible way to reduce to a large extent greenhouse gas emissions. Installing infrastructure for quick charging could enable EV adoption. However, integration of RCS into Radial Distribution Network (RDN) cause performance degradation. The location of RCS affects both the performance of RDN and the comfort of EV users. The optimal planning of charging station considering only power network is not feasible.

In this thesis, optimal planning of Rapid charging stations, Distributed Generators, and D-STATCOMs have been done on a proposed coupled network. Optimal number of charging connectors at each RCS was determined by employing queue theory based optimization approach. In the optimal planning, minimization of active power loss, voltage deviation, EV user cost, waiting time, RCS installation cost, and maximization of voltage stability index were considered. Further, the performance of power distribution system was enhanced by including the network reconfiguration technique in optimal planning. A novel metaphor less Rao 3 algorithm was utilized for optimizing single objective and multi objective problems. The results were verified by PSO, JAYA, and NSGA II algorithms.

6.2 Summary of Important findings

The summary of the findings from the current research is as follows:

It is important to consider EV user behaviour for RCSs planning while installing charging stations. This thesis presents a concise planning of RCSs and DGs to reduce power loss, voltage deviation, and EV user cost on a coupled network. Optimal RCSs planning has been analysed and compared for the following scenarios: i) RCSs alone, ii) Optimal DG planning with prior RCSs outcomes. iii) Concurrent planning of RCSs and DGs. The proposed planning was implemented by considering daily EV charging probability and load patterns. The use of metaphor less Rao 3 algorithm can ensure faster convergence with better performance for optimal planning of RCSs and DGs simultaneously.

Random interactions between candidate solutions and the ability to move candidate solutions towards the best optimal solution and away from the worst solution of Rao 3 algorithm, outperform both PSO and Jaya algorithms.

In this thesis, a planning approach of charging station that favours electrical network, EV user, and charging station owner has been proposed. Consideration of EV user loss, RCS installation cost, and waiting time in queue at RCS plays a vital role in obtaining optimal locations for RCS, and these objectives are conflicting in nature. To address the above issues, a two stage approach was proposed to determine the optimal size and locations of RCSs and DGs using pareto based multi objective approach. Optimal location of RCSs and optimal location and size of DGs are determined by minimizing power loss, voltage deviation, EV user cost and maximizing voltage stability index in the first stage. M1/M2/C queue theory model was used for finding the waiting in queue at RCS. Minimization of waiting time and installation cost of RCS were considered as objectives to determine the optimal number of connectors at RCS in second stage. During the analysis, the variation of various types of loads and the variation of probability of charging of EVs was considered. The simultaneous placement of RCSs and DGs resulted in 57.9% reduction in active power loss, 56.6% reduction in voltage deviation, and 22.6% improvement in VSI (compared to base case). The optimization problem was solved by Multi objective Rao optimization algorithm (MORA) and NSGA II. The ability of random interactions and move candidate solution close to the best solution and far away from the worst solution of MORA yielded better solutions than NSGA-II.

In this thesis, a two stage approach has been proposed for determining optimal placements and capacities for RCSs, DGs, and D-STATCOMs in a coupled network. At Stage 1, improvement of active power loss, reducing voltage deviation, EV user cost, and voltage stability index, were taken into consideration. Optimal connector count was determined by considering the minimization of waiting time at RCS and installation cost of RCS in Stage 2. Hourly load demand variation at various bus types and the hourly probability of EVs charging were taken in the analysis. The optimization problem was solved using Multi-Objective Rao Algorithm (MORA). It is clear from the results that the presence of RCSs worsened the voltage profile and increased power loss (Case 1). The installation of RCSs and DGs improved the performance of RDN (Case 2). Finally, providing reactive power support by concurrent planning of RCSs, DGs, and D-STATCOMs in Case 3 yielded better results than Base case, Case 1, and Case 2. The simultaneous placement of RCSs, DGs, and D-STATCOMs resulted in 64.76% reduction in active power loss, 62.76% reduction in voltage deviation, and 26.48% improve-

ment in VSI (compared to Base case). The spread of RCS in the coupled network was helped by the presence of DGs and D-STATCOMs, which led to a low value of EVUC (i.e EV user comfort). The ability of random interactions and move candidate solution close to the best solution and far away from the worst solution of MORA yielded better solutions than NSGA-II.

In this thesis, optimal planning of RCSs, DGs, and D-STATCOMs along with network reconfiguration of Radial Distribution Network (RDN) was proposed in a coupled network. Optimal planning was done through two stages. Stage 1 deals with network reconfiguration and optimal planning of RCSs, DGs, and D-STATCOMs by considering minimization of active power loss, EV user cost, voltage deviation, and improvement of voltage stability index. In Stage 2, queue model was employed in obtaining optimal connector count at each RCS. Minimization of waiting time and building cost of RCSs were considered in Stage 2. In the simulation, variation of various load types and EV charging was considered. Analyses included optimal planning of RCSs, DG, and D-STATCOMs without network reconfiguration as Case 1, applying network reconfiguration of RDN with the location obtained and sizes of RCSs, DGs, and D-STATCOMs from Case 1 as Case 2, and simultaneous optimal planning and network reconfiguration as Case 3. The reduction of 72.86 % active power loss, 72.69 % of MVD, and improvement of VSI_{min} from 0.6479 to 0.8357 in Case 3 (compared to Base case) by MORA algorithm showed that simultaneous optimal planning of RCSs, DGs, and D-STATCOMs along with network reconfiguration offers better performance for RDN. Here, the ability of random interactions among candidate solutions and moving the candidate solution toward the best and away from the worst solution yielded better solutions than NSGA II algorithm.

6.3 Future Scope

The following are the possible extensions of the current research work.

1. Optimal planning can be extended by considering the EV load and base load uncertainties.
2. Optimal planning can be extended by considering reliability indices like Average Energy Not Supplied (AENS), System Average Interruption Frequency Index (SAIFI), Customer Average Interruption Frequency Index (CAIFI), and etc.
3. Optimal planning can be extended by considering the improvement of resiliency of power network.

4. Utilization of advanced optimization techniques in the complex placement problems can be researched.

5. Optimal planning of RCS can be done by considering the realistic road network along with distribution network.

.

Bibliography

[1] J. Kennedy and R. Eberhart, "Particle swarm optimization," in *Proceedings of ICNN'95-international conference on neural networks*, vol. 4, pp. 1942–1948, IEEE, 1995.

[2] R. Rao, "Jaya: A simple and new optimization algorithm for solving constrained and unconstrained optimization problems," *International Journal of Industrial Engineering Computations*, vol. 7, no. 1, pp. 19–34, 2016.

[3] R. Rao, "Rao algorithms: Three metaphor-less simple algorithms for solving optimization problems," *International Journal of Industrial Engineering Computations*, vol. 11, no. 1, pp. 107–130, 2020.

[4] K. Deb, A. Pratap, S. Agarwal, and T. Meyarivan, "A fast and elitist multiobjective genetic algorithm: Nsga-ii," *IEEE transactions on evolutionary computation*, vol. 6, no. 2, pp. 182–197, 2002.

[5] R. V. Rao and H. S. Keesari, "Rao algorithms for multi-objective optimization of selected thermodynamic cycles," *Engineering with Computers*, vol. 37, pp. 3409–3437, 2021.

[6] E. Hadian, H. Akbari, M. Farzinfar, and S. Saeed, "Optimal allocation of electric vehicle charging stations with adopted smart charging/discharging schedule," *IEEE Access*, vol. 8, pp. 196908–196919, 2020.

[7] I. Frade, A. Ribeiro, G. Gonçalves, and A. P. Antunes, "Optimal location of charging stations for electric vehicles in a neighborhood in lisbon, portugal," *Transportation Research Record*, vol. 2252, no. 1, pp. 91–98, 2011.

[8] T. Ramachandra, B. H. Aithal, and K. Sreejith, "Ghg footprint of major cities in india," *Renewable and Sustainable energy reviews*, vol. 44, pp. 473–495, 2015.

[9] A. Miele, J. Axsen, M. Wolinetz, E. Maine, and Z. Long, "The role of charging and refuelling infrastructure in supporting zero-emission vehicle sales," *Transportation Research Part D: Transport and Environment*, vol. 81, p. 102275, 2020.

[10] A. König, L. Nicoletti, D. Schröder, S. Wolff, A. Waclaw, and M. Lienkamp, "An overview of parameter and cost for battery electric vehicles," *World Electric Vehicle Journal*, vol. 12, no. 1, p. 21, 2021.

[11] M. A. Hannan, F. Azidin, and A. Mohamed, "Hybrid electric vehicles and their challenges: A review," *Renewable and Sustainable Energy Reviews*, vol. 29, pp. 135–150, 2014.

[12] R. C. Green II, L. Wang, and M. Alam, "The impact of plug-in hybrid electric vehicles on distribution networks: A review and outlook," *Renewable and sustainable energy reviews*, vol. 15, no. 1, pp. 544–553, 2011.

[13] M. Muthukumar, N. Rengarajan, B. Velliyangiri, M. Omprakas, C. Rohit, and U. K. Raja, "The development of fuel cell electric vehicles–a review," *Materials Today: Proceedings*, vol. 45, pp. 1181–1187, 2021.

[14] S. Mehta, "Electric plug-in vehicle/electric vehicle, status report," *Electr. Eng*, pp. 1–15, 2010.

[15] T.-D. Nguyen, S. Li, W. Li, and C. C. Mi, "Feasibility study on bipolar pads for efficient wireless power chargers," in *2014 IEEE Applied Power Electronics Conference and Exposition-APEC 2014*, pp. 1676–1682, IEEE, 2014.

[16] H. Wu, "A survey of battery swapping stations for electric vehicles: Operation modes and decision scenarios," *IEEE Transactions on Intelligent Transportation Systems*, vol. 23, no. 8, pp. 10163–10185, 2021.

[17] S. Deb, K. Tammi, K. Kalita, and P. Mahanta, "Impact of electric vehicle charging station load on distribution network," *Energies*, vol. 11, no. 1, p. 178, 2018.

[18] D. Boston and A. Werthman, "Plug-in vehicle behaviors: An analysis of charging and driving behavior of ford plug-in electric vehicles in the real world," *World Electric Vehicle Journal*, vol. 8, no. 4, pp. 926–935, 2016.

[19] K. Morrow, D. Karner, and J. E. Francfort, "Plug-in hybrid electric vehicle charging infrastructure review," 2008.

[20] Y. Zheng, Z. Y. Dong, Y. Xu, K. Meng, J. H. Zhao, and J. Qiu, "Electric vehicle battery charging/swap stations in distribution systems: comparison study and optimal planning," *IEEE transactions on Power Systems*, vol. 29, no. 1, pp. 221–229, 2013.

[21] P. Morrissey, P. Weldon, and M. O'Mahony, "Future standard and fast charging infrastructure planning: An analysis of electric vehicle charging behaviour," *Energy policy*, vol. 89, pp. 257–270, 2016.

[22] T. Bräunl, "Synthetic engine noise generation for improving electric vehicle safety," *International journal of vehicle safety*, vol. 6, no. 1, pp. 1–8, 2012.

[23] D. Mayfield and C. F. Ohio, "Siting electric vehicle charging stations," *Editor Carlotta Collette*, 2012.

[24] J. Feng, S. X. Xu, and M. Li, "A novel multi-criteria decision-making method for selecting the site of an electric-vehicle charging station from a sustainable perspective," *Sustainable Cities and Society*, vol. 65, p. 102623, 2021.

[25] E. A. Rene, W. S. T. Fokui, and P. K. N. Kouonchie, "Optimal allocation of plug-in electric vehicle charging stations in the distribution network with distributed generation," *Green Energy and Intelligent Transportation*, p. 100094, 2023.

[26] Z. Huang, B. Fang, and J. Deng, "Multi-objective optimization strategy for distribution network considering v2g-enabled electric vehicles in building integrated energy system," *Protection and Control of Modern Power Systems*, vol. 5, pp. 1–8, 2020.

[27] W. Khan, F. Ahmad, and M. S. Alam, "Fast ev charging station integration with grid ensuring optimal and quality power exchange," *Engineering Science and Technology, an International Journal*, vol. 22, no. 1, pp. 143–152, 2019.

[28] G. H. Fox, "Electric vehicle charging stations: Are we prepared?," *IEEE Industry Applications Magazine*, vol. 19, no. 4, pp. 32–38, 2013.

[29] M. R. Khalid, M. S. Alam, A. Sarwar, and M. J. Asghar, "A comprehensive review on electric vehicles charging infrastructures and their impacts on power-quality of the utility grid," *ETransportation*, vol. 1, p. 100006, 2019.

[30] C. Luo, Y.-F. Huang, and V. Gupta, "Placement of ev charging stations—balancing benefits among multiple entities," *IEEE Transactions on Smart Grid*, vol. 8, no. 2, pp. 759–768, 2015.

[31] M. H. Khooban, M. ShaSadeghi, T. Niknam, and F. Blaabjerg, "Analysis, control and design of speed control of electric vehicles delayed model: multi-objective fuzzy fractional-order controller," *IET Science, Measurement & Technology*, vol. 11, no. 3, pp. 249–261, 2017.

[32] R. Ye, X. Huang, Z. Chen, and Z. Ji, "A hybrid charging management strategy for solving the under-voltage problem caused by large-scale ev fast charging," *Sustainable Energy, Grids and Networks*, vol. 27, p. 100508, 2021.

[33] N. K. Krishnamurthy, J. N. Sabhahit, V. K. Jadoun, D. N. Gaonkar, A. Shrivastava, V. S. Rao, and G. Kudva, "Optimal placement and sizing of electric vehicle charging infrastructure in a grid-tied dc microgrid using modified tlbo method," *Energies*, vol. 16, no. 4, p. 1781, 2023.

[34] M. Suhail, I. Akhtar, and S. Kirmani, "Objective functions and infrastructure for optimal placement of electrical vehicle charging station: a comprehensive survey," *IETE Journal of Research*, pp. 1–11, 2021.

[35] F. Ahmad, A. Iqbal, I. Ashraf, M. Marzband, *et al.*, "Optimal location of electric vehicle charging station and its impact on distribution network: A review," *Energy Reports*, vol. 8, pp. 2314–2333, 2022.

[36] V. Boddapati, A. R. Kumar, D. Prakash, and S. A. Daniel, "Design and feasibility analysis of a solar pv and biomass-based electric vehicle charging station for metropolitan cities (india)," *Distributed Generation & Alternative Energy Journal*, pp. 793–818, 2022.

[37] S. M. Shariff, M. S. Alam, S. Hameed, M. R. Khalid, A. Ahmad, E. A. Al-Ammar, I. Alsaidan, and H. Alrajhi, "A state-of-the-art review on the impact of fast ev charging on the utility sector," *Energy Storage*, vol. 4, no. 4, p. e300, 2022.

[38] P. V. K. Babu and K. Swarnasri, "Multi-objective optimal allocation of electric vehicle charging stations in radial distribution system using teaching learning based optimization," *International Journal of Renewable Energy Research*, vol. 10, no. 1, pp. 366–377, 2020.

[39] K. Gholami, S. Karimi, and A. Anvari-Moghaddam, "Multi-objective stochastic planning of electric vehicle charging stations in unbalanced distribution networks supported by smart photovoltaic inverters," *Sustainable cities and society*, vol. 84, p. 104029, 2022.

[40] M. Z. Zeb, K. Imran, A. Khattak, A. K. Janjua, A. Pal, M. Nadeem, J. Zhang, and S. Khan, "Optimal placement of electric vehicle charging stations in the active distribution network," *IEEE Access*, vol. 8, pp. 68124–68134, 2020.

[41] S. Davidov and M. Pantoš, "Optimization model for charging infrastructure planning with electric power system reliability check," *Energy*, vol. 166, pp. 886–894, 2019.

[42] H. Simorgh, H. Doagou-Mojarrad, H. Razmi, and G. B. Gharehpetian, "Cost-based optimal siting and sizing of electric vehicle charging stations considering demand response programmes," *IET Generation, Transmission & Distribution*, vol. 12, no. 8, pp. 1712–1720, 2018.

[43] Y. A. Alhazmi and M. M. Salama, "Economical staging plan for implementing electric vehicle charging stations," *Sustainable Energy, Grids and Networks*, vol. 10, pp. 12–25, 2017.

[44] L. Al-Ghussain, A. Darwish Ahmad, A. M. Abubaker, M. Alrbai, O. Ayadi, S. Al-Dahidi, and N. K. Akafuah, "Techno-economic assessment of photovoltaic-based charging stations for electric vehicles in developing countries," *Energy Sources, Part A: Recovery, Utilization, and Environmental Effects*, vol. 45, no. 1, pp. 523–541, 2023.

[45] P. K. Saurav, S. Mansani, and P. Kayal, "Optimal allocation and assessment of distributed generation units with multi-objective planning in unbalanced distribution networks," *Electric Power Components and Systems*, pp. 1–20, 2023.

[46] S. K. Injeti and V. K. Thunuguntla, "Optimal integration of dgs into radial distribution network in the presence of plug-in electric vehicles to minimize daily active power losses and to improve the voltage profile of the system using bio-inspired optimization algorithms," *Protection and Control of Modern Power Systems*, vol. 5, pp. 1–15, 2020.

[47] F. Ahmad, A. Iqbal, I. Ashraf, M. Marzband, and I. Khan, "The optimal placement of electric vehicle fast charging stations in the electrical distribution system with randomly placed solar power distributed generations," *Distributed Generation & Alternative Energy Journal*, pp. 1277–1304, 2022.

[48] W. S. T. Fokui, M. J. Saulo, and L. Ngoo, "Optimal placement of electric vehicle charging stations in a distribution network with randomly distributed rooftop photovoltaic systems," *Ieee Access*, vol. 9, pp. 132397–132411, 2021.

[49] Niharika and V. Mukherjee, "Intelligent electric vehicles charging coupled demand response of isolated microgrid," *Energy Storage*, vol. 4, no. 4, p. e326, 2022.

[50] K. Kathiravan and P. Rajnarayanan, "Application of aoa algorithm for optimal placement of electric vehicle charging station to minimize line losses," *Electric Power Systems Research*, vol. 214, p. 108868, 2023.

[51] K. E. Adetunji, I. W. Hofsajer, A. M. Abu-Mahfouz, and L. Cheng, "An optimization planning framework for allocating multiple distributed energy resources and electric vehicle charging stations in distribution networks," *Applied Energy*, vol. 322, p. 119513, 2022.

[52] F. Ahmad, I. Ashraf, A. Iqbal, M. Marzband, and I. Khan, "A novel ai approach for optimal deployment of ev fast charging station and reliability analysis with solar based dgs in distribution network," *Energy Reports*, vol. 8, pp. 11646–11660, 2022.

[53] F. Ahmad, A. Iqbal, I. Asharf, M. Marzband, and I. Khan, "Placement and capacity of ev charging stations by considering uncertainties with energy management strategies," *IEEE Transactions on Industry Applications*, 2023.

[54] K. Balu and V. Mukherjee, "Siting and sizing of distributed generation and shunt capacitor banks in radial distribution system using constriction factor particle swarm optimization," *Electric Power Components and Systems*, vol. 48, no. 6-7, pp. 697–710, 2020.

[55] M. Bilal and M. Rizwan, "Integration of electric vehicle charging stations and capacitors in distribution systems with vehicle-to-grid facility," *Energy Sources, Part A: Recovery, Utilization, and Environmental Effects*, pp. 1–30, 2021.

[56] A. Pratap, P. Tiwari, R. Maurya, and B. Singh, "A novel hybrid optimization approach for optimal allocation of distributed generation and distribution static compensator with network reconfiguration in consideration of electric vehicle charging station," *Electric Power Components and Systems*, pp. 1–26, 2023.

[57] B. Mahdad, "Optimal integration and coordination of distributed generation and shunt compensators using improved african vultures optimizer," *Engineering Optimization*, pp. 1–38, 2023.

[58] S. R. Gampa, K. Jasthi, P. Goli, D. Das, and R. Bansal, "Grasshopper optimization algorithm based two stage fuzzy multiobjective approach for optimum sizing and placement of distributed generations, shunt capacitors and electric vehicle charging stations," *Journal of Energy Storage*, vol. 27, p. 101117, 2020.

[59] L. Lin, S. Shen, Y. Liao, C. Wang, and L. Shahabi, "Shunt capacitor allocation by considering electric vehicle charging stations and distributed generators based on optimization algorithm," *Energy*, vol. 239, p. 122283, 2022.

[60] J. E. Anderson, M. Bergfeld, D. M. Nguyen, and F. Steck, "Real-world charging behavior and preferences of electric vehicles users in germany," *International Journal of Sustainable Transportation*, pp. 1–15, 2022.

[61] N. Kumar, T. Kumar, S. Nema, and T. Thakur, "A comprehensive planning framework for electric vehicles fast charging station assisted by solar and battery based on queueing theory and non-dominated sorting genetic algorithm-ii in a co-ordinated transportation and power network," *Journal of Energy Storage*, vol. 49, p. 104180, 2022.

[62] B. Zhang, M. Zhao, and X. Hu, "Location planning of electric vehicle charging station with users' preferences and waiting time: multi-objective bi-level programming model and hnsga-ii algorithm," *International Journal of Production Research*, vol. 61, no. 5, pp. 1394–1423, 2023.

[63] M. Noruzi Azghandi, A. A. Shojaei, S. Toosi, and H. Lotfi, "Optimal reconfiguration of distribution network feeders considering electrical vehicles and distributed generators," *Evolutionary Intelligence*, vol. 16, no. 1, pp. 49–66, 2023.

[64] R. Wu and S. Liu, "Multi-objective optimization for distribution network reconfiguration with reactive power optimization of new energy and evs," *IEEE Access*, vol. 11, pp. 10664–10674, 2023.

[65] A. Pahlavanhoseini and M. S. Sepasian, "Scenario-based planning of fast charging stations considering network reconfiguration using cooperative coevolutionary approach," *Journal of Energy Storage*, vol. 23, pp. 544–557, 2019.

[66] J.-M. Clairand, M. González-Rodríguez, R. Kumar, S. Vyas, and G. Escrivá-Escrivá, "Optimal siting and sizing of electric taxi charging stations considering transportation and power system requirements," *Energy*, vol. 256, p. 124572, 2022.

[67] P. Sadeghi-Barzani, A. Rajabi-Ghahnavieh, and H. Kazemi-Karegar, "Optimal fast charging station placing and sizing," *Applied Energy*, vol. 125, pp. 289–299, 2014.

[68] G. Ferro, R. Minciardi, L. Parodi, and M. Robba, "Optimal planning of charging stations in coupled transportation and power networks based on user equilibrium conditions," *IEEE Transactions on Automation Science and Engineering*, vol. 19, no. 1, pp. 48–59, 2021.

[69] A. M. Othman, H. A. Gabbar, F. Pino, and M. Repetto, "Optimal electrical fast charging stations by enhanced descent gradient and voronoi diagram," *Computers & Electrical Engineering*, vol. 83, p. 106574, 2020.

[70] S. N. Hashemian, M. A. Latify, and G. R. Yousefi, "Pev fast-charging station sizing and placement in coupled transportation-distribution networks considering power line conditioning capability," *IEEE Transactions on Smart Grid*, vol. 11, no. 6, pp. 4773–4783, 2020.

[71] A. Awasthi, K. Venkitusamy, S. Padmanaban, R. Selvamuthukumaran, F. Blaabjerg, and A. K. Singh, "Optimal planning of electric vehicle charging station at the distribution system using hybrid optimization algorithm," *Energy*, vol. 133, pp. 70–78, 2017.

[72] F. Ahmad, A. Iqbal, I. Ashraf, M. Marzband, and I. Khan, "Placement of electric vehicle fast charging stations in distribution network considering power loss, land cost, and electric vehicle population," *Energy Sources, Part A: Recovery, Utilization, and Environmental Effects*, vol. 44, no. 1, pp. 1693–1709, 2022.

[73] D. Paudel and T. K. Das, "Infrastructure planning for ride-hailing services using shared autonomous electric vehicles," *International Journal of Sustainable Transportation*, pp. 1–16, 2022.

[74] H. Zhang, J. Qiu, and Y. Wang, "Planning strategy of fast-charging stations in coupled transportation and distribution systems considering human health impact," *International Journal of Electrical Power & Energy Systems*, vol. 133, p. 107316, 2021.

[75] A. Shukla, K. Verma, and R. Kumar, "Multi-objective synergistic planning of ev fast-charging stations in the distribution system coupled with the transporta-

tion network," *IET Generation, Transmission & Distribution*, vol. 13, no. 15, pp. 3421–3432, 2019.

[76] A. Pal, A. Bhattacharya, and A. K. Chakraborty, "Allocation of electric vehicle charging station considering uncertainties," *Sustainable Energy, Grids and Networks*, vol. 25, p. 100422, 2021.

[77] S. Deb, K. Tammi, X.-Z. Gao, K. Kalita, and P. Mahanta, "A hybrid multi-objective chicken swarm optimization and teaching learning based algorithm for charging station placement problem," *IEEE Access*, vol. 8, pp. 92573–92590, 2020.

[78] G. G. Soma, F. Pilo, and S. Conti, "Multi-objective integrated planning of fast charging stations," in *2019 AEIT International Conference of Electrical and Electronic Technologies for Automotive (AEIT AUTOMOTIVE)*, pp. 1–5, IEEE, 2019.

[79] A. Amer, M. A. Azzouz, A. Azab, and A. S. Awad, "Stochastic planning for optimal allocation of fast charging stations and wind-based dgs," *IEEE Systems Journal*, vol. 15, no. 3, pp. 4589–4599, 2020.

[80] R. Sa'adati, M. Jafari-Nokandi, and J. Saebi, "Allocation of ress and pev fast-charging station on coupled transportation and distribution networks," *Sustainable Cities and Society*, vol. 65, p. 102527, 2021.

[81] M. Mozaffari, H. A. Abyaneh, M. Jooshaki, and M. Moeini-Aghtaie, "Joint expansion planning studies of ev parking lots placement and distribution network," *IEEE Transactions on Industrial Informatics*, vol. 16, no. 10, pp. 6455–6465, 2020.

[82] O. Hafez and K. Bhattacharya, "Queuing analysis based pev load modeling considering battery charging behavior and their impact on distribution system operation," *IEEE Transactions on Smart Grid*, vol. 9, no. 1, pp. 261–273, 2016.

[83] A. Pal, A. Bhattacharya, and A. K. Chakraborty, "Planning of ev charging station with distribution network expansion considering traffic congestion and uncertainties," *IEEE Transactions on Industry Applications*, 2023.

[84] A. Sadhukhan, M. S. Ahmad, and S. Sivasubramani, "Optimal allocation of ev charging stations in a radial distribution network using probabilistic load modeling," *IEEE Transactions on Intelligent Transportation Systems*, vol. 23, no. 8, pp. 11376–11385, 2021.

[85] M. Asna, H. Shareef, P. Achikkulath, H. Mokhlis, R. Errouissi, and A. Wahyudie, "Analysis of an optimal planning model for electric vehicle fast-charging stations in al ain city, united arab emirates," *IEEE Access*, vol. 9, pp. 73678–73694, 2021.

[86] S. Deb, K. Tammi, X.-Z. Gao, K. Kalita, P. Mahanta, and S. Cross, "A robust two-stage planning model for the charging station placement problem considering road traffic uncertainty," *IEEE Transactions on Intelligent Transportation Systems*, vol. 23, no. 7, pp. 6571–6585, 2021.

[87] S. A. Cook, "An overview of computational complexity," *ACM Turing award lectures*, p. 1982, 2007.

[88] S. Bandaru and K. Deb, "Metaheuristic techniques," in *Decision sciences*, pp. 709–766, CRC Press, 2016.

[89] C. Blum and A. Roli, "Metaheuristics in combinatorial optimization: Overview and conceptual comparison," *ACM computing surveys (CSUR)*, vol. 35, no. 3, pp. 268–308, 2003.

[90] X.-S. Yang, *Engineering optimization: an introduction with metaheuristic applications*. John Wiley & Sons, 2010.

[91] M. Abdel-Basset, L. Abdel-Fatah, and A. K. Sangaiah, "Metaheuristic algorithms: A comprehensive review," *Computational intelligence for multimedia big data on the cloud with engineering applications*, pp. 185–231, 2018.

[92] H. John, "Holland. genetic algorithms," *Scientific american*, vol. 267, no. 1, pp. 44–50, 1992.

[93] X.-S. Yang, "Firefly algorithm, stochastic test functions and design optimisation," *International journal of bio-inspired computation*, vol. 2, no. 2, pp. 78–84, 2010.

[94] D. Karaboga *et al.*, "An idea based on honey bee swarm for numerical optimization," tech. rep., Technical report-tr06, Erciyes university, engineering faculty, computer . . . , 2005.

[95] N. M. Al Salami, "Ant colony optimization algorithm," *UbiCC Journal*, vol. 4, no. 3, pp. 823–826, 2009.

[96] R. V. Rao, V. J. Savsani, and D. Vakharia, "Teaching–learning-based optimization: an optimization method for continuous non-linear large scale problems," *Information sciences*, vol. 183, no. 1, pp. 1–15, 2012.

[97] R. Rao, "Rao algorithms: Three metaphor-less simple algorithms for solving optimization problems," *International Journal of Industrial Engineering Computations*, vol. 11, no. 1, pp. 107–130, 2020.

[98] D. H. Wolpert and W. G. Macready, "No free lunch theorems for optimization," *IEEE transactions on evolutionary computation*, vol. 1, no. 1, pp. 67–82, 1997.

[99] S. Deb, K. Tammi, K. Kalita, and P. Mahanta, "Review of recent trends in charging infrastructure planning for electric vehicles," *Wiley Interdisciplinary Reviews: Energy and Environment*, vol. 7, no. 6, p. e306, 2018.

[100] S. Mirjalili, S. Saremi, S. M. Mirjalili, and L. d. S. Coelho, "Multi-objective grey wolf optimizer: a novel algorithm for multi-criterion optimization," *Expert systems with applications*, vol. 47, pp. 106–119, 2016.

[101] C. C. Coello and M. S. Lechuga, "Mopso: A proposal for multiple objective particle swarm optimization," in *Proceedings of the 2002 Congress on Evolutionary Computation. CEC'02 (Cat. No. 02TH8600)*, vol. 2, pp. 1051–1056, IEEE, 2002.

[102] S. Deb, K. Tammi, K. Kalita, and P. Mahanta, "Impact of electric vehicle charging station load on distribution network," *Energies*, vol. 11, no. 1, p. 178, 2018.

[103] H. Zhang, S. J. Moura, Z. Hu, and Y. Song, "Pev fast-charging station siting and sizing on coupled transportation and power networks," *IEEE Transactions on Smart Grid*, vol. 9, no. 4, pp. 2595–2605, 2016.

Publications

Refereed International Journal publications:

1. **Vijay, Vutla**, Chintham Venkaiah, and Vinod Kumar Dulla Mallesham. "Meta Heuristic Algorithm Based Multi Objective Optimal Planning of Rapid Charging Stations and Distribution Generators in a Distribution System Coupled with Transportation Network." Advances in Electrical and Electronic Engineering 20, no. 4 (2023): 493-504 (ESCI, VSB-Technical University of Ostrava).

2. **Vijay, Vutla**, Chintham Venkaiah, and DM Vinod Kumar. "Multi objective queue theory based optimal planning of rapid charging stations and distributed generators in coupled transportation and distribution network." Energy Storage, (2023): e484 (ESCI, John Wiley & Sons ltd, IF:3.2 (2023)).

Refereed International Journal publications communicated:

1. **Vutla Vijay**, Chintham Venkaiah, "Multi objective optimal planning of Rapid Charging Stations, Distributed Generators, and D-STATCOM in coupled network considering Waiting time". Energy Sources, Part A: Recovery, Utilization, and Environmental Effects. (SCIE, Taylor & Fransis).

2. **Vutla Vijay**, Chintham Venkaiah, "Multi-Objective Optimal Planning of Electric Vehicle Rapid Charging Stations in Coupled Network Considering Network Reconfiguration". Electrical Engineering. (SCIE, Springer).

Appendix A
IEEE 33 bus radial distribution system

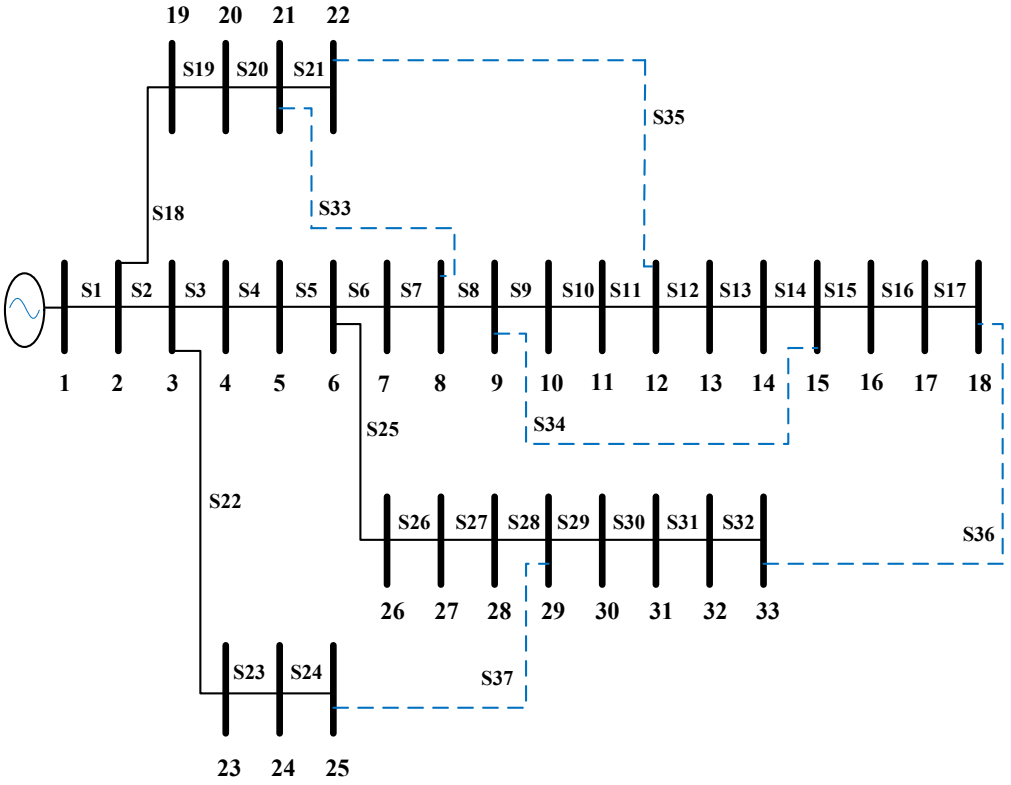

Figure 6.1: Single line diagram of IEEE 33 bus system

Table 6.1: IEEE 33 bus radial distribution system line data

Line No	Starting bus	End bus	R (p.u)	X (p.u)
1	1	2	0.0575	0.0298
2	2	3	0.3076	0.1567
3	3	4	0.2284	0.1163
4	4	5	0.2378	0.1211
5	5	6	0.5110	0.4411
6	6	7	0.1168	0.3861
7	7	8	1.0678	0.7706
8	8	9	0.6426	0.4617
9	9	10	0.6489	0.4617
10	10	11	0.1227	0.0406
11	11	12	0.2336	0.0772
12	12	13	0.9159	0.7206
13	13	14	0.3379	0.4448
14	14	15	0.3687	0.3282
15	15	16	0.4656	0.3400
16	16	17	0.8042	1.0738
17	17	18	0.4567	0.3581
18	2	19	0.1023	0.0976
19	19	20	0.9385	0.8457
20	20	21	0.2555	0.2985
21	21	22	0.4423	0.5848
22	3	23	0.2815	0.1924
23	23	24	0.5603	0.4424
24	24	25	0.5590	0.4374
25	6	26	0.1267	0.0645
26	26	27	0.1773	0.0903
27	27	28	0.6607	0.5826
28	28	29	0.5018	0.4371
29	29	30	0.3166	0.1613
30	30	31	0.6080	0.6008
31	31	32	0.1937	0.2258
32	32	33	0.2128	0.3308

Table 6.2: IEEE 33 bus radial distribution system load data

Bus No.	Real power (kW)	Reactive power (kW)
1	0	0
2	100	60
3	90	40
4	120	80
5	60	30
6	60	20
7	200	100
8	200	100
9	60	20
10	60	20
11	45	30
12	60	35
13	60	35
14	120	80
15	60	10
16	60	20
17	60	20
18	90	40
19	90	40
20	90	40
21	90	40
22	90	40
23	90	50
24	420	200
25	420	200
26	60	25
27	60	25
28	60	20
29	120	70
30	200	600
31	150	70
32	210	100
33	60	40

Appendix B

25 node road network

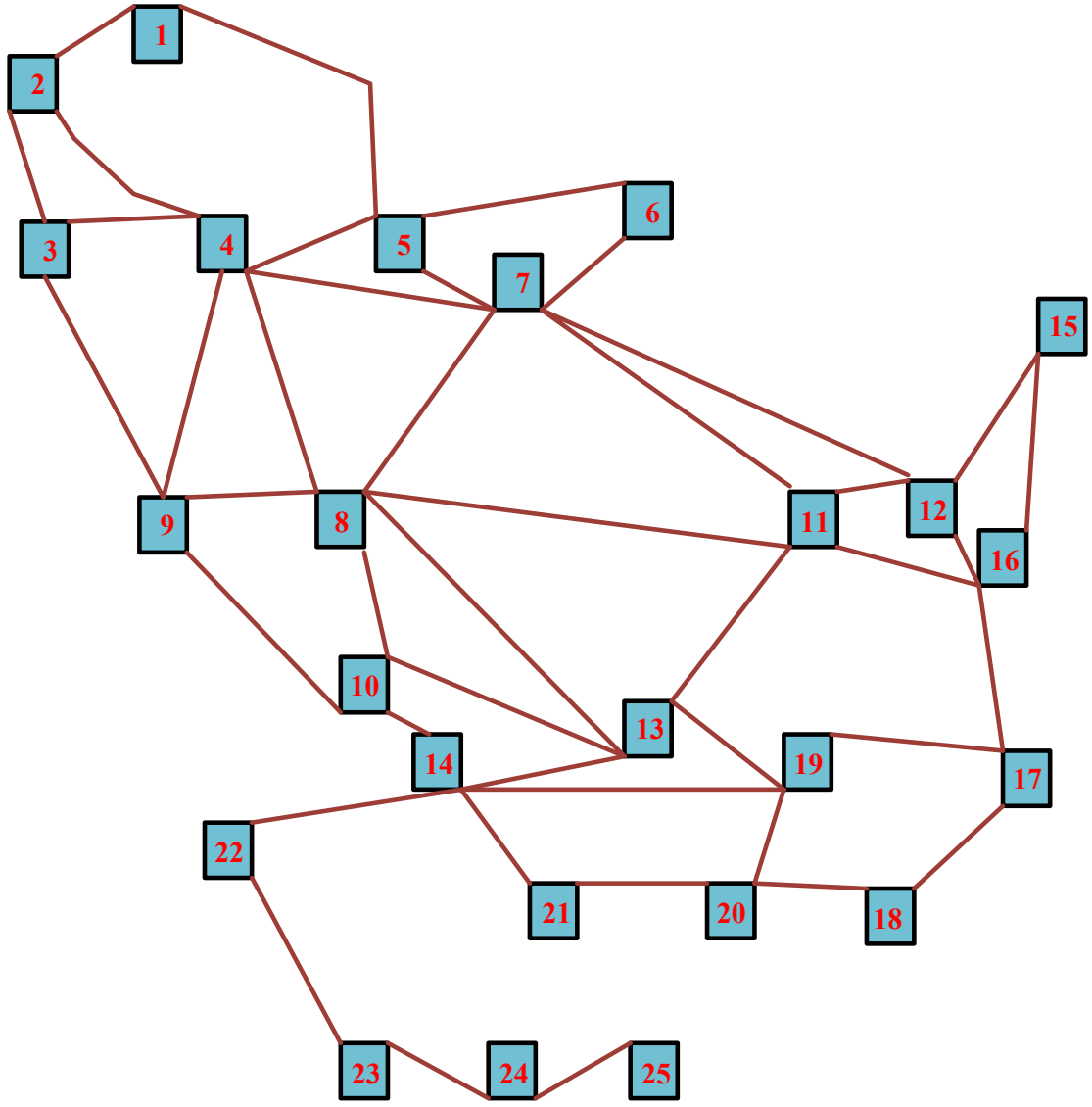

Figure 6.2: Single line diagram of 25 node road network

Table 6.3: Distance between nodes of 25 node road network

From node	To node	Distance (km)
1	2	4
1	5	5
2	3	3
2	4	4
3	4	4
3	9	4
4	9	7
4	8	5
4	7	5
4	5	3
5	6	5
5	7	5
6	7	3
7	8	3
7	11	8
7	12	9
8	9	6
8	10	6
8	11	7
8	13	7
9	10	6
10	13	6
10	14	3
11	13	3
11	16	7
11	12	2
12	15	4
12	16	4

From node	To node	Distance (km)
13	14	7
13	19	4
14	19	7
14	21	2
14	22	4
15	16	4
16	17	4
17	18	3
17	19	3
18	20	30
19	20	30
20	21	20
21	14	20
21	20	20
21	14	20
21	20	20
22	23	30
23	24	30
24	25	80
25	24	80

About Author

Vutla Vijay received M.Tech. from Jawaharlal Nehru Technological University Kondagattu, Jagityal, Karimnagar in 2018. Currently he is a research scholar in the Department of Electrical Engineering at National Institute of Technology (NIT) Warangal. His present research is in the area of optimal planning of DGs and Electric Vehicle charging stations. Artificial Intelligence applications in power system.